



Chair of Drilling and Completion Engineering

Master's Thesis



A Study of Ultrasonic
Measurement Technique to
Discriminate Fluids

Patrick Lutz, BSc

February 2023



MONTANUNIVERSITÄT LEOBEN
www.unileoben.ac.at

EIDESSTATTLICHE

Ich erkläre an Eides statt, dass ich diese Arbeit selbständig verfasst, andere als die angegebenen Quellen und Hilfsmittel nicht benutzt, und mich auch sonst keiner unerlaubten Hilfsmittel bedient habe.

Ich erkläre, dass ich die Richtlinien des Senats der Montanuniversität Leoben zu "Gute wissenschaftliche Praxis" gelesen, verstanden und befolgt habe.

Weiters erkläre ich, dass die elektronische und gedruckte Version der eingereichten wissenschaftlichen Abschlussarbeit formal und inhaltlich identisch sind.

Datum 06.02.2023

A handwritten signature in black ink, appearing to read 'Patrick Lutz', written over a horizontal line.

Unterschrift Verfasser/in
Patrick Lutz

Patrick Lutz
Master Thesis 2023
Petroleum Engineering

A Study of Ultrasonic Measurement Technique to Discriminate Fluids

Supervisor: Krishna Ravi
Co-supervisor/Advisor: Michael Prohaska,
Shwetank Krishna

Chair of Drilling Engineering

To my loving parents and family.

Acknowledgements

I want to thank my Supervisor Univ.-Prof. MBA PhD Kris Ravi, my advisors M. Tech PhD Shwetank Krishna and Ass. Prof. Dipl-Ing. Dr. mont. Michael Prohaska-Marchried for their continuous guidance during this thesis. Thank you for the opportunity to work on this project as a student assistance and giving me the chance to write this thesis.

Former and current office manager Patrizia Haberl and Elisabeth Koch created the helpful environment that made it possible to follow through the process of this thesis, for which I am very grateful.

I want to thank my colleagues Nico Masching, Stefan Weiskirchner, and Sahand Shams for always helping me in the laboratory when needed.

Eventually I wish to express my gratitude to my friends who I met during my studies. Their aid made it possible for me to push through the hardships I faced during the last years.

Finally, I want to thank my family for their continuous mental and financial support. Without them I would have never been able to study petroleum engineering.

Abstract

Cementing is a well-established practice in the oil and gas industry. Its main purpose is to protect the wellbore from the surrounding downhole environment which includes prevention of unwanted communication of formation fluids with the wellbore or other permeable horizons. During a cement job the existing mud in the wellbore will be displaced by the spacer, to clean the pipe and borehole wall, followed by cement and a displacement fluid which usually is a mud. The intermixing between these fluids (spacer, cement, and mud) could arise during the placement phase which tends to affect the specified cement properties and hence jeopardize the quality of a cement job. Thus, a better understanding of intermixing during the fluid displacement phase is required to improve the fluid compatibility in mitigating this problem.

The main goal of this thesis is to generate ultrasonic data for several commonly used materials in the oil and gas industry to prepare muds, spacers, and cements. A baseline study is conducted to measure the variation in sonic velocity of individual materials dispersed in water. The generated baseline database will serve as a reference point to predict the sonic velocity in the mixed fluid.

A feasibility study is conducted to determine the practicality of ultrasonic sensors to determine the sonic velocity of different fluids. The result of this study poses new questions which have been answered in the static single additive experiments. A total of thirteen (13) commonly used drilling and cementing additives are analyzed using a custom-made ultrasonic setup. Therefore, fluids of different concentration of each additive are mixed and the average sonic velocity determined. The results of this study give an intrinsic insight into the effect of each additive on the sonic velocity. Finally, a proof-of-concept experiment is presented to display how the acquired knowledge can be applied in the field. Therefore, two (2) muds of different density are mixed and displaced on a benchtop setup. Fluid discrimination, density evaluation, degree of intermixing calculation and required volume for full displacement prediction is successfully conducted and presented. Most of the objectives of this thesis are successfully achieved and are presented in detail.

Zusammenfassung

Zementieren ist eine etablierte Praxis in der Erdöl- und Gasindustrie. Der Hauptnutzen des Zements besteht darin, das Bohrloch vor der umgebenden Bohrlochumgebung zu schützen. Dies verhindert eine unerwünschte Kommunikation von Formationsfluiden mit dem Bohrloch oder anderen permeablen Horizonten. Während zementier arbeiten wird der vorhandene Bohrschlamm mit einen Spacer verdrängt, um das Rohr und die Bohrlochwand zu reinigen. Gefolgt wird dies mit Zement und einer Verdrängungsflüssigkeit, die normalerweise wieder ein Bohrschlamm ist. Die Vermischung zwischen diesen Flüssigkeiten (Spacer, Zement und Bohrschlamm) kann während der Verdrängungsphasen auftreten, welches die spezifizierten Zementeigenschaften beeinträchtigt und somit die Qualität einer Zementarbeit gefährdet. Aus diesem Grund ist ein besseres Verständnis des Vermischens während der Verdrängungsphasen erforderlich, um die Fluidkompatibilität zu verbessern und das Vermischen zu verhindern. Das Hauptziel dieser Arbeit ist die Ausarbeitung von Ultraschalldaten für häufig verwendete Materialien, zur Herstellung von Bohrschlämmen, Spacern und Zementen, in der Erdöl- und Gasindustrie. Es wird eine Grundstudie durchgeführt, um die Schwankungen der Schallgeschwindigkeit einzelner in Wasser verteilten Materialien zu messen. Die generierte Basisdatenbank dient als Referenzpunkt, um die Schallgeschwindigkeit in gemischten Flüssigkeiten vorherzusagen. Eine Machbarkeitsstudie wird durchgeführt, um die Praktikabilität von Ultraschallsensoren zur Bestimmung der Schallgeschwindigkeit verschiedener Flüssigkeiten zu bestimmen. Das Ergebnis dieser Studie wirft neue Fragen auf, die in den statischen Einzeladditivversuchen beantwortet werden. Insgesamt dreizehn (13) häufig verwendete Bohr- und Zementierzusätze werden mit einem selbst gebauten Ultraschallaufbau analysiert. Dazu werden Flüssigkeiten unterschiedlicher Konzentration jedes Additivs gemischt und die durchschnittliche Schallgeschwindigkeit bestimmt. Die Ergebnisse dieser Studien geben einen intrinsischen Einblick in die Wirkung jedes Additivs auf die Schallgeschwindigkeit. Abschließend wird ein Proof-of-Concept-Experiment vorgestellt, um zu zeigen, wie das erworbene Wissen in der Praxis angewendet werden kann. Daher werden zwei (2) Schlämme unterschiedlicher Dichte gemischt und auf einem Benchtop-Aufbau verdrängt. Flüssigkeitsdiskriminierung, Dichtemessung, Berechnung des Mischungsgrades und das erforderliche Volumen für die Vorhersage der vollständigen Verdrängung wurden erfolgreich angewandt und präsentiert. Die meisten Ziele dieser Arbeit wurden erfolgreich erreicht und werden im Detail dargestellt.

Table of Contents

Acknowledgements.....	vii
Abstract.....	ix
Zusammenfassung.....	x
Chapter 1.....	13
1.1 Background and Context.....	13
1.2 Scope and Objectives.....	14
1.3 Achievements.....	14
1.4 Technical Issues.....	15
1.5 Overview of Thesis.....	15
Chapter 2.....	17
2.1 Ultrasonic Measurement.....	17
2.2 Additives.....	22
Chapter 3.....	29
3.1 Concept of fluid intermixing and Sonic velocity.....	29
3.2 Design of Experiment.....	30
3.3 Test Preparation.....	31
3.4 Testing.....	33
3.5 Results.....	35
3.6 Summary Feasibility Study.....	39
Chapter 4.....	41
4.1 Design of Experiment.....	41
4.2 Setup Error Determination.....	55
4.3 Experimental Preparation and Investigation.....	56
Chapter 5.....	65
5.1 Experimental Results.....	65
Chapter 6.....	115
6.1 Summary.....	115
6.2 Evaluation.....	116
6.3 Future Work.....	116
References.....	119

Chapter 1

Introduction

1.1 Background and Context

Cementing is a well-established practice in the oil and gas industry. Its main purpose is to protect the wellbore from the surrounding downhole environment which includes prevention of unwanted communication of formation fluids with the wellbore or other permeable horizons. This practice is part of well integrity principle known as two-barrier system. A two-barrier system requires a primary and secondary barrier throughout the lifecycle of a drilled well. For example, while drilling an intermediate section the overbalanced mud is considered to be the primary barrier and the surface casing cement, the surface casing, the wellhead and the blow-out preventer are considered to be the secondary barrier (Khalifeh and Saasen 2020).

During a cement job the existing mud in the wellbore will be displaced by the spacer, to clean the pipe and borehole wall, followed by cement and a displacement fluid which usually is a mud. The intermixing between these fluids (spacer, cement, and mud) could arise during the placement phase which tends to affect the specified cement properties and hence jeopardize the quality of a cement job. In addition, the presence of mud or filter cake can alter and reduce the ability of the cement to adhere with the borehole wall and casing. Thus, a better understanding of intermixing during the fluid displacement phase is required to improve the fluid compatibility in mitigating this problem (Chen et al. 2014; Shadravan et al. 2015).

Several companies have developed fluid displacement simulation software to better prepare for cement jobs. Primarily, these software determines the fluid velocity field in the system and then solve the advection diffusion equation to simulate intermixing. However, experimental validation of the simulated results is often not available due to the lack of appropriate testing infrastructure. Therefore, by generating the necessary experimental data, models can be confirmed or improved, leading to a better understanding of intermixing. A combination of

pressure, flowrate, resistivity, density, displacement efficiency and level of intermixing measurements are used to gather necessary experimental data.

In this master thesis, ultrasonic measurement technique will be focused to establish a database to understand and evaluate the feasibility of the mud, spacer, and cement interaction. The sensor will capture the density variation both in static system and flowing conditions in real-time (Paul Wagner 2020b; Sven Curis 2022a; Adamowski et al. 1995). There are limited publications that provide ultrasonic data for different muds and spacers. The available literature mainly focuses on different muds while not considering the effect of individual ingredients on the ultrasonic velocity (Wiklund et al. 2010). Whereas, a lot of data is available for cements since an ultrasonic compressive strength test is conducted during API testing (Jandhyala et al. 2018; Tay et al. 2020; Mahmood et al. 2022).

1.2 Scope and Objectives

The objective of this master thesis is to capture the effect of intermixing between commonly used fluids in the drilling industry. Especially the intermixing between muds and spacers. The ultrasonic velocity of single ingredients, pure, and intermixed fluids will be determined to generate baseline data. Initially, the mentioned baseline data will be captured in a static fluid sample. After this initial study, a dynamic flow test on the benchtop will be conducted to capture intermixing between the testing fluids.

Outcome:

- Sonic velocity of single materials at different concentration in water
- Static fluid measurement of muds and spacers
- Semi-dynamic measurement of a water-mud fluid displacement on the benchtop
- Determination of “degree of intermixing” using ultrasonic data
- Compilation and analysis of the obtained data to determine the effect of ingredients in water-based muds.

1.3 Achievements

The feasibility showed that it is possible to determine a density/average sonic velocity relationship. During the feasibility study additional questions were developed. Those posed questions were answered during the static single additive experiments. In total 13 different additives have been analyzed using the custom-made ultrasonic setup. Each fluid was mixed at different concentration (each additive) and the average sonic velocity was measured. This resulted in a base understanding of the ultrasonic interaction with different commonly used

additives. Finally, an experiment is presented to show how the acquired knowledge can be applied in the field. Fluid discrimination, density evaluation, degree of intermixing calculation and required volume for full displacement prediction was successfully conducted and presented.

1.4 Technical Issues

While testing viscosifiers not all bubbles could be removed. Therefore, some data is not as accurate. The applied piezoelectric sensors cannot create a strong enough ultrasonic wave to have a good signal that can be received. Therefore, some data is not as accurate when measuring insoluble weighting agents. Furthermore, only a semi-dynamic test was conducted, because the used piezoelectric elements cannot be attached to a curved surface.

1.5 Overview of Thesis

First a feasibility study is conducted to evaluate the possible use of ultrasonic sensors to determine the degree of intermixing and density. The result are additional questions posed by the findings of this study. To answer those questions thirteen (13) different additives are tested to achieve an understanding on how the average sonic velocity measurement is affected by those additives. Their average sonic velocity is compared to a variety of fluid properties (e.g., density, viscosity, gel strength, etc.). Finally, a proof-of-concept experiment is presented to show that the measurement can be used in the field to determine the degree of intermixing, density and to predict the required volume for full displacement. Furthermore, it was proven that fluid discrimination is possible. The system is easy to use with brines but faces some challenges when used on muds which have insoluble weighting agents. All the measurement approaches, test setups, software settings, the analyzed data and the findings are presented in this master thesis.

Chapter 2

Literature Review

This section of the master thesis mainly focuses on the thirteen (13) additives used for the experiment of the sonic velocity study and the principles of ultrasonic measurements. Each additive is reviewed to understand its purpose in the oil and gas industry and if an ultrasonic sensor study was conducted in the past. The additives used during this study are polyanionic cellulose (PAC), xanthan gum, bentonite, laponite, carboxymethyl-cellulose (CMC), flowzan, barite, calcium carbonate (CaCO_3), potassium carbonate (K_2CO_3), sodium carbonate (Na_2CO_3), citric acid, caustic soda and gypsum. Furthermore, the basis of ultrasonic measurements and the physical effects that can be encountered during those measurements will be discussed in the section below.

2.1 Ultrasonic Measurement

Ultrasonic measurement is a non-destructive and non-invasive evaluation technique that uses high frequency sound waves (frequencies higher than 20kHz) to evaluate the properties of materials or detect defects. The principles of ultrasonic measurement are based on the behaviour of sound waves in materials and the interaction of these waves with defects and material boundaries. In ultrasonic measurement, a transducer (piezoelectric element is used in this thesis) generates high frequency sound waves that are directed into the material being evaluated. These sound waves propagate through the material, encountering any defects or material boundaries along the way. The behaviour of the sound waves is then analysed to determine the presence and nature of any defects or material properties. One of the key principles of ultrasonic measurement is the concept of reflection and refraction. When a sound wave encounters a material boundary or a defect, some of the energy is reflected back towards the transducer, while some continues to propagate through the material. The amount of energy reflected and refracted depends on the properties of the material, the size and shape of the

defect, and the frequency of the sound wave. Another important principle of ultrasonic measurement is the concept of attenuation, or the loss of energy in a sound wave as it travels through a material. Attenuation is affected by several factors such as temperature, material properties, and the presence of defects. The amount of attenuation can be used to determine the material properties and the presence of defects. The time of flight, or the time it takes for a sound wave to travel through a material and return to the transducer, is another important principle in ultrasonic measurement. By analysing the time of flight, it is possible to determine the thickness of the material, the velocity of the sound wave, and the presence of any defects. This principle is applied during all the presented tests of this thesis. In summary, the principles of ultrasonic measurement are based on the behaviour of sound waves in materials, including reflection and refraction, attenuation, and time of flight. These principles allow for the non-destructive evaluation of material properties and the detection of defects in a wide range of applications. (Halmshaw 1996; Krautkrämer and Krautkrämer 1990; POVEY 1997)

2.1.1 Acoustic propagation through liquid mediums

In liquids, several different types of ultrasonic wave forms can propagate, including longitudinal waves and shear waves. Longitudinal waves, also known as compressional waves, are the most used wave form in ultrasonic testing. These waves propagate through a material in the direction of the wave propagation, and the particle displacement is parallel to the direction of the wave. Longitudinal waves are generated by a transducer (e.g., piezoelectric element) that vibrates in the axial direction, creating pressure variations that propagate through the material. Shear waves, on the other hand, are transverse waves that propagate perpendicular to the direction of the wave propagation. In a shear wave, the particle displacement is perpendicular to the direction of the wave. Shear waves can be generated in materials that support transverse elastic waves, such as metals and some polymers. In liquids, shear waves can also propagate, although they are typically slower and have higher attenuation than longitudinal waves. Shear waves are often used in ultrasonic testing for specialized applications, such as thickness measurements in multi-layer materials or material characterization. Overall, the type of wave form that is used in ultrasonic testing is dependent on the material being tested and the specific application. In liquids, both longitudinal and shear waves can propagate and be used for a variety of ultrasonic measurements. (POVEY 1997)

2.1.2 Reflection and Refraction

Reflection and refraction describe the behaviour of ultrasonic waves as they encounter different materials or interfaces. Reflection occurs when an ultrasonic wave encounters an interface between two materials with different acoustic impedances and bounces back into the same

material from which it originated. The amount of energy reflected depends on the angle of incidence and the acoustic impedance mismatch between the two materials. Reflection can be used to determine the presence of interfaces within a material or to study the mechanical properties of a material, such as its thickness or elastic modulus. Refraction occurs when an ultrasonic wave travels from one material into another material with a different acoustic impedance, causing it to change direction. The amount of refraction depends on the angle of incidence, the acoustic impedance mismatch between the two materials, and the wavelength of the wave. Refraction can be used to study the spatial distribution of mechanical properties within a material, such as the distribution of inhomogeneities or cracks. In ultrasonic testing, both reflection and refraction are used to generate images of the internal structure of materials, to measure the thickness and elastic properties of materials, and to detect and quantify flaws and defects in materials. Understanding the principles of reflection and refraction is therefore an important aspect of ultrasonic testing. Two types of interfaces occur in the custom-made ultrasonic test setup used in this thesis. The first type is the interface between the transducer and receiver with the testing chamber. It is important to have a good coupling between the piezoelectric sensor and the acrylic glass of the test chamber. A bad coupling will result in the loss of most of the energy; hence making it impossible to properly measure the testing fluid. To even further improve the transmission of the ultrasonic wave an ultrasonic gel is applied onto the sensor before attaching it to the testing chamber. The second type of interface is in between different materials i.e., the acrylic glass of the testing chamber and the testing fluid or the testing fluid and air bubbles in suspension.

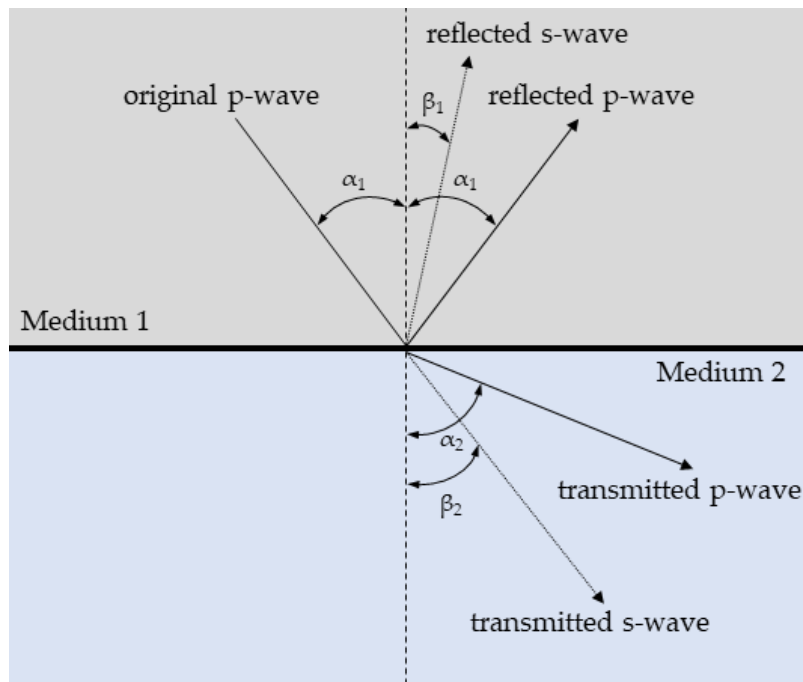


Figure 1: Depiction of refraction from medium 1 into medium 2

(Burrascano et al. 2015)

2.1.3 Attenuation

Attenuation is an important concept in ultrasonic testing and refers to the reduction of the amplitude (or wave energy) of an ultrasonic wave as it propagates through a material. Attenuation is a result of several physical processes, including absorption, scattering, and dispersion, which cause the energy of the wave to be dissipated into the material. The magnitude of attenuation depends on several factors, including the frequency of the wave, the elastic properties of the material, density and thickness of the material. Higher frequency waves are generally more susceptible to attenuation, and materials with higher densities and lower elastic moduli tend to exhibit higher levels of attenuation. Attenuation can have a significant impact on the accuracy and reliability of ultrasonic testing, as it reduces the sensitivity and resolution of the measurement. To obtain accurate measurements, it is important to understand and quantify the level of attenuation in the material being tested, and to take steps to mitigate its effects, such as using low-frequency transducers or compensating for the effects of attenuation in the data analysis process. This approach taken in this paper is the adjustment of the frequency of the signal to improve the resolution of the measurement. There are several methods for measuring and characterizing the attenuation of ultrasonic waves in materials, including pulse-echo measurements, through-transmission measurements, and frequency-domain measurements. These methods can provide valuable information about the mechanical properties of materials and can be used for a wide range of applications, including quality control, material characterization, and non-destructive testing. An example for attenuation can be seen in Figure 2 and Figure 3. To capture both figures the same settings were used and it is clearly visible how the barite attenuates the signal resulting in a lower amplitude. (Halmshaw 1996; Krautkrämer and Krautkrämer 1990; POVEY 1997; Bitok J.K. 2013; O’Leary et al. 2015)

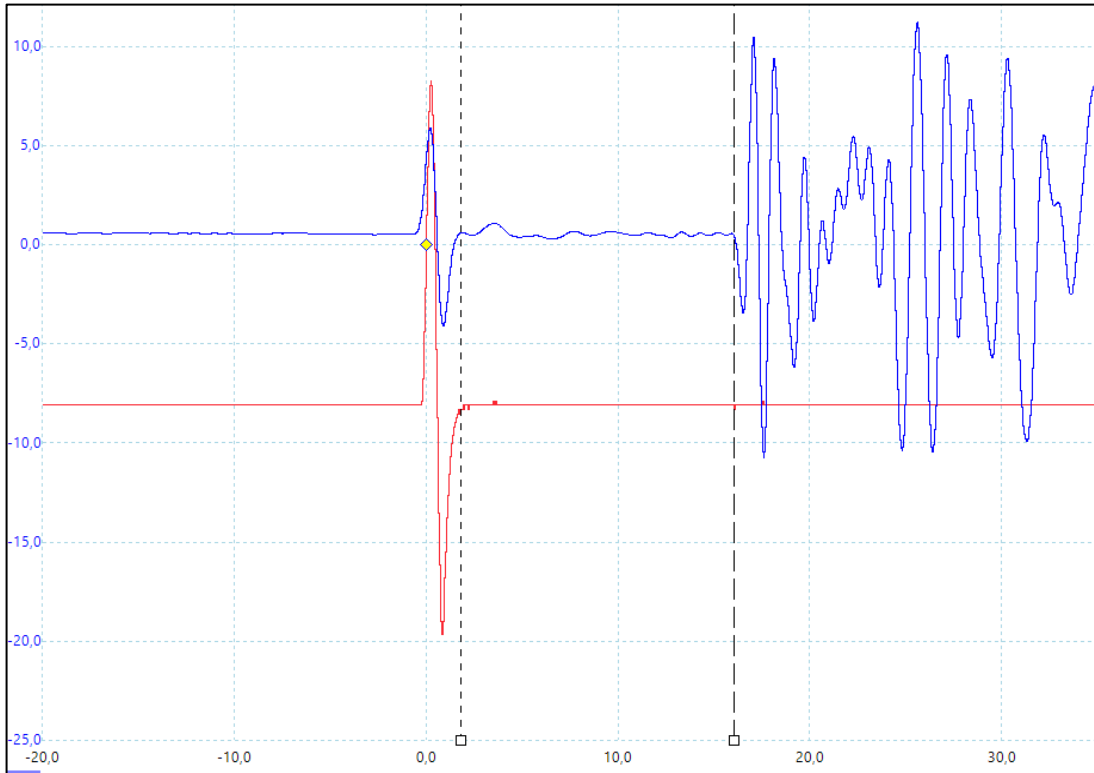


Figure 2: 9ppg barite ultrasonic measurement

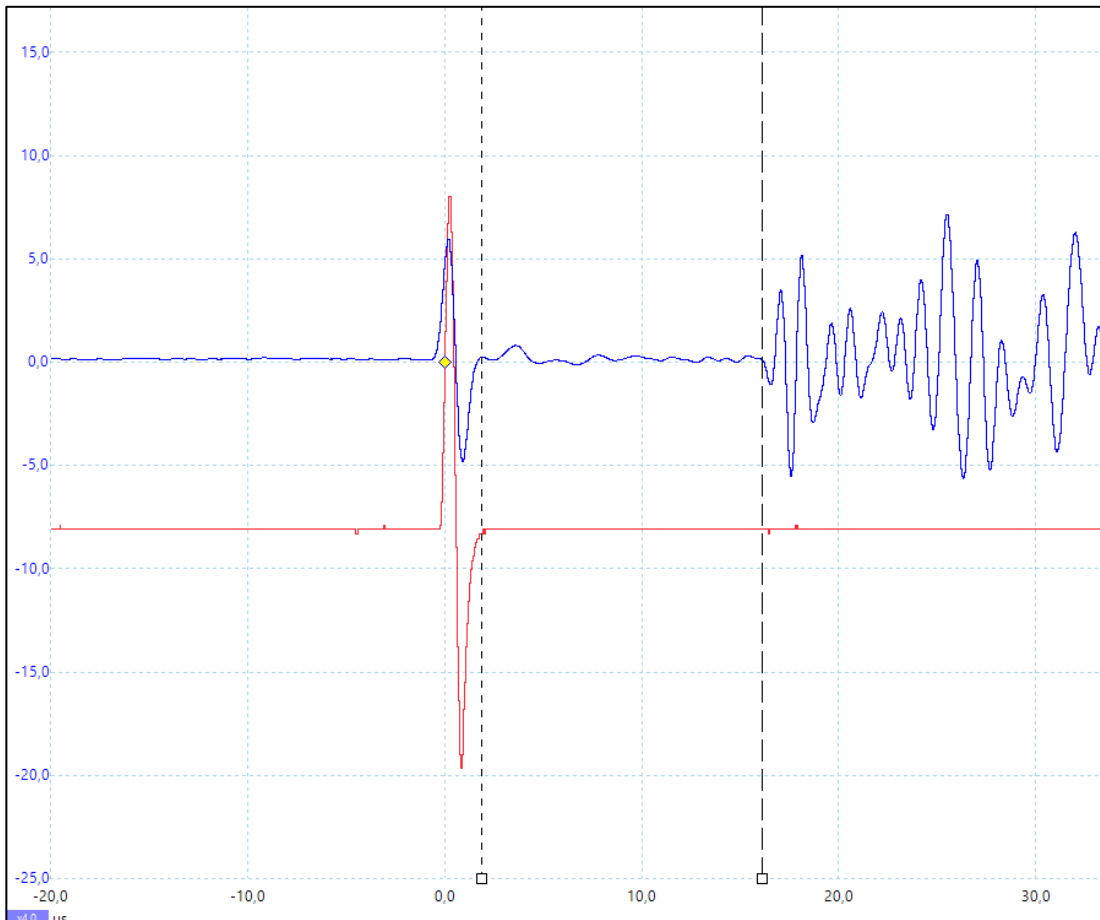


Figure 3: 10ppg barite ultrasonic measurement

2.1.4 Dispersion

In ultrasonic testing, dispersion refers to the variation in the velocity of an ultrasonic wave as a function of frequency. In other words, the velocity of an ultrasonic wave can change depending on the frequency of the wave. In many materials, including liquids, the velocity of an ultrasonic wave is a function of both the frequency and the wavelength of the wave. At lower frequencies, the velocity of an ultrasonic wave is typically higher, while at higher frequencies, the velocity is lower. This relationship between frequency and velocity is referred to as dispersion. Dispersion has important implications for ultrasonic testing, as it can affect the accuracy of measurements and the interpretation of data. For example, dispersion can cause ultrasonic waves to spread out as they travel through a material, reducing the energy and resolution of the waveform. Dispersion can also cause the formation of multiple modes or harmonics (*“any oscillatory motion in which the restoring force is proportional to displacement may be called harmonic” (POVEY 1997)*), each with its own velocity and attenuation characteristic. This can result in the reflection and refraction of the wave at interfaces within the material, leading to complex wave behavior that can be difficult to interpret. To address the effects of dispersion in ultrasonic testing, various techniques have been developed, including the use of multi-frequency probes, correction algorithms, and imaging methods. These techniques can help to minimize the impact of dispersion and improve the accuracy and resolution of ultrasonic measurements. Overall, the understanding and control of dispersion is an important aspect of ultrasonic testing, as it can affect the ability to accurately measure and interpret ultrasonic data. For this study tests were conducted to check how significant the impact of dispersion is on the captured signal. For the frequencies used during the static single additive experiments it is deemed insignificant as such no further regards to dispersion have been made in this study. (POVEY 1997; Krautkrämer and Krautkrämer 1990)

2.2 Additives

This subsection of the literature review project focuses on the thirteen used additives for this master thesis. Each additives main usage in the oil and gas industry is mentioned as well as previous ultrasonic work. A good understanding of each materials' effect on sonic velocity is crucial to determine the degree of intermixing, density or even when applying ultrasonic sensors in velocity profiling as presented by (Krishna et al. 2022).

2.2.1 Viscosifier

2.2.1.1 Polyanionic Cellulose (PAC)

PAC is a commonly used drilling fluid additive. Its molecular structure is close to CMC. However, PAC has better filtration reduction, anti-salt, collapse prevention, and high temperature (up to 150°C) capabilities. Furthermore, it is often added to muds to increase the viscosity to improve the hole cleaning performance. (TCI China 2021)

2.2.1.2 Xanthan Gum

Xanthan gum, also known as XC Polymer, is a natural biopolymer. Its main application in the oil and gas industry is in drilling muds. A non-Newtonian mud rheology is the result when mixing it with water. The xanthan gum powder swells when it is in contact with water and takes on a gel-like consistency. Furthermore, it has a flat velocity profile which benefits the annular flow and cutting transportation especially in low density muds. Moreover, xanthan gum develops a gel strength which benefits the cutting suspension when the pumps are turned off. Xanthan gum has a tolerance for salinity and the temperature tolerance varies on the water used and the temperature (degradation starts between 93 °C and 121 °C). Extreme pHs or hardness are not well suited with for Xanthan gum, and it is susceptible to bacteria attack resulting in the development of a stench when left sitting for prolonged times. The addition of bactericide can prevent this effect. (SLB Energy Glossary - Xanthan Gum 2023; Xanthan Suspensions | Resolute Oil 2023)

2.2.1.3 Bentonite

Bentonite is a clay material that shows considerable swelling when exposed to water. This material property and the worldwide availability is the motivation why it is used in the oil and gas industry as a viscosifier and filtration control. It is often combined with other viscosifiers such as CMC or starch to achieve the desired rheological properties. Another benefit of bentonite is its ability to cool, lubricate and protect (against corrosion) the drill bit. Furthermore, bentonite creates a gel strength which benefits the cuttings suspension when the pumps are turned off. Its shear thinning property makes it possible to break the gel strength without a great risk of damaging the surrounding formation. Moreover, bentonite forms a filter cake by entering in the borehole wall, swelling and hardening; hence creating a protective layer against influx from the borehole into the formation and vice versa. (SLB Energy Glossary - Bentonite 2023; NEA Group 2023)

Bentonite formations have been analyzed with ultrasonic sensors. Research has shown that when the clay formation is saturated with water it increases the sonic velocity of the formation. (Kimura et al. 2018) Additionally, the acoustic velocity of seismic while drilling used bentonite

in their analysis. (Poletto et al. 2002) Both of the mentioned papers have not analyzed the effect of bentonite in drilling muds on its own. The presented work in subsection 5.1.1.3 is a novel approach to better understand the effect of bentonite on the sonic velocity.

2.2.1.4 Laponite

Laponite is a fairly new additive in the oil and gas industry, but found its use already in paints, inks, household cleaning materials, cosmetics and shampoos. (Lee, L., Rogers, P., Oakley, V. L., & Navarro, J. 1997). Laponite is a synthetic hectorite clay which swells when in contact with water. Hence, the main use of laponite is as a viscosifier. Specifically, the addition of laponite to a mud will result in an increase in apparent viscosity with almost no change to plastic viscosity. Furthermore, it has lubricative and fluid loss prevention properties. When drilling shale formations laponite can be added to the mud, since it effectively plugs shale pores resulting in reduced surface area and volume of exposed shale formation. (Huang et al. 2021)

2.2.1.5 Carboxymethyl cellulose (CMC)

CMC is a modified natural polymer which is often used to increase the viscosity, control fluid loss, and improve the flow conditions at high temperature, pressure and salinity. (Menezes et al. 2010) A byproduct of when producing CMC is NaCl (up to 20 wt %), consequently for some applications PAC, which shares a lot of similarities with CMC, is preferred (lower NaCl concentration). Furthermore, there is a distinction between high viscous and low viscous grade CMC. The impact of viscosity is mainly governed by the molecular weight of the cellulose material used in production. (SLB Energy Glossary - CMC 2023)

A little bit of research has been conducted with ultrasonic sensors on CMC. One paper (Abdul Kareem J- Al-Bermamy and Nadia Hussein Sahib 2013) presents that the sonic velocity is increasing with an increase in concentration. The same trend is presented by (Guru et al. 2008) (study of sonic velocity on a blend of Pullulan and CMC), but in a smaller velocity range as compared to (Abdul Kareem J- Al-Bermamy and Nadia Hussein Sahib 2013). A comparison to these two papers and a conclusion is presented in subsection 5.1.1.5.

2.2.1.6 Flowzan

Flowzan is a high purity xanthan gum polymer, thus finding the same use as xanthan gum. Therefore, refer to the section above for a more detailed review of xanthan gum. The main advantage of flowzan over xanthan gum is that less material is required to achieve the same properties. (Chevron Phillips Chemical 2023)

2.2.2 Weighting Material

2.2.2.1 Barite

Barite, also known as barium sulphate, is the most used weighting agent in the oil and gas industry. It's specific gravity (4,5) and the wide availability of the additive make it the primary mineral to increase the density of drilling fluids. The importance of density in overbalanced drilling is to ensure to stay within the mud weight window. As such it not only prevents formation fluids from entering the wellbore but also provides stability during drilling. Furthermore, due to its great availability it is more cost effective than other weighting materials (i.e., celestite, witherite and hematite), it is relatively inert, non-toxic (very important in regards to disposal costs), insoluble, relatively soft (does not wear out drilling equipment) and, it is nonmagnetic (does not interfere with downhole instruments used for logging). (Bleiwas and Miller 2015).

In 1998 an ultrasonic study was conducted to analyse the effects of a barite/bentonite mud on sonic velocity. It was discovered that with an increase in barite in the mud the attenuation effect increases; hence lowering the sonic velocity. The presented data from the paper can be seen in subsection 5.1.2.1 where it is compared to the results gathered for this master thesis. (Motz et al. 1998)

2.2.2.2 Calcium Carbonate (CaCO_3)

Calcium carbonate is a preferred weighting agent when drilling the pay-zone. The main benefit of using CaCO_3 instead of barite for drilling the production zone is that CaCO_3 is soluble in acids (i.e., hydrochloric acid). Therefore, it can be more easily removed after drilling is completed. This results in less skin caused by the filter cake. (Gogoi and Talukdar 2015) CaCO_3 is also often used as a bridging material in drill-in, completion and workover fluids. This in water and oil insoluble material has a specific gravity of 2,7 and it is recommended to only be used for muds with a density of up to 12 ppg. (SLB Energy Glossary - calcium carbonate 2023)

2.2.2.3 Potassium Carbonate (K_2CO_3)

K_2CO_3 (specific gravity of 2,3) forms potassium muds which are most used when drilling water sensitive shales. The in water dissolved K^+ ions attach to the surface of the clay; hence improving its strength. This results in more stable layers of clay. Furthermore, potassium muds help to prevent the drilled clay to break into fine particles, which counter acts a change in viscosity of the drilling fluid. Due to the tendency of the K^+ ions to stick to clay particles it is not recommended to combine those muds with bentonite. Instead viscosifiers like CMC or PAC should be used. (SLB Energy Glossary - potassium mud 2023) There are some environmental concerns when using big quantities of potassium muds. They might increase the pH of bodies

of water which may harm aquatic life. (Oxy 2013) This is especially a concern during offshore drilling.

A lot of studies have been conducted with potassium carbonate, but only one study was found that measured the sonic velocity of potassium carbonate. (O'Leary et al. 2015) discovered that an increase in concentration of potassium carbonate is resulting in higher sonic velocity. He stipulates that the change in sonic velocity of carbonate liquids is due to the adiabatic compressibility of the mixed fluid. Thus, a lower adiabatic compressibility results in a higher sonic velocity and vice versa. This effect can also be seen when comparing the results of potassium carbonate (subsection 5.1.2.3) and sodium carbonate (subsection 5.1.2.4). Na_2CO_3 has a lower adiabatic compressibility compared to K_2CO_3 , thus Na_2CO_3 has a higher sonic velocity. Furthermore, an increase in concentration of dissolved K_2CO_3 increases the sonic velocity of the fluid.

2.2.2.4 Sodium Carbonate (Na_2CO_3)

Sodium carbonate, also known as soda ash, is not often referred to as a weighting agent, but during this study it was purposed as such. It has a specific gravity of 2,5 and is soluble in water. During this thesis only a density range of 8,5 to 9,25 ppg is investigated. This low density due to the limitation of the low solubility (21,4g/l) in water at room temperature. Hence, the main purpose of sodium carbonate in the field is to treat calcium ion contamination in water-based muds. Another common application of sodium carbonate is for soda-ash treatment. Calcium ions from drilling gypsum or anhydrite cause clay flocculation, lower pH and lead to polymer precipitation. Sodium carbonate counteracts the pH change and reduces the effect of calcium ions. (SLB Energy Glossary - Sodium carbonate 2023)

No mud specific ultrasonic measurement studies have been found investigating the effect sodium carbonate has on the average sonic velocity. (O'Leary et al. 2015) also investigated the effect of Na_2CO_3 and discovered that with an increase in concentration the sonic velocity of the fluid increases.

2.2.3 Other additives

2.2.3.1 Citric Acid

Citric acid is available as a powder or in already premixed solutions. During this thesis citric acid powder is used to analyse the effect it has on the average sonic velocity. The main use of citric acid in the field is to reduce the pH of drilling fluids, remove dissolved calcium from flowers and to treat the mud for cement contamination. It is also used as a dispersant in cement slurries. (Persianutab 2021; SLB Energy Glossary - Citric acid 2023). Furthermore, citric acid had been used as an iron-control agent in combination with HCl to mitigate the precipitation of ferric hydroxide and/or iron sulfide. (Alkhaldi et al. 2009; Barnard, JR. 1960; Hall and Dill 1988) (Barnard, JR. 1960; Hall and Dill 1988; Taylor et al. 1999) A study from 2009 also investigated the application of citric acid in stimulation treatments of calcite. (Alkhaldi et al. 2009)

An investigation by (Jathi Ishwara Bhat et al. 2010) conducted acoustic measurements to determine the effects of citric acid in water based media. The presented results show that citric acid only has a small influence on the sonic velocity, but the recorded trend was that with an increase in concentration the sonic velocity increased. This trend is similar to other dissolving agents such as Na_2CO_3 or K_2CO_3 .

2.2.3.2 Caustic Soda (NaOH)

Caustic soda, also known as sodium hydroxide, finds a wide variety of different applications in the oil and gas industry. In the refining process of petroleum it is used to absorb carbon dioxide in light petroleum fractions, as an absorbent of sulphides in the purification process and in combination with hypochlorite to sweeten crude oil by removing sulphur compounds. (Westlake Chemical 2018) During drilling operations caustic soda is added to water-based muds to increase and maintain the pH. It is classified as a hazardous material, since it is very caustic and has an exothermal reaction when added to water. (SLB Energy Glossary - Caustic soda 2023). Another application is in alkaline flooding (chemical enhanced oil recovery) which increases the oil sweep efficiency. (Hemmati-Sarapardeh et al. 2022)

(Bitok J.K. 2013) conducted experiments to investigate the effect of various soluble materials in aqueous solutions including NaOH. A trend (comparable to other soluble materials) was discovered that an increase in concentration leads to an increase in sonic velocity. Comparable results were achieved during this study as are presented in subsection 5.1.3.2.

2.2.3.3 Gypsum

Gypsum, also known as calcium sulphate dihydrate, is used as an additive in muds to drill sections of gypsum, anhydrite, and salt stringers. It also performs well in preventing shale swelling and it is commonly combined with various viscosifiers to keep them suspended and to improve the fluid loss control capabilities of the mud. (SLB Energy Glossary - Gyp mud 2023) Furthermore, gypsum is also an additive used in cements to control the setting of cement, hence increasing the workable time.

Some research for gypsum is available, but only for the hydration process of gypsum in cement slurries. (Korte and Brouwers 2011) and (de Acj Arie Korte and H. J. H. Brouwers 2010) both studied the change in sonic velocity in regards to the hydration of the gypsum in a fresh cement slurry. Neither of them analysed gypsum on its own. Therefore, the results are different from the ones presented in this thesis.

Some of the additives above did not mention any previous ultrasonic studies or ultrasonic studies different fields. For those additives no comparable ultrasonic study has been found during the literature review of this master thesis. Hence, no data is available to be compared to the acquired data of the static additive tests. This lack of information of so many additives is one of the main incentives why this master thesis came to be.

Chapter 3

Feasibility Study

This part of the thesis will focus on the feasibility study for the ultrasonic sensors. The study was conducted to confirm the initial theory described in section 3.1, to develop an approach for ultrasonic measurement, learn the operation of ultrasonic sensors and develop a fundamental understanding of the gathered data.

3.1 Concept of fluid intermixing and Sonic velocity

The concept of intermixing is that when two different pure fluids of varying characteristics mix together, the resulting fluid will be a mixture of both. Thus, not having the physical property of the pure single fluid but physical properties most likely in between them. To further stipulate this notion, a pure fluid (Fluid 1) has a specific sonic velocity, if it is mixed with a different fluid (Fluid 2) of different sonic velocity, the resulting fluid will have a sonic velocity in between pure Fluid 1 and pure Fluid 2. This relation is theorized to be a linear one, if no chemical reaction occurs between the two fluids. Therefore, it is hypothesized that the resulting data will follow a linear trendline with the formula (Equation 1).

$$y(x) = kx + d \quad (1)$$

In Equation 1, 'k' is the slope of the trendline, and 'd' is the intersection on the y-axis. This equation can then be used to determine the degree of intermixing between two known fluids with unknown degree of intermixing. Even if the result of the feasibility study is not as expected, the ultrasonic capability to discriminate fluids is tested to reliably locate the fluid in the system.

3.2 Design of Experiment

A total of four pure fluids are used to test the initial theory. These four fluids are mixed at different known ratios. Each fluid sample is stored in 400 ml containers for safe transportation and long-term storage. In total, 19 fluids are tested. Each fluid is measured with a pressurized mud balance to determine the density in pounds per gallon (ppg). After mixing and determining the density, the sonic velocity is measured using ultrasonic sensors mounted on a container with known dimensions. Each measurement is taken three times and then an average sonic velocity is calculated. Furthermore, a steel insert is used to reduce the distance of the container to simulate the presence of steel pipe in a borehole.

3.2.1 Personal Protective Equipment

All the required personal protective equipment (PPE) will be used during the preparation of the fluids. This includes a lab coat and goggles to protect from spills and unwanted splashes while using the pressurized mud balance or the mixer, gloves while handling the additives and cleaning. All weighing of material was done under a fume hood to reduce the fine particle concentration in the air.

3.2.2 Required Equipment

The required equipment for this feasibility study is:

- Weighing scale to measure the additives weight.
- Pressurized mud balance
- Variable speed mixer
- Eighteen (18) 400 ml screw top plastic containers
- 1 Transportation/Storage Box
- 1 Test chamber (Acrylic cube)
- 1 carbon steel sheet metal with spacers attached to have a constant distance to the acrylic wall.
- 1 ultrasonic sensor
- 1 ultrasonic control/capture device
- 1 laptop for data acquisition and storage

3.2.3 Fluid Design

The four fluids used are:

Table 1: Fluid description feasibility study

Fluid Name	Fluid Number	Density Target [ppg]	Volume to Mix [ml]
Water	1	8,3	1400
K ₂ CO ₃ Brine	2	9	2400
Barite Mud 1	3	13	1400
Barite Mud 2	4	15	2400

Fluid 1 is tap water from the lab facilities. It will not be stored in a plastic bottle, but instead will be poured fresh whenever needed.

Fluid 2 is a potassium carbonate mud with the composition of 1 weight percent (wt %) laponite, 0,4 wt % bentonite and required concentration of K₂CO₃ to reach the desired density of 9 ppg.

Fluid 3 is a barite mud with the composition of 1,25 wt % laponite and required concentration of barite to reach 13 ppg.

Fluid 4 is another barite mud with a composition of 1,5 wt % laponite and required concentration of barite to reach 15 ppg.

Laponite, barite, bentonite and potassium carbonate were chosen because of their low environmental impact. Hence, they can be disposed in the lab and no concerns arise during the cleaning process of the equipment.

3.3 Test Preparation

To conduct the test, first a research and development (R&D) facility with all the necessary equipment for the study needs to be gathered. Close to the Montanuniversität Leoben a startup named Octogon opened shop, their focus is on custom made ultrasonic sensors. The R&D wing of this company was contacted and agreed to help with the feasibility study.

3.3.1 Fluid Preparation

All the necessary additives are calculated, weight and put into the mixer. A standard fluid mixing program was used. The additives were added within the first 15s of mixing at lower rotations per minute (RPM), followed by 60s of high RPM mixing.

Table 2: Feasibility study amount of additives

Additive	Fluid 2 - 9ppg K ₂ CO ₃ Mud	Fluid 3 - 13ppg Barite Mud	Fluid 4 - 15ppg Barite Mud
Water [g]	2392,8	1395,8	2392,8
Laponite [g]	23,93	17,45	35,89
K ₂ CO ₃ [g]	180,20	1267,88	3342,39
Bentonite [g]	9,57	0	0

Fluid 1 is pure water taken from the tap in the lab. The K₂CO₃ brine is mixed without any complications and the mud balance reading was close enough to the desired density. Bentonite was also added in addition to laponite. K₂CO₃ creates a brine with a high pH which tends to reduce the viscous property of laponite. Hence, bentonite is added to counter this anomaly.

During the preparation of barite muds, additional amount of barite is added to achieve acceptable densities. This is attributed to the lack of viscosifier in solution. It is also observed that barite tends to settle down right after mixing. Thus, a higher concentration of laponite or a different viscosifier would be better for future tests. After completing the pure fluids, mixtures at ratios 1:1, 1:2, 1:3, 2:1, 3:1, were blended, density determined with the pressurized mud balance and finally stored in plastic containers. The acquired densities can be seen in Table 3 and the fluids in their storage containers can be observed in Figure 4.

Table 3: Feasibility study-mixing ratios and measured densities

Fluid No.	Mixing Ratio	Measured Density [ppg]
1	1	8,3
2	1	8,85
3	1	13,1
4	1	14,7
1 and 2	1:1	8,6
	1:2	8,65
	1:3	8,7
	2:1	8,45
	3:1	8,4
2 and 4	1:1	11,6
	1:2	12,7
	1:3	13,2
	2:1	10,75
	3:1	11
3 and 4	1:1	13,7
	1:2	14,1
	1:3	14,3
	2:1	13,65
	3:1	13,55

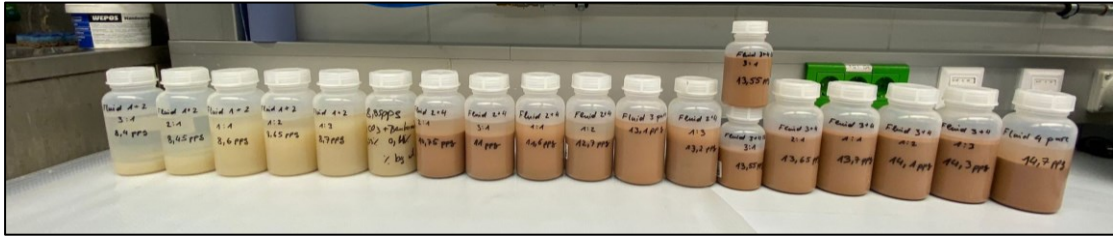


Figure 4: All mixed fluids for the feasibility study

3.4 Testing

All the required equipment was transported to Octogon, a local company specialized in ultrasonic sensor measurements, to perform the feasibility study. A schematic of the test setup is shown in Figure 5. The ultrasonic sensor used can emit at a frequency of up to 2,5 MHz and was powered between 50 and 60 V for the conducted experiments. This ultrasonic sensor can emit and receive the sonic pulses. To use such a sensor, a conventional oscilloscope can't be utilized, instead a special sender/receiver module is employed. Since, this module does not have its own software, Octogon provided a software to change the settings of the device. This specific setup will not be used in later experiments of this master thesis instead a two-sensor setup (one sender / one receiver) will be used. Still, the data acquired in the feasibility study should comply with the data gathered with this one sensor setup.

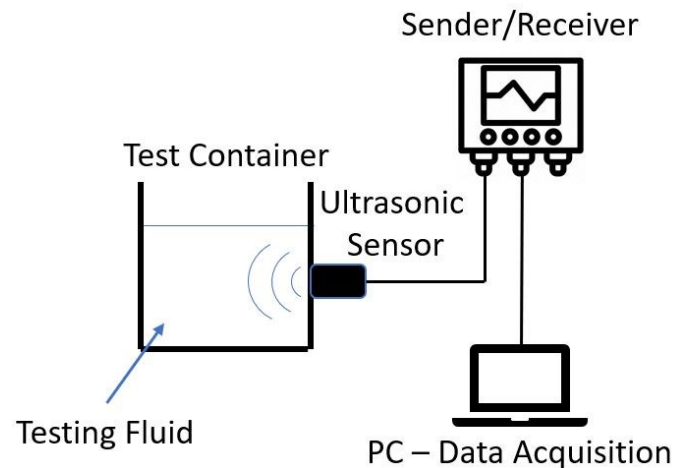


Figure 5: Schematic for feasibility study

The setup was first tested with water as a calibration fluid to determine the right frequency and power for the sensor. Figure 6 shows the data acquisition program and the used parameters for water. Note that the ultrasonic velocity here is halved because the ultrasonic wave needs to travel through the testing fluid is then reflected at the air/acrylic glass boundary and travels back through the testing medium. This two-way-travel time usually needs to be halved to acquire the required time for calculating the ultrasonic velocity, but by halving the setting this

step can be skipped. The ultrasonic velocity (v) is calculated using Equation 2, where ‘s’ is the distance between the sensor and the other side of the container, or the carbon steel plate and ‘t’ is the measured time.

$$v = \frac{s}{t} \quad (2)$$

The software developed by Octogon is intended to determine the wall thickness of steel samples. Therefore, the software has the capability to set a specific (known) sonic velocity and measure the distance between two points. Hence, there is another option to test if the result is correct. The reliability of the measurement can be tested after inserting the steel plate and the previously calculated sonic velocity. During the test, it was discovered that with denser testing fluid the energy of ultrasonic wave is attenuated resulting in no reflected signal being received. This issue is mitigated by inserting the carbon steel plate to reduce the signal travel-time.



Figure 6: Octogon inhouse software

3.4.1 Testing Procedure

The testing procedure to test the fluids is presented below.

1. The testing fluid is mixed using a variable speed mixer. The fluid density is measured using a pressurized mud balance. If the measured density is acceptable, the fluid is transferred into the storage container, otherwise additional additives need to be added.
2. After the fluid is transferred into the storage container, it is transported to the testing facility. The setup is prepared by connecting it with the computer, changing the

software settings to desired values, applying ultrasonic gel, and attaching the sensor to the test chamber.

3. The fluid is transferred into the test chamber and three measurements are conducted. An average velocity is calculated, and the data is stored in an online document for easy access at multiple locations.
4. After the test is done, the fluid is transferred back into the storage container and sealed.
5. The test chamber is cleaned using the tap water.
6. Repeat steps form 2-5, until all prepared fluids have been tested, all data is collected and stored.
7. Perform the analysis on the measured data to get the valuable insights.

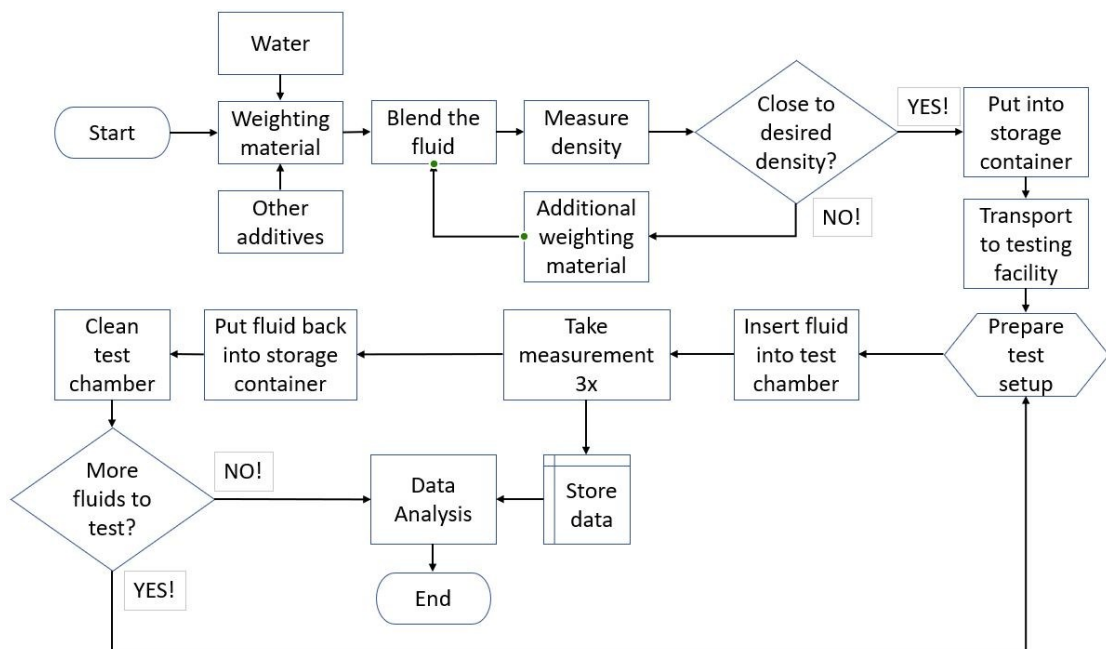


Figure 7: Flowchart for the feasibility study

3.5 Results

Table 4 shows the gathered results of the feasibility study. It confirms one of the initial theories partially. For instance, the average sonic velocity of pure Fluid-1 and Fluid-2 are 1490 m/s and 1571m/s, respectively. The mixtures of these fluids (1 and 2) have their sonic velocity in between those of the pure fluids. Furthermore, a trend can be observed that with increase in density the sonic velocity increases. The mixture of Fluid 2 and 4 supports the theory of sonic velocities being in between the two pure fluids, but they do not share the trend of increased velocity with increase in density. Instead, it is a reverse relation, the density increases and the sonic velocity decreases. This is attributed to the suspended weighting materials in the solution

that tends to absorb the ultrasonic wave, hence dampening the signal. Since, K_2CO_3 is dissolved in the water entirely this particular effect is negligible. However, with the increase density the same volume is occupied by more particles which allows for better transmission of the ultrasonic wave through the brine. This theory is further supported by the mixture of Fluid 3 and 4, where the observed signal responds was even further damped. The data acquisition for this combination was even harder due to this effect. Therefore, different frequencies and power were supplied to the sensor for gathering some data. Fluid 3 and 4 also have an outlier in this data set. The 2:1 combination has a sonic velocity of 1458,5 m/s which is above the sonic velocity of either pure fluid. The standing theory is that this is a human error in the measurement due to the posed difficulty stated earlier.

Table 4: Acquired data of the feasibility study.

Fluid	Mixing Ratio	Measured Density [ppg]	Average Sonic Velocity [m/s]
1	1	8,3	1490
2	1	8,85	1571
3	1	13,1	1452,2
4	1	14,7	1457,66
1 and 2	1:1	8,6	1529,84
	1:2	8,65	1545,44
	1:3	8,7	1560,58
	2:1	8,45	1525,3
	3:1	8,4	1512
2 and 4	1:1	11,6	1525
	1:2	12,7	1498,52
	1:3	13,2	1482,8
	2:1	10,75	1528,6
	3:1	11	1548,92
3 and 4	1:1	13,7	1456,46
	1:2	14,1	1454,42
	1:3	14,3	1453,4
	2:1	13,65	1458,5
	3:1	13,55	1456,46

Figure 8 shows that each fluid combination follows a trend, but it is clearly showing that each fluid combination has a different range of average sonic velocity response. Thus, it can be concluded that each fluid combination needs to be investigated separately to find a specific trendline. Figure 9 shows a clear trend with only a few outliers most likely to accuracy in the measurement. Further, the previously discussed trend of increased sonic velocity with increased density is clearly visible. For effective understanding, a linear trendline is inserted in the plot.

Figure 10 shows a clear trend with only one outlier, most likely to accuracy in the measurement. In this figure, the reverse trend with a decreased sonic velocity with increased density is clearly visible. This is due to the absorption of the sonic wave energy into the suspended weighting material (barite). For effective understanding, a linear trendline is inserted in the plot.

Figure 11 represents the data of the fluids with the highest density. Due to the difficulty of measuring such highly dense fluid the data is showing a lot of variations. It is also important to consider that the range of sonic velocity is approximately from 1450 m/s to 1460 m/s which represents only a small difference in sonic velocity. In Figure 11, the data is erratic thus the inserted linear trendline does not represent the data effectively.

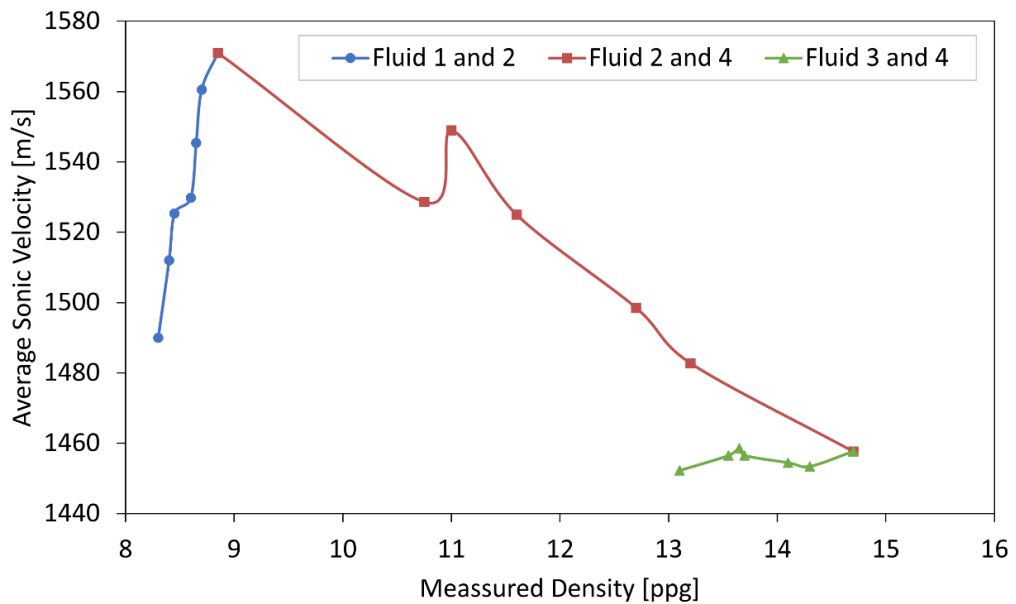


Figure 8: All feasibility data represented in one graph.

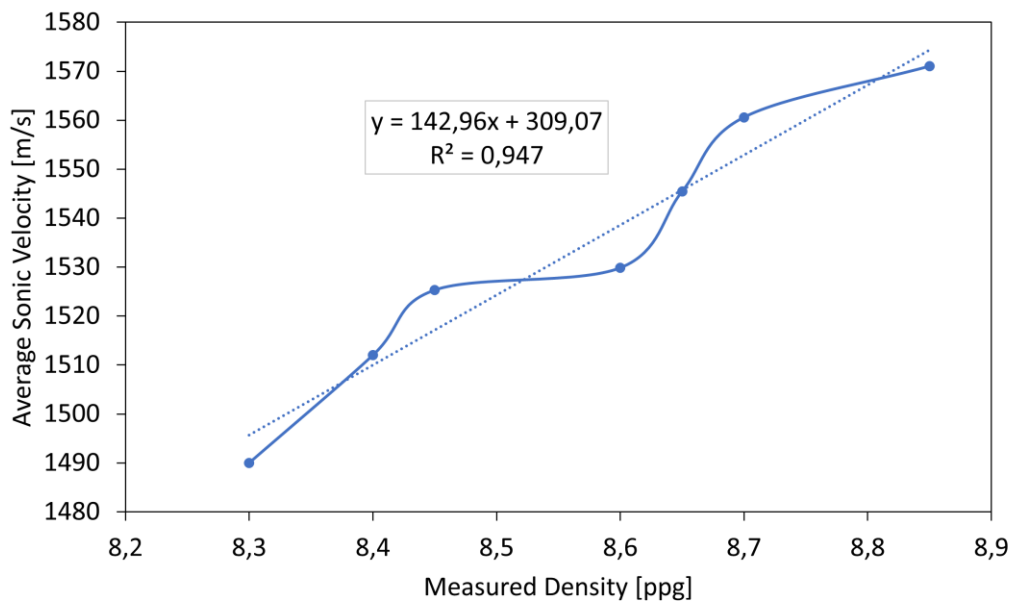


Figure 9: Average sonic velocity [m/s] with reference to measured density [ppg] of fluid 1 & 2

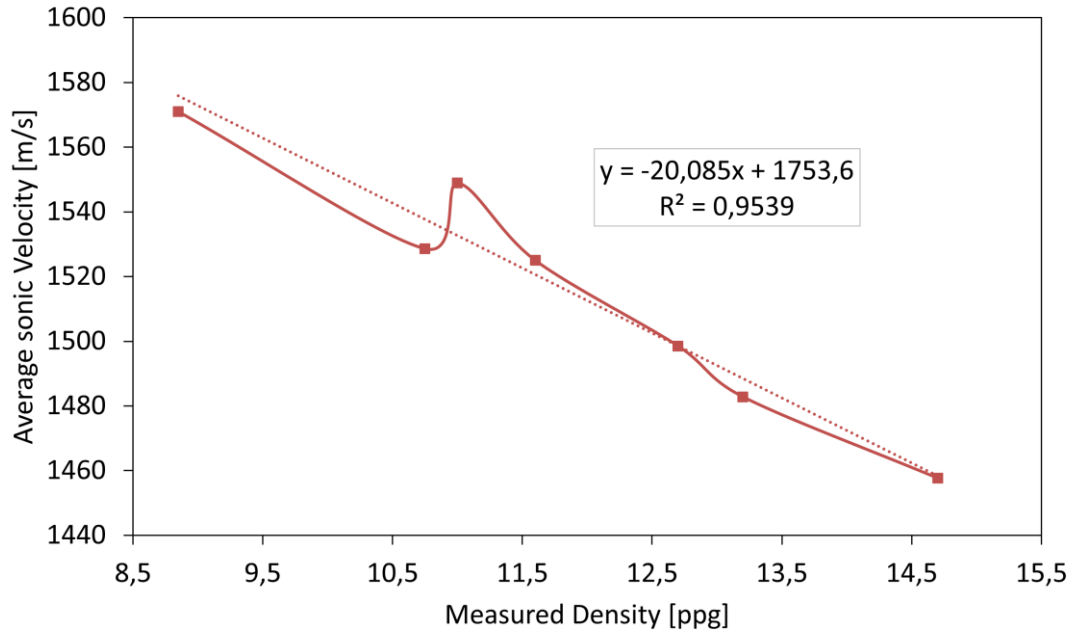


Figure 10: Average sonic velocity [m/s] with reference to measured density [ppg] of fluid 2 & 4

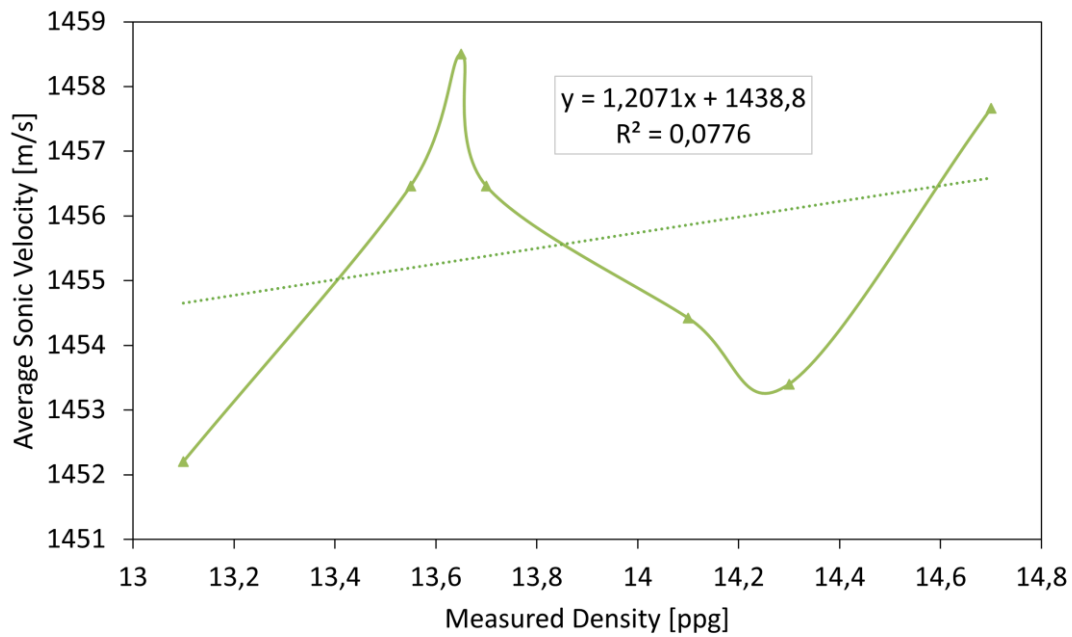


Figure 11: Average sonic velocity [m/s] with reference to measured density [ppg] of fluid 3 & 4

3.6 Summary Feasibility Study

The feasibility study was conducted and deemed successful. Fluid discrimination with ultrasonic sensors is possible, but the study uncovered new challenges and questions that need to be answered. For instance, only mixed fluids have been tested. What additive in said mixed fluid contributed to the change in sonic velocity. Another question that arose is the effect of gel strength development on the sonic velocity. Does the sonic velocity increase or decrease as a gel strength develops.

The feasibility study has also shown that when using barite, a lot of the energy of the transmitted wave is lost, thus rendering the measurement almost not feasible. It is important to find out the limitation of the measurement when conducting the next experiments.

The acquired testing procedure was deemed good and will be used and slightly adjusted in the next experiments.

The experiments were conducted with the assistance of ultrasonic specialists and high-end equipment. The acquired data from the ultrasonic sensors will be used for calibration of the inhouse ultrasonic setup to determine the error.

Chapter 4

Ultrasonic Experiments

4.1 Design of Experiment

The main goal for the ultrasonic experiments is to determine the ultrasonic velocity of commonly used additives in the oil and gas industry. This master thesis focuses mainly on additives used in water-based muds and spacers. A lot more information is already known and available for cements due to the common usage of ultrasonic compressive strength analysis in API 10B-2 and 10A testing procedures. Furthermore, the selected additives are readily available, and are not harmful to the environment and thus, can be disposed easily in the lab facilities. The experimental setup uses piezoelectric elements and follows the same principle employed by (Sven Curis 2022b). The primary difference between Curis study and mine is that he used the sensors on cured cement samples and the current study focuses primarily for testing on the Newtonian and non-Newtonian fluids. (Sven Curis 2022b; Paul Wagner 2020a)

4.1.1 Testing Methodology

Step 1: Construction of test set-up:

A test chamber is required to facilitate the testing fluid during the measurement. Therefore, the cube used during the feasibility study is being used. Additionally, a small test container is planned, manufactured and constructed to replace the carbon steel plate. The carbon steel plate will not work with this test setup, because of the application of two sensor setup. The ultrasonic wave travels through the fluid only once (with one sensor two-way travel time is measured) and is not reflected at the carbon steel plate to be captured again with the same sensor. Next the test setup is assembled following the same approach as (Sven Curis 2022b; Paul Wagner 2020a). An error determination is conducted after the test setup is built.

Step 2: Testing Fluid preparation:

A variety of fluids is tested in the described test setup. Therefore, an additive classification is introduced to better group the tested media. The classification is split in three groups namely “Viscosifier”, “Weighting Agent” and “Other Additives”. All these are mixed in water at different concentrations to create a baseline study. Once the baseline study is completed a combination of these additives will be mixed into a non-Newtonian testing fluid to study whether there is a possibility to discriminate these fluids.

Step 3: Experimental investigation:

To conduct the required experiments an oscilloscope (to capture the data), two piezoelectric elements (send and receive the ultrasonic signal) and rheological data is required. A non-Newtonian testing fluid will be poured into the testing chamber and the ultrasonic velocity will be determined by measuring the transit time of the ultrasonic wave through the medium. The time between the actuations of the first and second element can be captured by the oscilloscope. By applying Equation 2, the sonic velocity can be determined. If multiple fluids are used in a flowing system, the captured data can be used to discriminate between the displacing and displaced fluid. Furthermore, when the ultrasonic velocity of intermixed fluids is known the degree of intermixing can be determined as well.

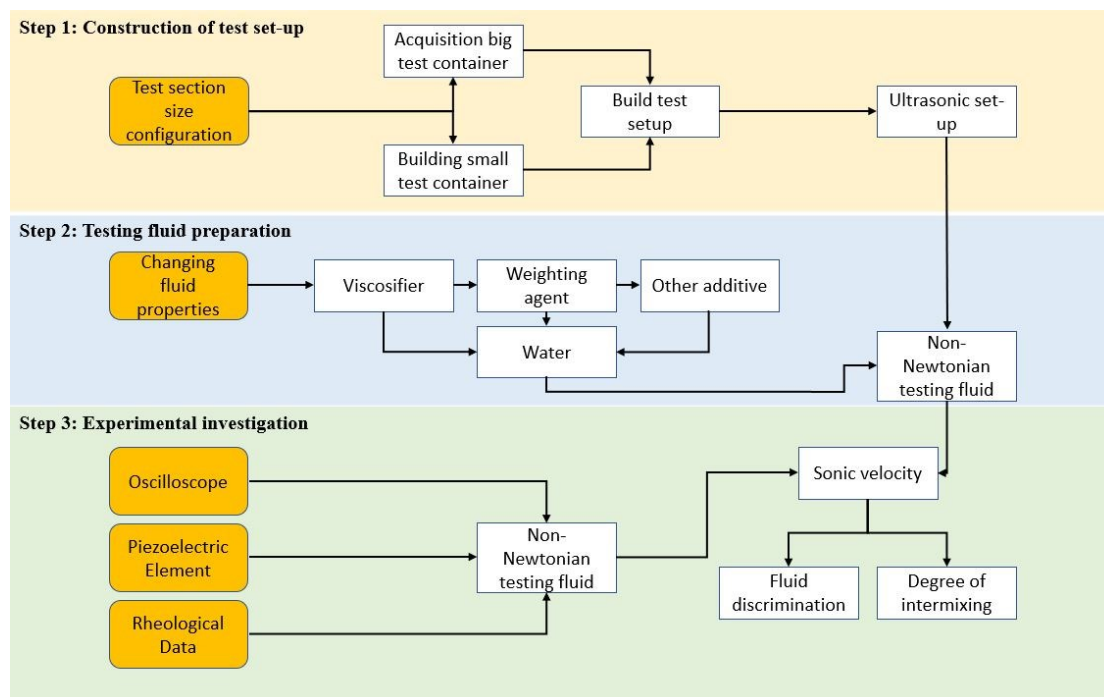


Figure 12: Testing methodology

4.1.2 Experimental Setup

The experimental setup for the current study is different from the one used during the feasibility study. In the current setup, two piezoelectric elements are used instead of using a single sensor (with sender and receiver). One element function as the emitter and the second one captures the ultrasonic wave and transfers it to the oscilloscope. The data acquisition software of the oscilloscope can then be used to determine the ultrasonic velocity.

4.1.2.1 New Small Testing Chamber

The carbon steel plate has been disregarded in reference to flow-loop project. Since two piezoelectric elements are used, a new testing container needs to be constructed. Therefore, acrylic glass of the same thickness from the bigger cube was used. The change in container size does not change the result of the sonic velocity since time and distance are proportional (Equation 2). The sonic velocity of the testing fluid is not affected by the change in container size. The benefit of the reduced container size is that the total absorbed power by the fluid is less over a shorter distance compared to the bigger container. The only negative aspect to this change is that it is more difficult to analyses the data owing to the increase in noise and shorter measuring time.

To construct the new test chamber following equipment was used permanent marker, Angle ruler, caliper, Dremel, disc grinder, heavy duty gloves, safety goggles, clamps, wooden board, acrylic glue, and thick needle. First the new test chamber was designed considering the distance of the new annular space in the flow-loop and the width of the piezoelectric elements. Figure 13 shows the length specifications for the cube. All measurements are given in milli meters (mm), and the wall thickness of each piece is 2,8 mm. Then a piece of acrylic glass was salvaged from an old acrylic cube. The five required pieces (one base plate, two wide walls and two slim walls) were then transferred onto the acrylic glass. It is advised to give enough extra material to allow for it to be ground to size and allowing for a square wall. After the pieces have been traced onto the acrylic glass the big acrylic sheet is placed onto a piece of relatively thin wood (~1,5cm) and clamps are used to secure acrylic sheet. The wood is used to not damage the work area and the wood can be replaced easily and cheaply. A Dremel is used to cut out the traced pieces. After the pieces are separated a disc grinder is used to grind them down to length. This is done over several phases over all sides of the work piece because each side of the wall needs to have a 90° angle to its neighboring walls. Next the walls are glued. Figure 14 shows the acrylic pieces before being glued. One wall after another is attached to the base plate with acrylic glue while attempting to maintain a right angle to the base plate. The acrylic glue can fill gaps, thus some mistakes during construction can be fixed easily. Last a needle is used to

put acrylic glue into all the edges of the cube to ensure proper sealing. After 24 hours of curing, the test chamber is ready to be used as you can see in Figure 15.

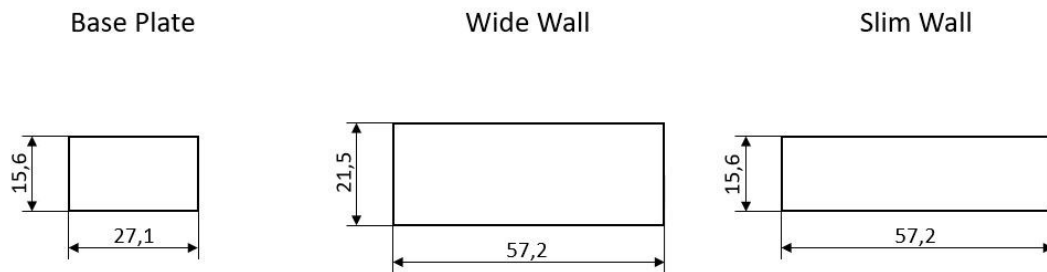


Figure 13: Measurement for each surface of the acrylic cube (in mm)

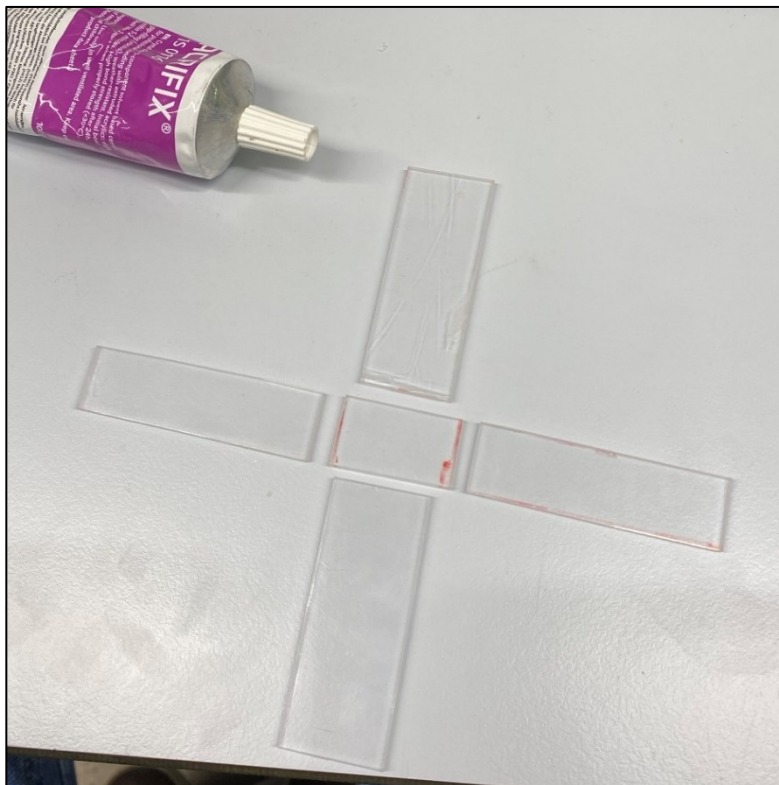


Figure 14: All pieces of the acrylic cube before assembling.



Figure 15: Finished acrylic cube.

4.1.2.2 Test Setup Schematic

Figure 16 shows the schematic for the experimental setup. Compared to the feasibility study more parts are required to run the experiments (given below).

The required equipment to run the experiments are:

- Function generator
- Amplifier
- 2x Piezoelectric elements - transmitter and receiver
- Oscilloscope
- Laptop for data acquisition
- Test chamber - big one for brines and other materials that the ultrasonic wave can pass through easily and small one for materials that absorb the ultrasonic wave.
- Ultrasonic gel

The function generator is built into the oscilloscope and can be setup with the PicoScope software after the oscilloscope is connected to the PC via a USB connection. The oscilloscope is connected to the amplifier. The function generated wave is sent into the amplifier to increase the voltage of the signal (original voltage of the oscilloscope is 1V or 2V). The amplifier is usually set to approximately 10V but has been adjusted in several experiments to receive a better ultrasonic signal. This change does not alter the received time between sender and receiver but changes the intensity of the signal. This allows for a better analysis of the denser fluids.

Both sender and receiver need to be attached to the test chamber. This can be done with zip-lock ties or any sticky tape. In the following experiments electrical tape was used. It does not possess a high degree of stickiness, but its capability to stretch made it possible to have a good downward force onto the sensors to ensure a good connection with the acrylic glass. Furthermore, an ultrasonic gel is placed between the piezoelectric elements and the acrylic glass. This allows the wave to be transmitted flawlessly from the element to the acrylic glass and finally into the testing medium.

Figure 17 shows the actual setup. The orange tape is the mentioned electrical tape and covers both piezoelectric elements. The cube shown in the picture is the big cube with an inside distance of 70,3 mm. The setup is connected as shown in Figure 16.

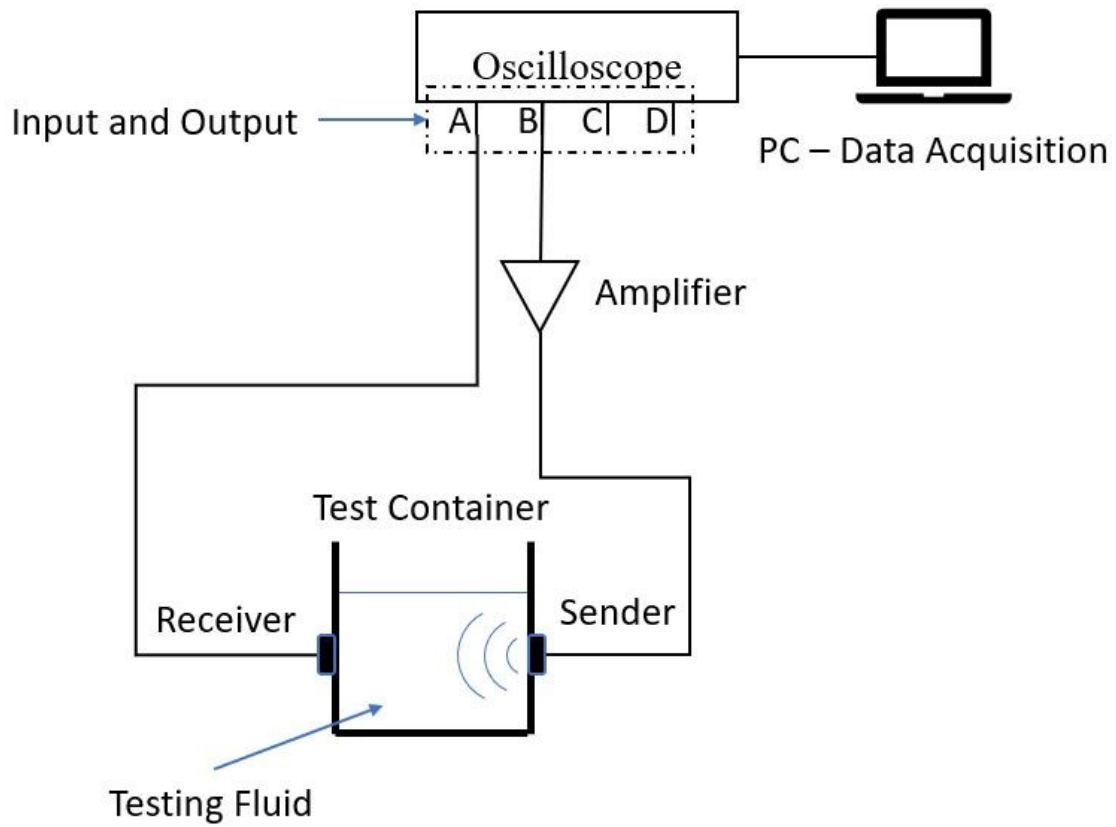


Figure 16: Schematic of the experimental setup

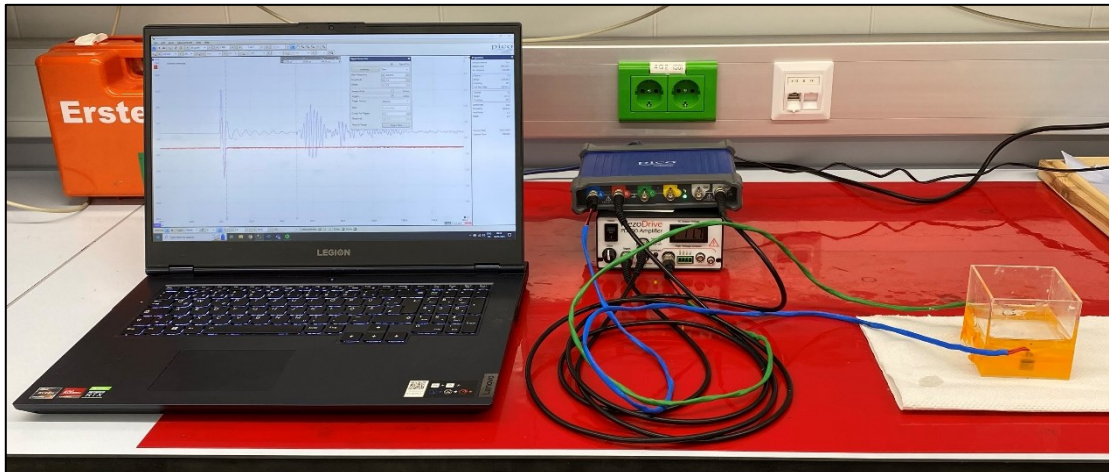


Figure 17: Custom-made ultrasonic test setup with big testing chamber

4.1.3 Fluid Classification

To specify which additives to choose, a classification system needs to be employed to better visualize and select the appropriate materials for the experiment. Therefore, the classification by the International Association of Drilling Contractors (IADC) was selected as such fluid additives can be classified in categories:

1. Alkalinity or pH control (lime, caustic soda, bicarbonate of soda, etc.)
2. Bactericides (paraformaldehyde, caustic soda, lime, starch, etc.)
3. Calcium removers (caustic soda, soda ash, bicarbonate of soda, etc.)
4. Corrosion inhibitors (hydrated lime, amine salts, etc.)
5. Defoamers (alcohol based defoamers, etc.)
6. Emulsifiers (modified lignosulfonates, etc.)
7. Filtrate/Fluid loss (bentonite, CMC, pregelatinized starch, etc.)
8. Foaming agents (nonionic surfactants and polymeric materials)
9. Lost Circulation Material (LCM) (cedar fiber, sawdust, drilling paper, magma fiber, etc.)
10. Extreme-pressure lubricants (graphite powder, soaps, etc.)
11. Shale control inhibitors (gypsum, sodium silicate, etc.)
12. Surfactants
13. Thinner and dispersants (various polyphosphates, lignitic materials)
14. Viscosifiers (bentonite, CMC, attapulgite clays, asbestos fibers, etc.)
15. Weighting materials (barite, lead compounds, iron oxide, etc.)

Table 5 shows all chosen additives. The orange marks in the table represents to which category the additives belong. The respective category description with a few examples can be found above the table. The additives were chosen based on the availability, their impact on the environment (environmentally friendly materials are easier to dispose) and to have a good coverage. The only categories that have not been filled are corrosion inhibitors (4), defoamers (5), emulsifiers (6), foaming agents (8), extreme pressure lubricants (10), surfactants (12) and thinner/dispersants (13). The other eight categories have been covered either with one or with multiple additives.

Table 5: Chosen materials and their categories

Additive Name / Category	1	2	3	4	5	6	7	8	9	10	11	12	13	14	15
Bentonite							■							■	
CMC							■		■					■	
Laponite							■							■	
Xanthan Gum							■		■					■	
PAC							■							■	
Flowzan							■							■	
Barite															■
Calcium Carbonate															■
Potassium Carbonate															■
Sodium Carbonate	■		■												■
Citric Acid	■	■													
Caustic Soda (NaOH)	■	■	■												
Gypsum											■				

(Manager 2017; Nabiyev; foaming_agent 2022; Manual 2021; Bisley International 2022; Xiong et al. 2019; Navarrete et al. 2000; eritia 2018)

4.1.3.1 Viscosifiers

Viscosifiers are used in the oil and gas industry to create a viscous fluid. Viscosity is defined as a fluid's internal resistance against flow. This is achieved by attraction and cohesion of nearby molecules in the fluid. It is of utmost importance during the drilling process to not only keep the drilled material suspended when pumps are turned off (also known as gel strength) but also to ensure proper hole cleaning. The properties measured in viscos fluids are apparent and plastic viscosity, yield point, and gel strength. All these parameters can be determined with an API standardized viscometer. (Manual 2020)

On a drill site additional measurement are taken in accordance with API standards, such as filtrate test, sand content, solids content, oil content, and water content (Manual 2022). These measurements are not of interest in this master thesis, thus none of them have been conducted. Gel strength develops over time and occurs due to inter-particle attraction and friction between suspended fine solids. There are three types of gel strength developments, high-flat, progressive, and low-flat. Where, high-flat and progressive are undesirable and low-flat is desirable. High-flat and low-flat shows consistent gel strength with time. Whereas progressive increases with time. It has a low 10 second gel strength but can develop a high gel strength over time. Low-flat gel strength has a low gel strength compared to the other two. It increases slightly over time but doesn't reach very high gel strengths. This type of gel strength is desired because it can keep solids suspended and doesn't require high pressure to break the gel strength. Too high pressures while breaking the gel can lead to wellbore damage which is undesirable.

The viscosifiers will be tested at different weight percent of water. In addition to the viscosity measurement, a gel strength test will be conducted after 10 seconds and 10 minutes of rest time. The rest time starts after the fluid has been agitate for at least 30 seconds at 600RPM. The sonic velocity will also be measured once the material is transferred into the testing container, after 10 seconds, and 10 minutes of rest time (Rig Worker 2022). Since no automated agitation is possible, a stir rod has been used to agitate the fluid vigorously before the time started. This measurement is conducted to see the influence of the gelling on the sonic transmit ability. Table 6 shows all the chosen wt % for each additive. The wt % were chosen according to the experience of lab workers at Montanuniversity Leoben.

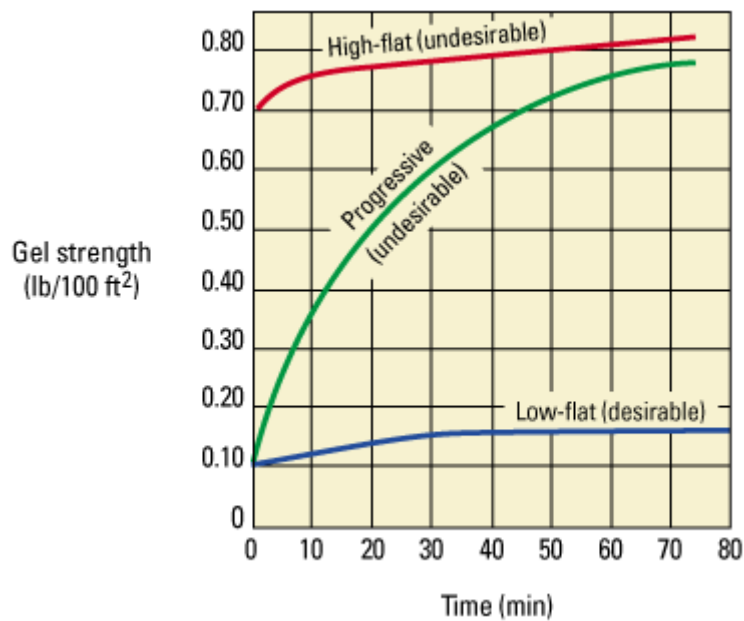


Figure 18: Types of gel strength in muds

Source: (SLB Glossary 2022)

Table 6: Selected viscosifiers with respective wt %

Additive Name	Weight Percent of Water		
	Bentonite	0,5	1
CMC	1	1,5	2
Laponite	0,5	1	1,5
Xanthan Gum	0,28	0,42	0,56
PAC	1	1,5	2

4.1.3.2 Weighting Materials

Weighting materials are used in the oil and gas industry to ensure proper density of drilling fluids. The required density for a section of drilled well can be determined with the mud weight window which considers the pore pressure and the fracture pressure of the formation. In

addition, a safety factor is applied to both values. This master thesis focuses on different weighting materials and how their sonic velocity changes with density. K_2CO_3 and sodium carbonate are forming brines, thus no solids need to be suspended to achieve the desired density. Barite and calcium carbonate are solids that need to be suspended to achieve the desired density. Therefore, laponite is used as a viscosifier because its impact on the sonic velocity is minimal. This viscosifier won't falsify the results of these weighting materials and the gathered sonic velocity can be corrected. For Barite a concentration of 1,5 wt % and 2 wt % of laponite is used for $CaCO_3$. Even though barite is heavier than $CaCO_3$ a higher percentage of laponite is required to suspend the $CaCO_3$. The $CaCO_3$ used in this experiment has a medium grain size compared to the barite's small grain size. Therefore, $CaCO_3$ grains did not stay in suspension when using laponite with only 1,5 wt % of water.

All the densities are measured with either a pressurized or atmospheric mud balance. Additionally, the volume and weight will be measured to calculate the density in SI Units, but only for the soluble weighting agents, because during testing it was discovered that the pressurized mud balance has a systematic error and needs to be recalibrated. This is also the reason why all other experiments used an atmospheric mud balance to determine the density of testing fluids. Table 7 shows the chosen weighting materials and the target density in ppg. K_2CO_3 and Na_2CO_3 have a lower target density because of their maximum solubility in water being 111,5 g/l (at 20°C) and 21,4 g/l (at 20°C) respectively. (Solubility Table of Compounds in Water at Temperature 2022)

Table 7: Selected weighting materials with target density

Additive Name	Target Density [ppg]						
Barite	9	10	11	12	13	14	15
Calcium Carbonate							
Potassium Carbonate	9	9,25	9,5	9,75	10	10,25	10,5
Sodium Carbonate	8,5	8,625	8,75	8,875	9	9,125	9,25

4.1.3.3 Other Additives

Other additives are those who are not classified in weighting material or viscosifier. In Table 8 all other additives with the respective wt % are listed.

Table 8: Chosen other additives with target wt % (eritia 2018).

Additive Name	Weight Percent of Water		
Citric Acid			
Caustic Soda	0,5	1	1,5
Gypsum			

The weight percent of water is based on the experience of lab workers at Montanuniversity Leoben and through online research.

The range of weight added to the tested fluid is 2,5 g (0,5 wt %) to 7,5 g (1,5 wt %). This amount of additive is not significant; thus, the density is not measured. All these additives do not develop any viscosity; thus, viscosity is not measured. The additives' effect on pH is measured using a waterproof pH-meter as seen in Figure 19. Furthermore, to ensure that the pH measurement is correct a pH-strip quick test (Figure 20) is conducted. It is less accurate, but it shows if the pH-meter is in the right pH range. It is not expected that the pH has an influence on the sonic velocity.



Figure 19: Waterproof pH-meter

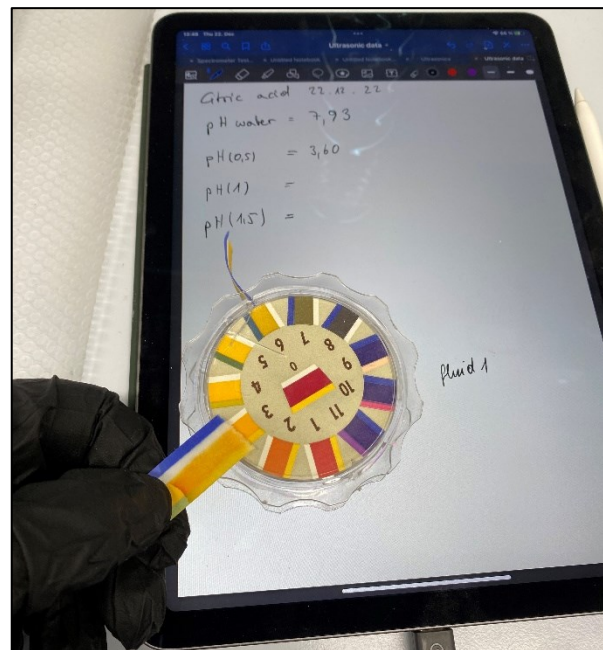


Figure 20: pH-strip quick test of fluid 1 at 0,5wt %

4.1.4 Personal Protective Equipment

All the required PPE is to be used during the preparation of the fluids. This includes a lab coat and goggles to protect from spills and unwanted splashes while using the pressurized mud balance or the mixer, and gloves while handling the additives and cleaning. All weighting of material was done under a fume hood to reduce the fine particle concentration in the air.

4.1.5 Testing Procedure

The testing procedure to test the fluids is presented below.

1. The testing fluid is mixed using variable speed mixer. When testing weighting agents, the fluid density is measured using a pressurized or atmospheric mud balance. When testing a viscosifier, a viscometer is used to capture the shear rate and shear stress.

2. If the measured density or viscosity readings are acceptable, the fluid is transported to the testing facility. The setup is prepared after it is connected to the workbench (computer), changing the software settings to desired values, applying ultrasonic gel, and attaching the sensor to the test chamber.
3. The fluid is transferred into the test chamber and three measurements are conducted. An average velocity is calculated, and the data is stored in an online document for easy access at multiple locations.
4. After the test is done the fluid is transferred back into the mixing container and the test setup is cleaned using tap water.
5. If not all tests for a weighting agent or viscosifier have been conducted, the fluid is transported back to the mixing area where additional water, weighting material or viscosifier is added to achieve the next fluid mixture.
6. Repeat step 2-5 until all prepared fluids have been tested, all data is collected and stored.
7. Perform the data analysis using the previously online stored data. Plots are created that visualize the relationship between density and measured sonic velocity.

When testing with viscosifiers, it is important to remove as many bubbles as possible after mixing to counter any discrepancies. The easiest solution is to pour the fluid from the mixing container into another container of sufficient volume. By repeating this process several times, the bubbles on the surface will pop. This will ensure a correct measurement of viscosity and density.

Figure 21 shows a flow-chart of the main testing procedure.

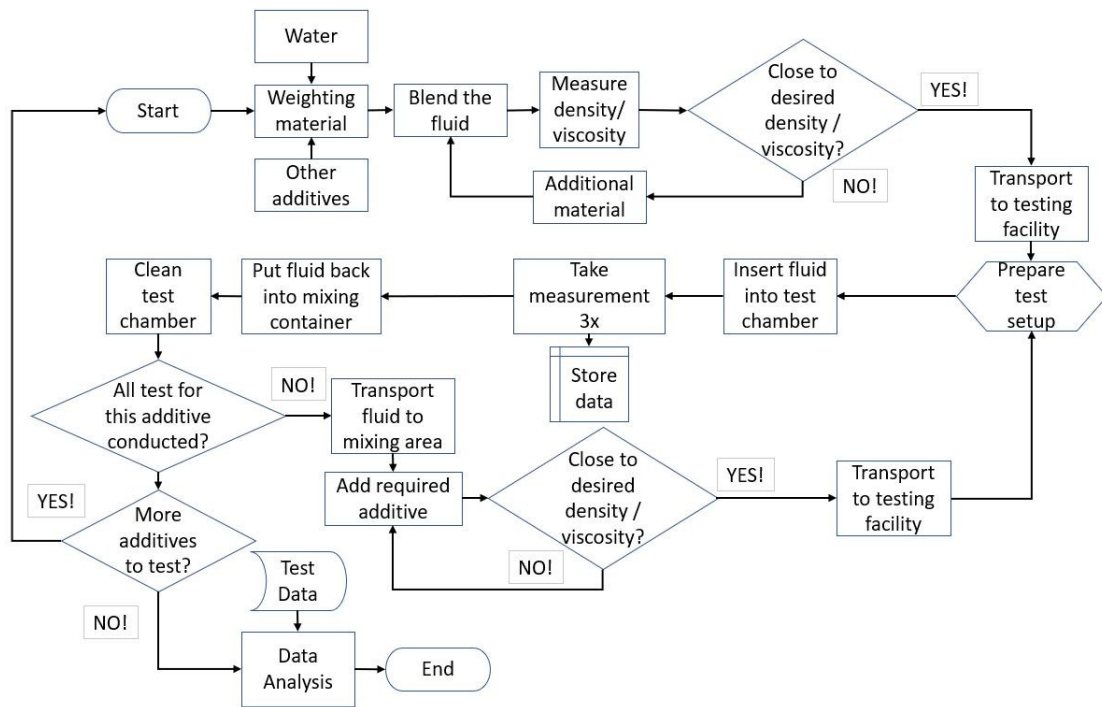


Figure 21: Testing procedure for main experiment

4.1.6 Proof of Concept Experiment

After the baseline is study is finished an understanding for each of the tested additives is established. To show how this method can be applied in the field a semi-dynamic test will be conducted. Therefore, a benchtop setup is used to displace one fluid (located in the test section) with another fluid of a different density. Both fluids are K_2CO_3 brines with the same amount of PAC to achieve some viscosity. Before the displacement test is conducted, the two pure fluids are prepared. Then mixtures with the ratios 1:1, 1:2, 1:3, 3:1 and 2:1 are prepared and tested on the ultrasonic test setup using the big testing chamber. For the pure fluids and the mixtures, the density is measured (atmospheric mud balance), an average ultrasonic velocity is determined and a relation to the degree of intermixing is made (linear trendline). Based on these data, an understanding of the baseline fluid is deduced and pave the pathway to conduct the semi-dynamic test. The experiment is considered semi-dynamic, because the intermixed samples are taken at the disposal line which is difficult to access. Therefore, the valve leading to the disposal line was opened and closed in between each sample. This resulted in an irregular fluid flow motion in the test section which is not comparable to a real-world scenario. Nevertheless, the main purpose of this experiment is to achieve random mixtures between the two pure fluids and to determine the degree of intermixing. A total of seven samples are taken one after another with volumes of at least 100 ml. The captured volume is too small to use a mud balance; hence, the volume and weight are measured to determine the density. The random mixtures are then

measured in the ultrasonic setup to determine the average sonic velocity of the liquid. The measured velocity can then be inserted into the Equation 1. By doing so the degree of intermixing can be determined. Furthermore, by plotting all data points and using predictive tools in excel it is possible to predict how much additional volume is required for full displacement. The conducted tests are:

- **Experiment 1:** Fluid 1 (lighter) is displaced by Fluid 2 (heavier) at low flowrate.
- **Experiment 2:** Fluid 1 is displaced by Fluid 2 at a higher flowrate.
- **Experiment 3:** Fluid 2 is displaced by Fluid 1 at similar flowrate to Experiment 2.

4.1.6.1 Benchtop Setup

The schematic design of the benchtop setup is shown in Figure 22. The setup can be split into two sections, namely Fluid Storage and Circulation System (1), and Testing Section (2). All tests run on the benchtop are in the laminar flow-regime.

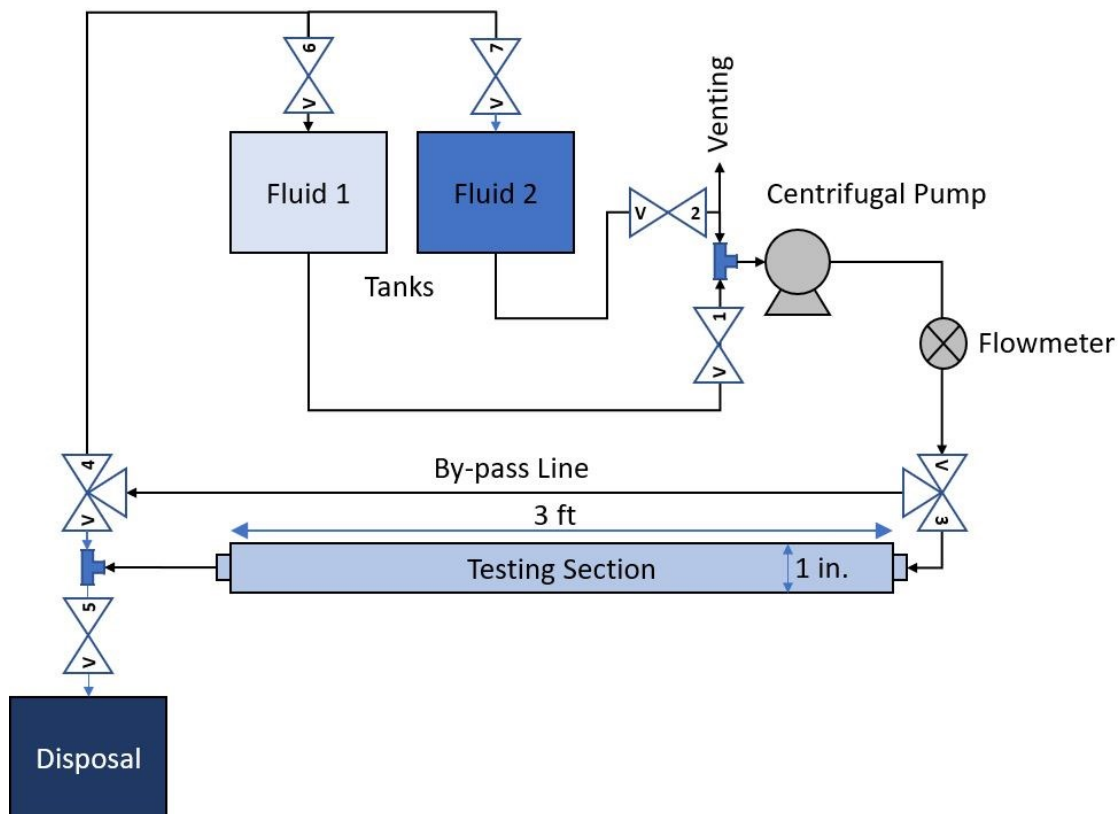


Figure 22: Schematic design of the benchtop experimental setup

- (1) **Fluid Storage and Circulation System:** This system is connecting all parts in the benchtop. It consists of a two fluid storage tanks and one disposal tank, multiple valves, a centrifugal pump, a flowmeter and a by-pass line. The centrifugal pump, with a flowrate range from 0,02 – 1,16 L/s (for water), is used to transport the testing fluids

from the storage tanks to the testing section. A flowmeter is installed in between the by-pass/testing section and the centrifugal pump to accurately measure the flowrate during an experiment. The by-pass line is parallel to the testing section and is used to fill the system with a different fluid without interfering with the fluid prepared in the testing section.

- (2) **Testing Section:** A horizontal acrylic transparent pipe of 3 ft long and 1-inch diameter is the testing section of the setup which is simulating flow through a pipe.

4.2 Setup Error Determination

The test setup has been built in the lab facilities of the Department of Petroleum Engineering. To determine its validity, it is compared to the feasibility study, an error determination has been conducted to ensure accurate measurements. Therefore, the fluid samples, which had been stored in sealed containers (during the feasibility study) are used to compare their previously determined sonic velocity with the inhouse captured sonic velocity. Every fluid will be tested and compared to the original result. This error determination is done once for the big testing chamber and once for the small one. Both testing chambers used water and fluids of varying density range. For the big cube, the density range is 8,4 ppg to 10,75 ppg and for the small cube the range is 11 ppg to 14,7 ppg. This step is taken to ensure accurate measurements of the denser fluids, since it has been observed that denser fluids tend to reduce the intensity of the signal, thus making it more difficult to evaluate the measurement. Three measurements have been taken and an average has been calculated. Equation 3 is used to determine the error between the inhouse average velocity and external average velocity:

$$Error = \frac{\overline{v_{internal}} - \overline{v_{external}}}{\overline{v_{internal}}} \quad (3)$$

As seen in Table 9 the error ranges from -0,63 % to 0,09 % averaging at -0,22 % and from -1,05 % to 0,71 % averaging at 0,27% for the big testing chamber and small testing chamber respectively. This range has been deemed appropriate hence the test setup can be used to determine the sonic velocity.

Table 9: Error determination - comparison external and local data

Actual Density [ppg]	Sonic Velocity External [m/s]	Average Sonic Velocity Local [m/s]	Error	Note
8,3	1490	1489,05	-0,06%	big testing chamber
8,3	1490	1491,29	0,09%	small testing chamber
8,4	1512	1502,45	-0,63%	big testing chamber
8,45	1525,3	1515,92	-0,61%	big testing chamber
8,6	1529,84	1529,49	-0,02%	big testing chamber
8,65	1545,44	1544,75	-0,04%	big testing chamber
8,7	1560,58	1553,93	-0,43%	big testing chamber
8,85	1571	1571,10	0,01%	big testing chamber
10,75	1528,6	1529,47	0,06%	big testing chamber
11	1548,92	1563,59	0,95%	small testing chamber
11,6	1525	1522,10	-0,19%	small testing chamber
12,7	1498,52	1482,81	-1,05%	small testing chamber
13,1	1452,2	1464,44	0,84%	small testing chamber
13,2	1482,8	1483,04	0,02%	small testing chamber
13,55	1456,46	1457,78	0,09%	small testing chamber
13,65	1458,5	1463,76	0,36%	small testing chamber
13,7	1456,46	1465,76	0,64%	small testing chamber
14,1	1454,42	1461,77	0,51%	small testing chamber
14,3	1453,4	1463,76	0,71%	small testing chamber
14,7	1457,66	1461,77	0,28%	small testing chamber

4.3 Experimental Preparation and Investigation

All samples were mixed with a starting volume of 500 ml water with the recommended practice of API 13B-1. Testing fluids are prepared as per their classification (mentioned below) based on to the primary materials used to prepare these fluids.

4.3.1 Viscosifier

The viscosifiers are mixed according to the concentrations presented in Table 6. First the lowest concentration is tested and then additional viscosifier is added. This will reduce the amount of additive required to perform all tests. The testing fluid tends to have high bubble concentration when mixed with Xanthan Gum and Flowzan. To reduce the concentration of these bubbles, multiple transfers between two containers are carried out.

For Xanthan Gum it was observed that a substantial amount of liquid is adhered to the wall of the mixing container. Therefore, the next higher concentration did not contain the initial 500ml of water. For very viscous fluids, it is recommended to mix every concentration from scratch to ensure more accurate results.

4.3.2 Weighting Material

The weighting material is distinguished between two types, insoluble and soluble weighting agents. Materials that can be dissolved into a water-based solution are defined as soluble weighting agents such as K_2CO_3 or Na_2CO_3 . Insoluble weighting agents are for instance barite or $CaCO_3$.

To determine how much weighting agents needs to be added to achieve the desired density, Equation 4 is used.

$$V_{additive} = \frac{V_{water} * (\rho_{target} - \rho_{water})}{\rho_{additive} - \rho_{target}} \quad (4)$$

Where ρ_{target} the density (kg/m^3) of the desired fluid, ρ_{water} and $\rho_{additive}$ the density of water and the tested additive respectively, and V_{water} is the water volume (m^3). To convert the calculated volume into a weight it is divided by the density of the weighting agent (Equation 5).

$$m_{additive} = \frac{V_{additive}}{\rho_{additive}} \quad (5)$$

4.3.2.1 Insoluble Weighting Agents

Before mixing any of the insoluble weighting agents a surplus of viscous fluid is mixed using laponite as stipulated in the DOE. The mixed laponite is then left to sit idle for around 10 minutes to ensure good hydration to fully develop its viscous properties. This fluid is then not only used to mix the weighted fluid but also to reduce the density if needed. This will ensure that the testing fluids keeps its viscous properties to suspend the weighting agent.

The required mass of each weighting material is determined using Equation 3 and 4, is measured and prepared. Then a mud mixer is used to mix the premixed viscous fluid with the weighting agent. The density is determined using an atmospheric mud balance. If the density is satisfactory the ultrasonic measurement can be taken, otherwise additional weighting agent is added to increase the density or additional viscous base fluid is added to reduce it. To reduce the required amount of additive used for experiments using the same weighting agent, the lowest density is mixed first and then the density is increased by adding additional weighting material.

4.3.2.2 Soluble Weighting Agents

Equation 4 and 5 does not consider the increase in volume due to the added weighting material. Therefore, after adding the weighting material the volume was precisely measured using a graduated cylinder with an accuracy of ± 1 ml and the weight was also captured using a digital

scale with an accuracy of $\pm 0,01$ g. A formula was derived to calculate how much water or additive is required to reach the desired density. By applying a data analysis in Excel, the required volume is automatically calculated.

The initial density ρ_1 and the density of the next fluid ρ_2 can be described with Equation 6 and Equation 7. In Equation 6 the variables m_1 (kg) and V_1 (m^3) are the measured mass and the measured volume of the initial fluid.

$$\rho_1 = \frac{m_1}{V_1} \quad (6) \quad \rho_2 = \frac{m_2}{V_2} \quad (7)$$

In Equation 7 m_2 and V_2 can be expressed using Equation 8 and Equation 9. Equation 8 shows that the mass after mixing (m_2) is described as the initial mass (m_1) added to the mass of the added additive (Δm). Equation 9 shows that the volume after mixing (V_2) is described as the initial volume (V_1) added to the volume the added additive occupies (ΔV).

$$m_2 = m_1 + \Delta m \quad (8) \quad V_2 = V_1 + \Delta V \quad (9)$$

Equation 6 can be rewritten to accommodate the change in mass and volume. This equation can then be further changes to represent Equation 10.

$$\Delta V = \frac{\Delta m}{\rho_{additive}} \quad (10)$$

By inserting Equation 8, 9 and 10 into Equation 7 the resulting Equation 11 is formed.

$$\rho_2 = \frac{m_1 + \Delta m}{V_1 + \frac{\Delta m}{\rho_{additive}}} \quad (11)$$

Equation 12 represents the multiplication of the denominator in Equation 11.

$$\rho_2 * V_1 + \frac{\rho_2 * \Delta m}{\rho_{additive}} = m_1 + \Delta m \quad (12)$$

Equation 13 is a complimentary equation to show that all Δm are brought to one side of the equation:

$$\rho_2 * V_1 - m_1 = \Delta m * \left(1 - \frac{\rho_2}{\rho_{additive}}\right) \quad (13)$$

Equation 14 is the final equation of the derivation and shows how the additional weight can be calculated using the measured mass and volume, the density of the additive and the known desired density.

$$\Delta m = \frac{\rho_2 * V_1 - m_1}{1 - \frac{\rho_2}{\rho_{additive}}} \quad (14)$$

If the current density is insufficient more weighting material can be added, thus $\rho_{additive} = \rho_{weighting\ material}$, but if the density needs to be reduced $\rho_{additive} = \rho_{water}$.

To reduce the amount of additive that is required to run all the tests, the highest density is mixed first and water has been added to the fluid to reduce the density to the next target density. The achieved densities can be seen in Table 30 and Table 31. Only the density converted to ppg is included in those tables. The weight and volume of the test fluid has been tracked in SI-Units. The density was calculated ($\rho = \frac{m}{v}$) and then using a conversion factor of $1\text{ppg} = 119,83\text{ kg/m}^3$. During testing a discrepancy between the mud balance data and the converted value is discovered. It has been confirmed that the pressurized mud balance has a systematic error therefore, it was decided to use the converted density for analysis.

4.3.3 Other Additives

The other additives are mixed according to the concentrations presented in Table 8. First the lowest concentration is tested, and then additional additive is added. This will reduce the amount of additive required to perform all tests. During mixing it was observed that gypsum settles down at higher concentrations. Therefore, it is recommended to add some viscosifier (for instance laponite) to ensure a more accurate measurement.

4.3.4 Software Settings

The software used is PicoScope 6. To achieve a consistently good result the following base settings are used. The subsequent section can only be followed if the setup is connected as suggested in Figure 16 (Pico 2020).

Capture Setup Toolbar:

The capture setup toolbar controls the time/frequency-related settings of the oscilloscope.

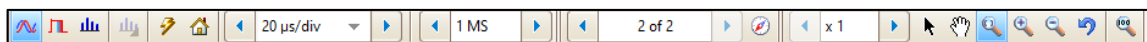


Figure 23: Capture setup toolbar

- All measurements are conducted using the scope mode.
- The collection time is set to 20 μm/div. (changing this value will stretch or shrink the signal in the X-Axis)
- The number of samples is kept at the standard value of 1 MS.

Channel Controls:

The channel controls allow adjustments to each input channel.

- Channel A and Channel B are activated all other channels are turned off.

- Channel A input range is set to ± 100 mV (changing this value will stretch or shrink the signal in the Y-Axis)
- Advanced settings of Channel A (opened by clicking the A next to input range)
 - Active lowpass filter and set to 400 kHz.
 - Set Axis Scaling Scale to 4 (changing this value will stretch or shrink the captured signal)
 - The lightning bolt next to DC Offset can be clicked but due to interference* from surrounding electrical devices and the fact that the collection time is so short the effect from this setting is minimal.
- Channel B input range is set to “Auto” and the advanced settings are kept at standard settings.

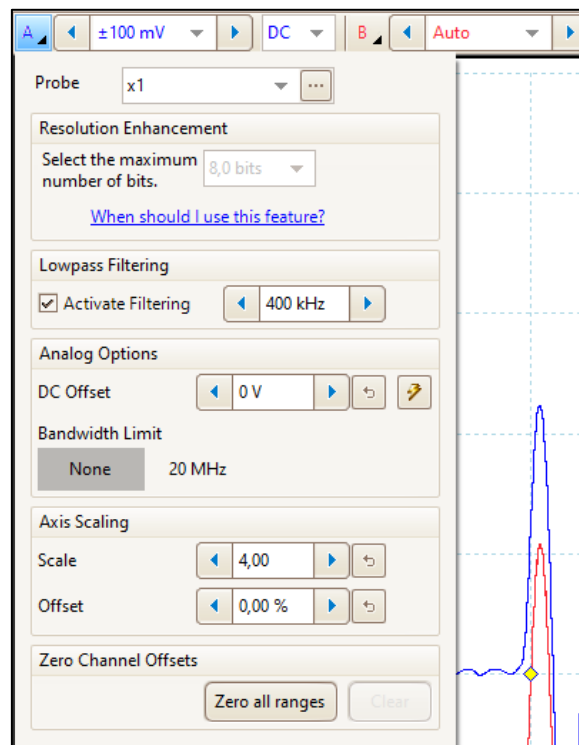


Figure 24: channel controls

*It was observed and calculated that the resulting interference is from the surrounding equipment and is precisely 50 Hz which conforms with the frequency of the Austrian power grid (APG Netzfrequenz 2023). It is recommended to run the tests in a room with only a small number of electrical devices to reduce this effect.

Signal Generator:

The signal generator allows for a signal to be generated. It is important to note that not all PicoScopes can use this function.

- Set the wave type to Sine to generate a sine curve.
- Set Start Frequency to 200 kHz (changing this value will widen or tighten the generated wave).
- Amplitude can either be set to 1 V or 2 V it does not change the result.
- Tick the box at Triggers and set the Trigger Source to Manual.

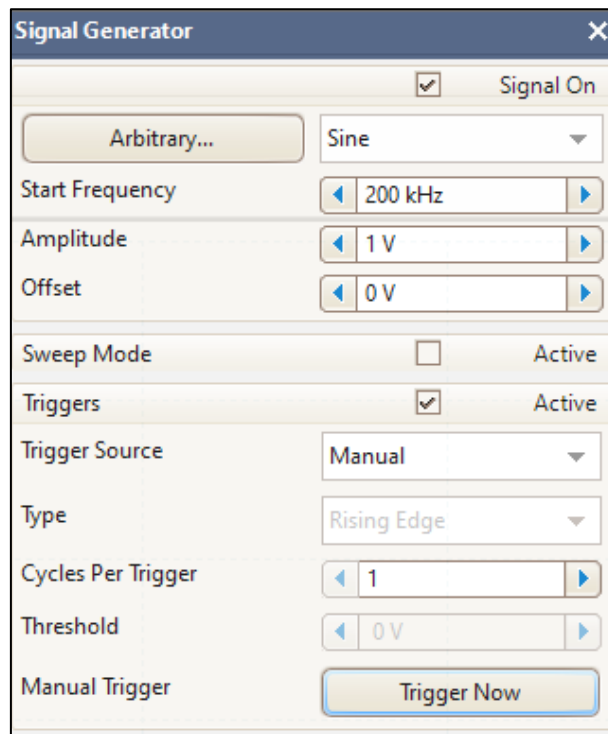


Figure 25: Signal generator settings

Trigger Controls:

The trigger controls tell the PicoScope when to start capturing.

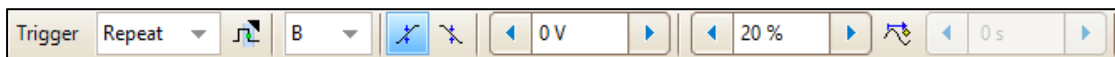


Figure 26: Trigger control settings

- Set the trigger mode to Repeat – when clicking the “Trigger Now” button seen in Figure 25 the signal will keep running in the background thus clicking the button again will instantly capture the next measurement.
- Set the trigger channel to B
- Set trigger to rising edge.

- Set threshold to 0 V – If the data is not captured properly this value can be changed to maybe get it working again.
- Set the pre-trigger to 20%. (Changing this value will change the amount of data captured before the “Trigger Now” button was pressed.)

These settings are further adjusted for each additive and fluid tested to ensure a good signal. Not every change in the settings will be noted in this master thesis.

4.3.5 Preparation and Investigation: Proof of Concept Experiment

Two K_2CO_3 brines (9ppg and 10ppg) with 1,5 wt % PAC are mixed. Therefore, the additives are calculated and mixed in batches of 7-liter and 4-liter totaling in 11 liters for each fluid. It is recommended to first add the K_2CO_3 to the water and let it stir for several minutes until everything is dissolved. Not all water is used in this process. Two (2) liters (for the 7-liter batch) and 1 liter (for the 4-liter batch) are set aside to premix the viscosifier. While the K_2CO_3 is dissolving a highly concentrated PAC mixture is prepared. Once the weighting material is fully dissolved, the concentrated PAC mixture is added to the batch. Furthermore, the 9 ppg fluid is dyed using blue food grade dye. If the K_2CO_3 and the PAC are added at the same time a viscous layer will form on top of the fluid. While the K_2CO_3 is dissolving bubbles form which are also captured in that layer as seen in Figure 27. An atmospheric mud balance is used to confirm that the density is close to the desired value. Furthermore, the viscosity of the pure fluids is also measured using a viscometer to confirm that they are pumpable by the centrifugal pump of the benchtop setup. Once the batches are mixed, mixtures of different ratios are prepared. First the density is measured and then they are analyzed using the ultrasonic test setup to determine the average sonic velocity. The mixing ratio, volumes and the measured density is shown in Table 10. Zero percent (0 %) intermixing is representing pure Fluid 1 and 100 % intermixing represents pure Fluid 2. The degree of intermixing is determined using Equation 15.

$$\text{Degree of Intermixing} = \frac{V_2}{V_1 + V_2} \quad (15)$$

The mixtures can be disposed after the average ultrasonic velocity is determined for the fluids. The pure fluids are then transferred into the storage containers of the benchtop. For Experiment 1 the test section is prefilled with Fluid 1. Then, the test section is closed off and the by-pass is used to fill the system with fluid 2. The pump is set to the lowest possible flowrate which corresponds to 0,07 L/s. The pump speed for Experiment 2 and 3 are set to medium flowrate which corresponds to a flowrate of 0,16 L/s. The valve connecting the by-pass and the test section is turned to let Fluid 2 pass through the test section. The valve at the disposal line is opened and the fluid is captured in 100ml containers. For Experiment 3 the fluid order is

reversed. The captured fluids of Experiment 2 and Experiment 3 can be seen in Figure 28 and Figure 29 respectively. The Volume and mass of the captured fluid is measured, and the density is calculated using Equation 16.

$$\rho = \frac{m}{V} \tag{16}$$

Where, ρ is the density of the captured fluid, m is the measured mass and V the measured volume. The uncertainty of the used scale is $\pm 0,01$ g and of the graduated cylinder ± 1 ml. After the density is determined, the fluid is transferred to the ultrasonic test setup where the fluid is poured into the big testing chamber. Three ultrasonic measurements are taken and an average sonic velocity is calculated. The degree of intermixing and the density can be determined using the Equation 1 and the coefficients of the initial intermixed study. The theoretical volume required to achieve full displacement can also be determined using Excel.

Table 10: Mixing Ratios and Corresponding Measured Density

Ratio	Degree of Intermixing	V1 [ml]	V2 [ml]	Measured Density [ppg]
1:0	0,00%	300	0	9,15
1:1	50,00%	150	150	9,7
1:2	66,67%	100	200	9,85
1:3	75,00%	75	225	9,9
3:1	25,00%	225	75	9,5
2:1	33,33%	200	100	9,55
0:1	100,00%	0	300	10,1



Figure 27: 10ppg K_2CO_3 mud viscous separation with bubbles captured in it.



Figure 28: Fluid 1 displaced by Fluid 2 at medium flowrate.



Figure 29: Fluid 2 displaced by Fluid 1 at medium flowrate.

Chapter 5

Results and Discussion

5.1 Experimental Results

This section of the master thesis will present the gathered results of the static and semi-dynamic fluid tests. To capture, the results the ‘Ruler’ tool in the PicoScope 6 software is used. Initially the two squares appear in the bottom left corner of the diagram. One of the squares is pulled towards the end of the emitted signal (red line). The second square is dragged to the end of the “silent phase” (area where the ultrasonic wave transmits through the testing medium). The difference in time is then displayed in the top. An example is shown in Figure 30 where the measured time difference is 46,72 μs .

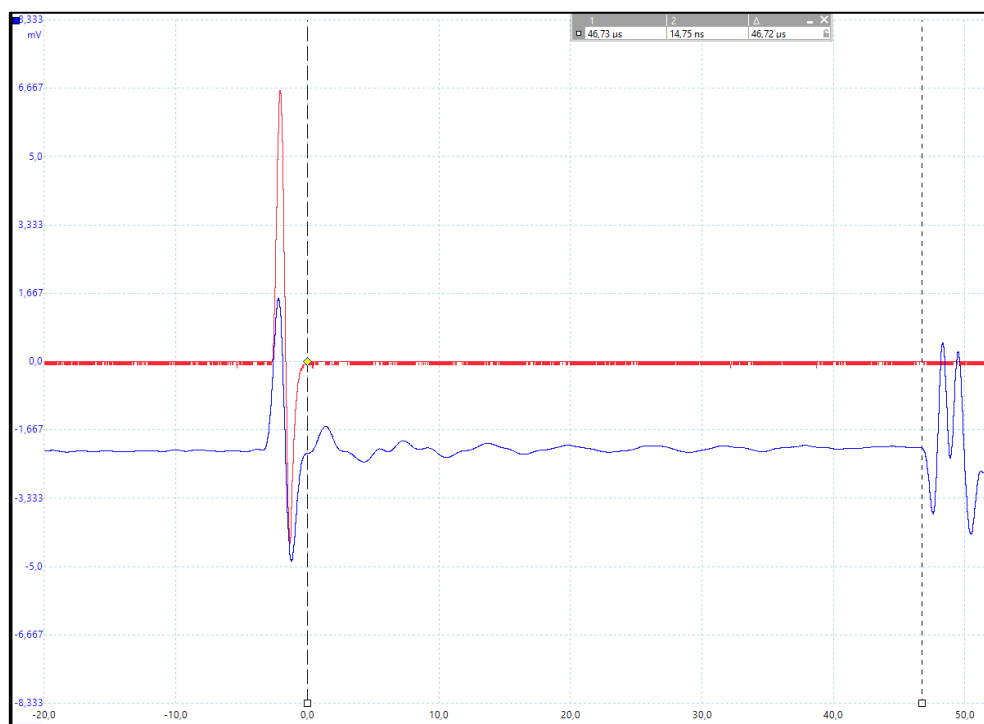


Figure 30: Ultrasonic signal - water 2nd measurement

5.1.1 Viscosifier

All viscosities are captured using a Chandler Viscometer. First the shear rate in RPM is increased and the shear stress is captured. Afterwards the viscometer is turned off for a couple of seconds and the procedure is repeated from high to low RPM. Finally, a shear stress average is calculated. The collected data is transferred into a regression analysis software (RAS) fluid library where the best fluid model is fit to the results and plastic viscosity and yield point are displayed. A minimum of four viscometer readings are required to get a confident result. Some fluids have data outliers thus they been removed to increase the accuracy of the prediction program.

The RAS uses various fluid models to determine the plastic viscosity and the yield point. Equation 17 shows the general Herschel Bulkley (GHB) model which is similar to the Herschel Bulkley (HB) model (Equation 18), but a reference shear rate has been introduced.

$$\left(\frac{\tau}{\tau_{ref}}\right)^m = \left(\frac{\tau_0}{\tau_{ref}}\right)^m + \left(\frac{\mu_\infty * \gamma}{\tau_{ref}}\right)^n \quad (17)$$

$$\tau = \tau_0 + \mu_\infty * \gamma^n \quad (18)$$

In Equation 17 τ is the shear stress, γ is the shear rate, τ_0 is the fluid stress (i.e. shear stress at near-zero shear rate), μ_∞ is the finite high shear limiting viscosity, m is the variable shear stress exponent in GHB rheological model, n is a variable shear rate exponent, and τ_{ref} is a reference that equals 47,88 Pa = 1 lb/ft². Equation 19 shows the equation used to calculate a Power Law fluid.

$$\tau = \mu_\infty * \gamma^n \quad (19)$$

Equation 20 shows the equation used to calculate a Bingham fluid.

$$\tau = \tau_0 + \mu_\infty * \gamma \quad (20)$$

5.1.1.1 Polyanionic Cellulose (PAC)

Viscosity Data:

This fluid is best described using the Bingham model, according to the RAS fluid analysis.

Table 11: PAC - plastic viscosity and yield point

	PAC 1%	PAC 1,5%	PAC 2%
Plastic Viscosity [cp]	11,97	27,09	52,13
Yield point [lbf/100ft ²]	0,01	0,01	0,01

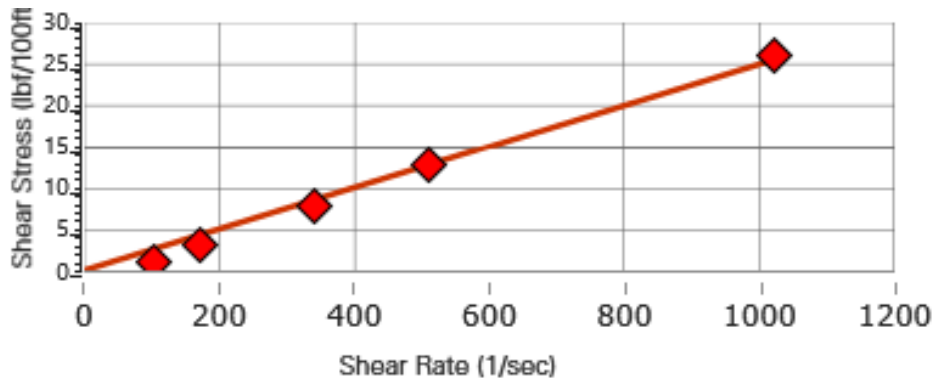


Figure 31: PAC 1% RAS analysis

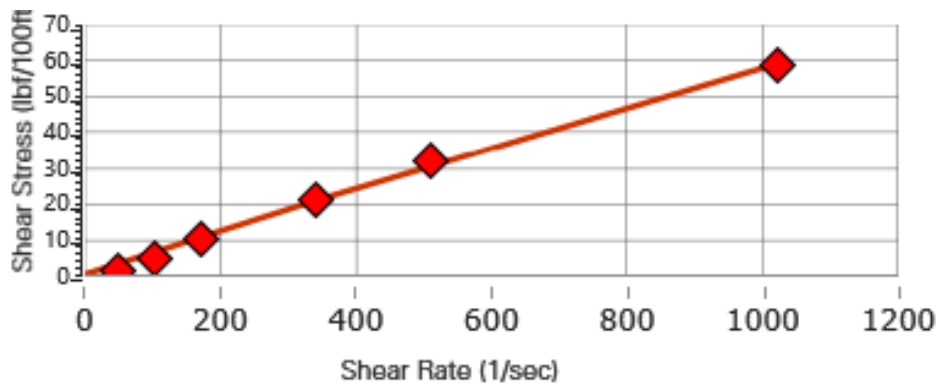


Figure 33: PAC 1,5% RAS analysis

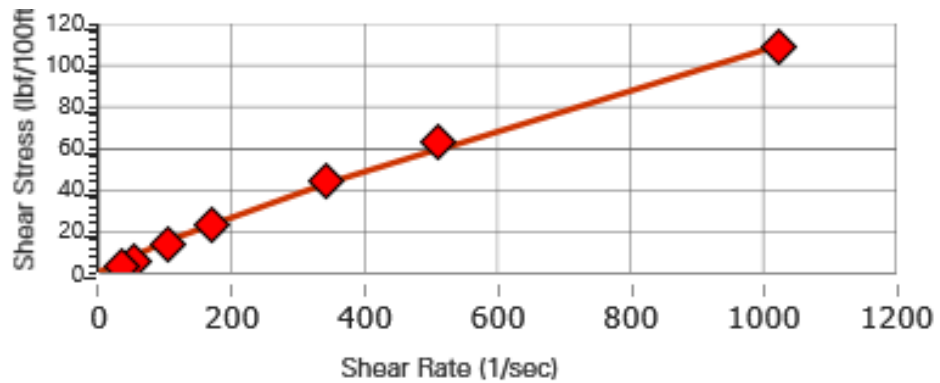


Figure 32: PAC 2% RAS analysis

Plastic Viscosity – Average Sonic Velocity Comparison:

The color scheme used in Table 12 represents the corresponding data in the figures below. Figure 34 shows that there is no linear correlation between the average sonic velocity and the plastic viscosity when testing PAC. Between the lowest (1 wt %) and the highest (2 wt %) concentration only a difference of 4 m/s in sonic velocity is measured. Even 1,5 wt % shows a slightly higher sonic velocity compared to the highest concentration.

Table 12: Plastic viscosity - average sonic velocity PAC

Concentration [wt %]	Plastic Viscosity [cp]	Average Sonic Velocity [m/s]
1	11,97	1528,80
1,5	27,09	1533,68
2	52,13	1532,24

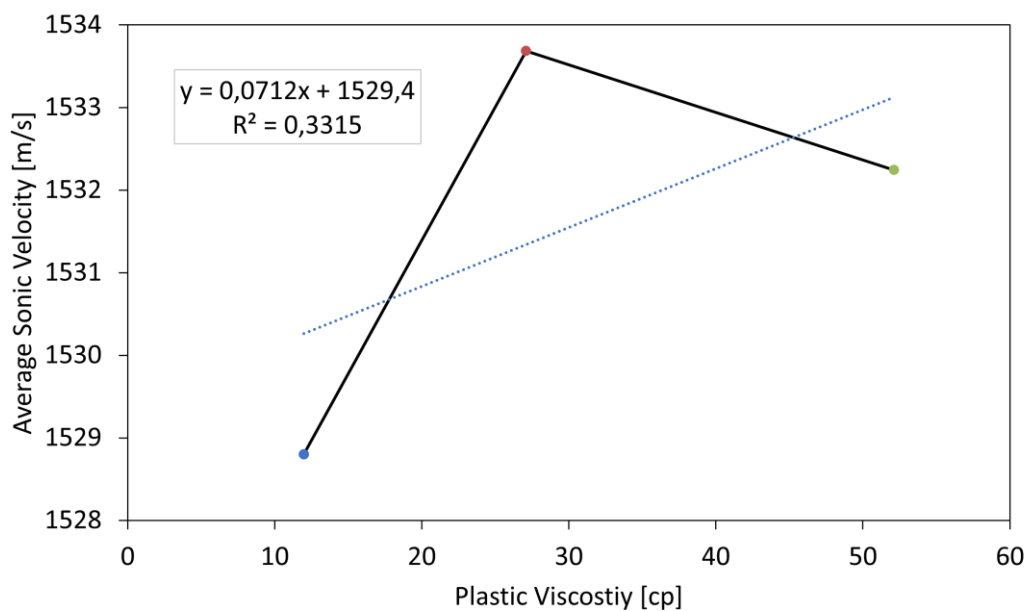


Figure 34: Plastic viscosity [cp] vs. average sonic velocity [m/s]: PAC

Gel Strength Data:

As seen in Figure 35, PAC does not develop any gel strength over time. Therefore, a comparison with sonic velocity is not shown.

Table 13: Gel strength - average sonic velocity PAC

Concentration [wt %]	Time [hh:mm:ss]	Shear rate [lbf/100ft ²]	Average Sonic Velocity [m/s]
1	00:00:10	0	1527,48
	00:10:00	0	1529,46
1,5	00:00:10	0	1537,79
	00:10:00	0	1528,80
2	00:00:10	0	1537,79
	00:10:00	0	1533,57

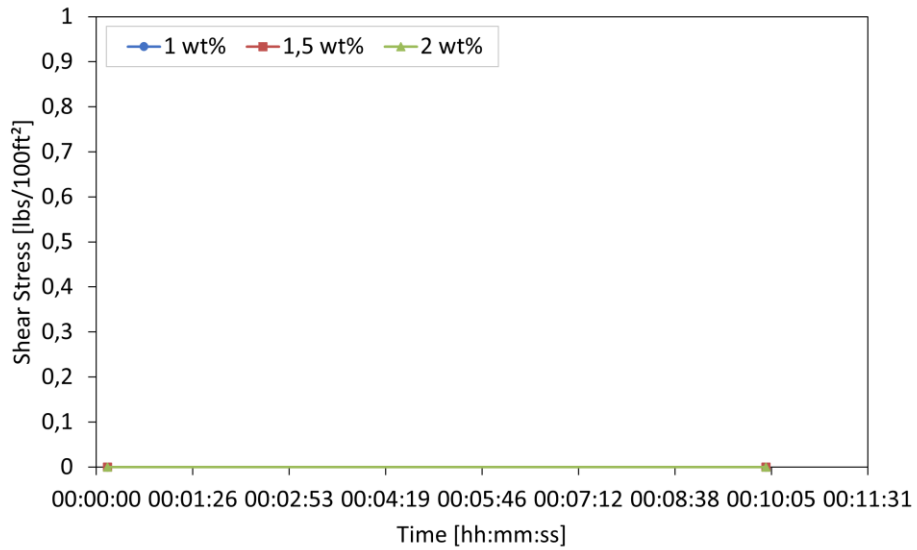


Figure 35: Gel strength [lbf/100ft²] PAC

Concentration Impact on Average Sonic Velocity:

As seen in Figure 36, the concentration has almost no impact on the sonic velocity when using PAC as a viscosifier.

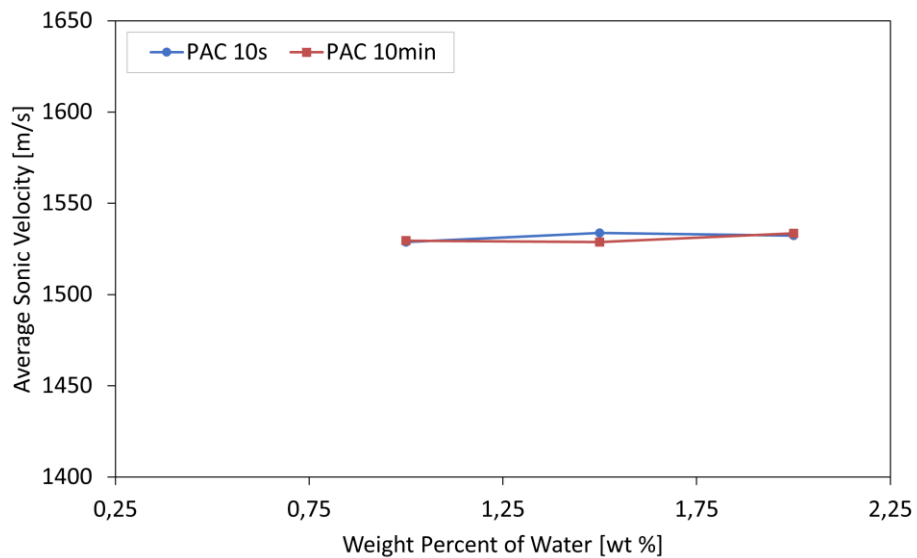


Figure 36: Weight % of water vs. Average sonic velocity [m/s]: PAC

5.1.1.2 Xanthan Gum

Viscosity Data:

This fluid is best described using the GHB model, according to the RAS fluid analysis.

Table 14: Plastic viscosity and yield point xanthan gum

	XGUM 0,28%	XGUM 0,42%	XGUM 0,56%
Plastic Viscosity [cp]	2,65	2,18	1
Yield point [lbf/100ft ²]	12,859	20,56	27,73

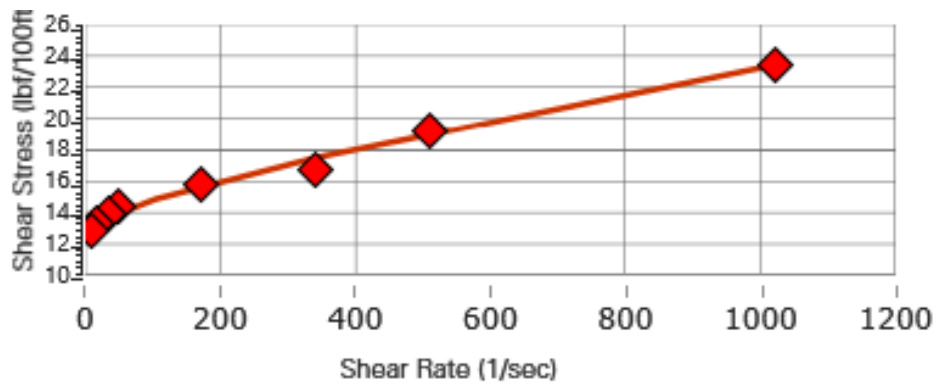


Figure 38: XGUM 0,28% RAS analysis

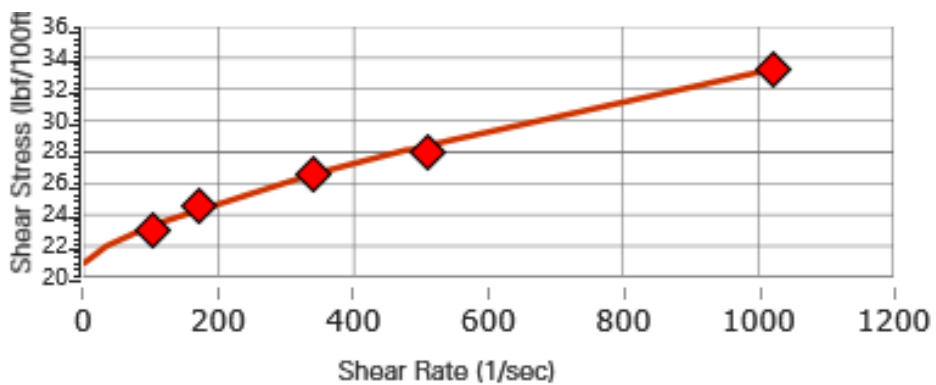


Figure 37: XGUM 0,42% RAS analysis

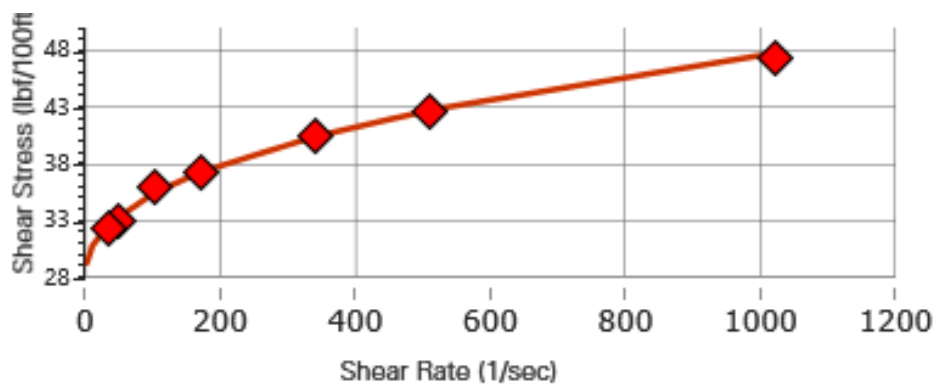


Figure 39: XGUM 0,56% RAS analysis

Plastic Viscosity – Average Sonic Velocity Comparison:

The colors in Table 15 represent the corresponding data points in the figures below. The data shown in Figure 40 represents invers linear trend. The highest concentration (lowest plastic viscosity) has the lowest sonic velocity whereas the lowest concentration (highest plastic viscosity) showed the highest sonic velocity. When testing the fluid, it is observed that the highest concentration fluid had a very thick consistency. For this fluid, it is especially difficult to get a good signal. A comparison can be seen by looking at Figure 41, which is the third measurement of the 0,28 wt % concentration, and Figure 42, which is the third measurement of the 0,56 wt % fluid. To achieve the signal shown in Figure 42 some settings, namely the lowpass filter and the starting frequency of the signal generator, needed to be adjusted to receive the image displayed. Still, it is very difficult to ascertain the location when the “quite time” ends. This phenomenon is attributed to the increased concentration of Xanthan Gum particles lead to increase in number of bubbles in suspension results in higher attenuation of the generated signal thus resulting in a lower velocity.

Table 15: Plastic viscosity - average sonic velocity xanthan gum

Concentration [wt %]	Plastic Viscosity [cp]	Average Sonic Velocity [m/s]
0,28	2,65	1489,45
0,42	2,18	1475,75
0,56	1	923,65

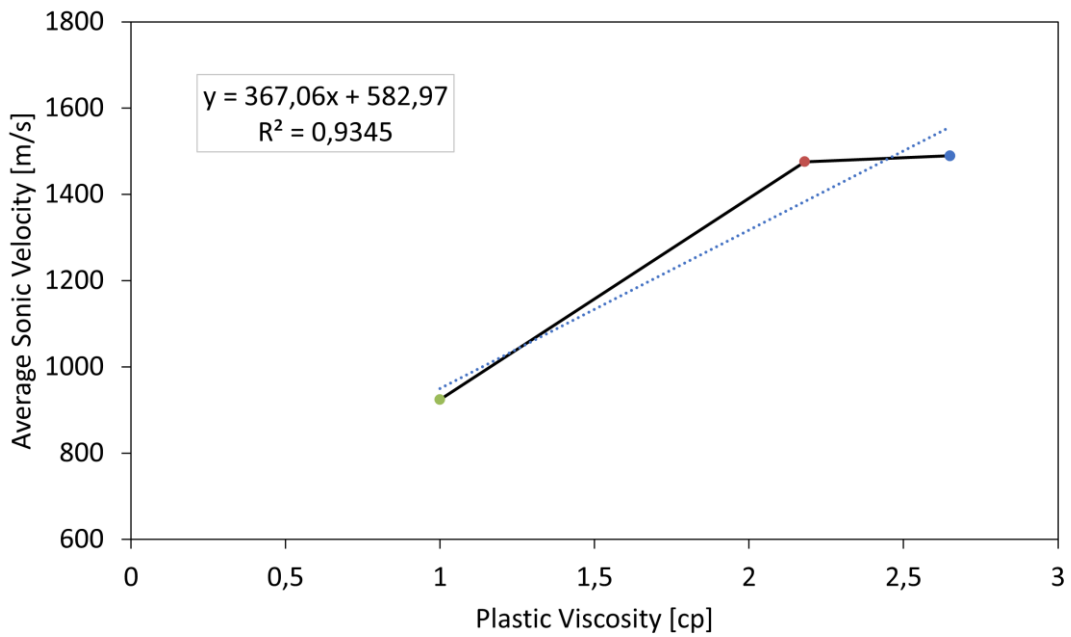


Figure 40: Plastic viscosity[cp] vs. average sonic velocity [m/s]: xanthan gum

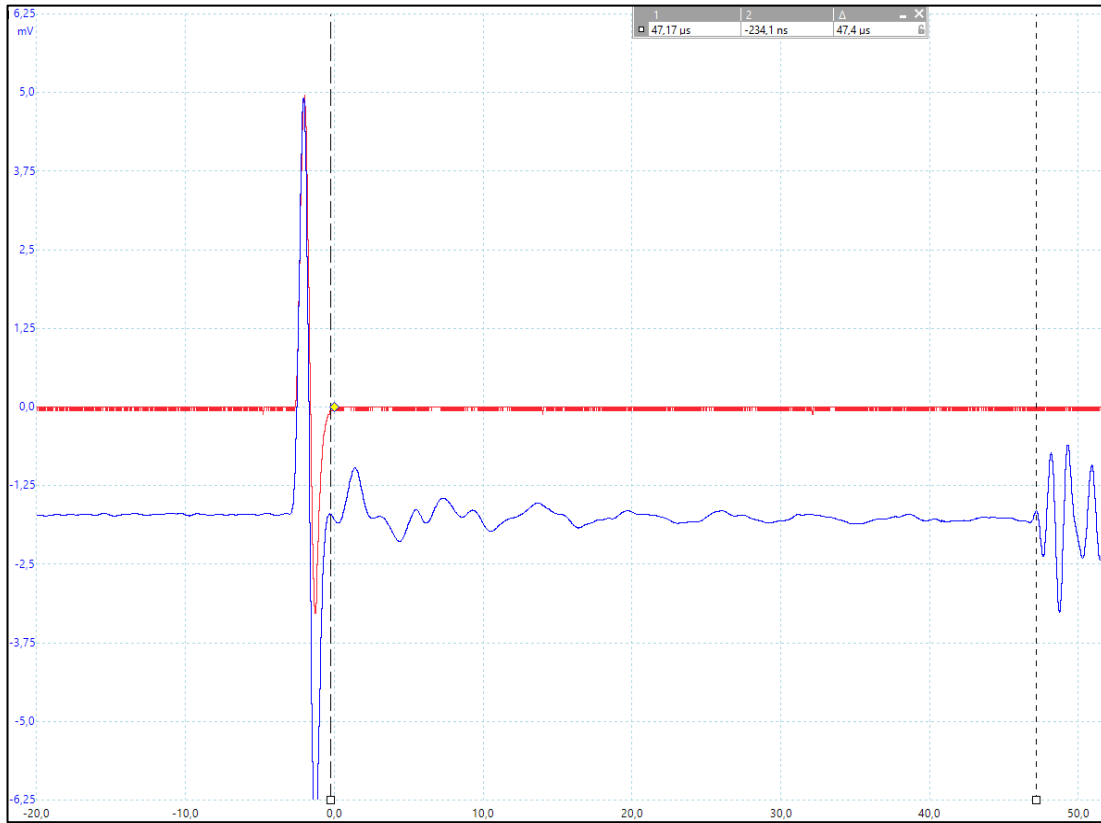


Figure 42: Ultrasonic signal 0,28 wt % xanthan gum

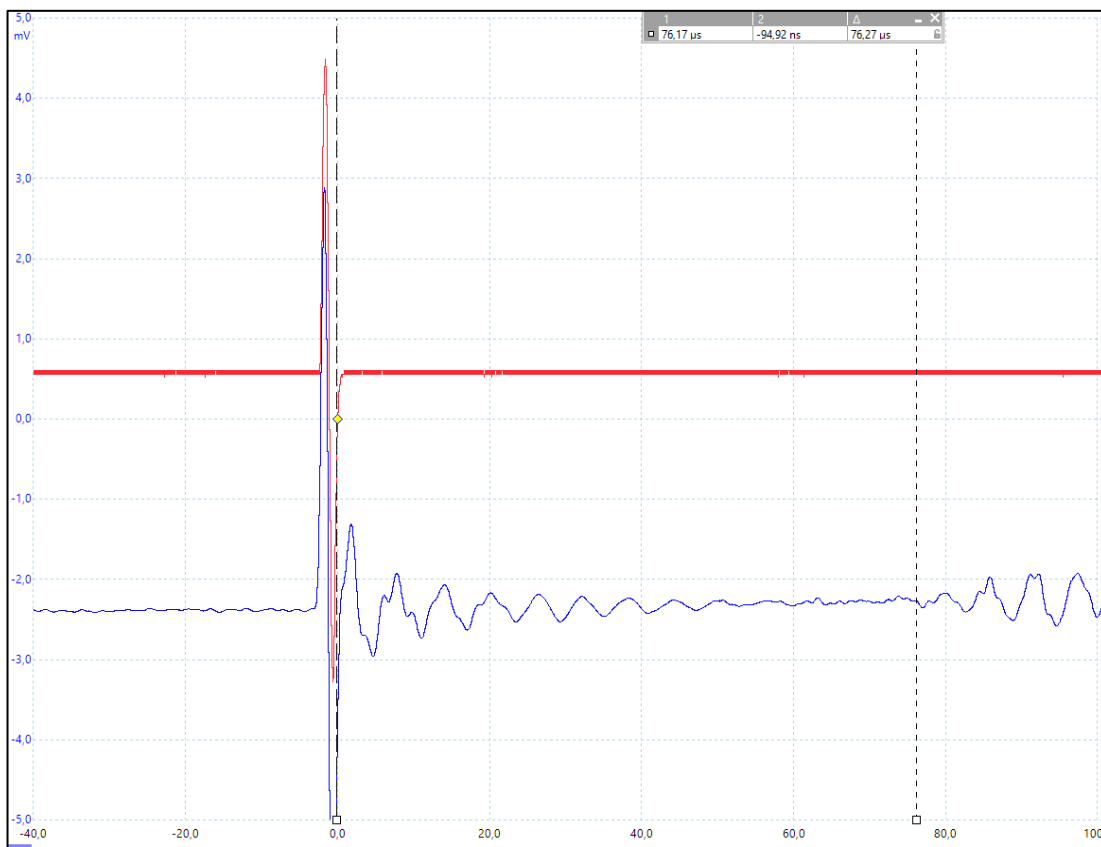


Figure 41: Ultrasonic signal 0,56 wt % xanthan gum

Gel Strength Data:

Figure 43 shows that a fluid containing xanthan gum will develop a gel strength. With increased concentration the shear stress increases. Furthermore, the difference between the 10-second reading and 10-minute reading also increases with increased concentration as seen in Table 16. Figure 44 shows a comparison between the initial and 10-minute gel strength. At 0,56 wt % the sonic velocity drastically drops. Figure 45 shows how the average sonic velocity changes from 10-seconds to 10-minute after the fluid has been poured into the test chamber. 0,28 wt % and 0,56 wt % show a small decrease in sonic velocity whereas 0,42 wt % shows a small increase in the sonic velocity.

Table 16: Gel strength - average sonic velocity xanthan gum

Concentration [wt %]	Time [hh:mm:ss]	Shear Stress [lbf/100ft ²]	Average Sonic Velocity [m/s]
0,28	00:00:10	13	1489,45
	00:10:00	15	1486,00
0,42	00:00:10	23	1475,75
	00:10:00	28	1487,36
0,56	00:00:10	34	923,65
	00:10:00	40	911,80

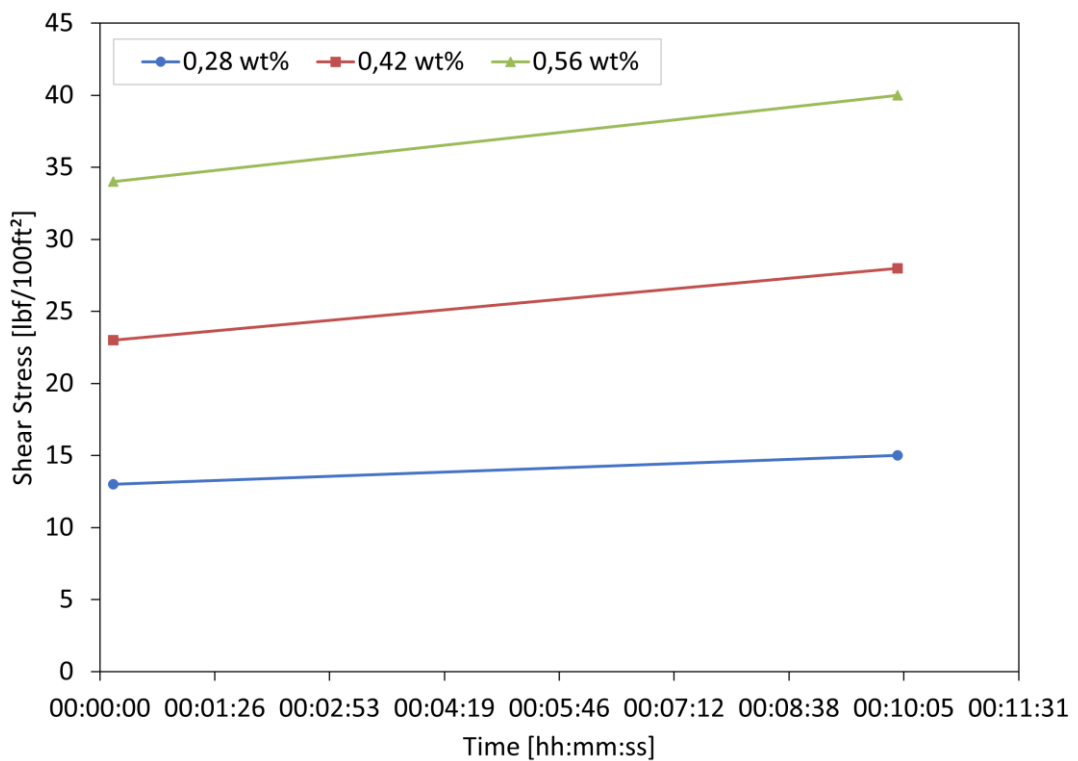


Figure 43: Gel strength [lbf/100ft²]: xanthan gum

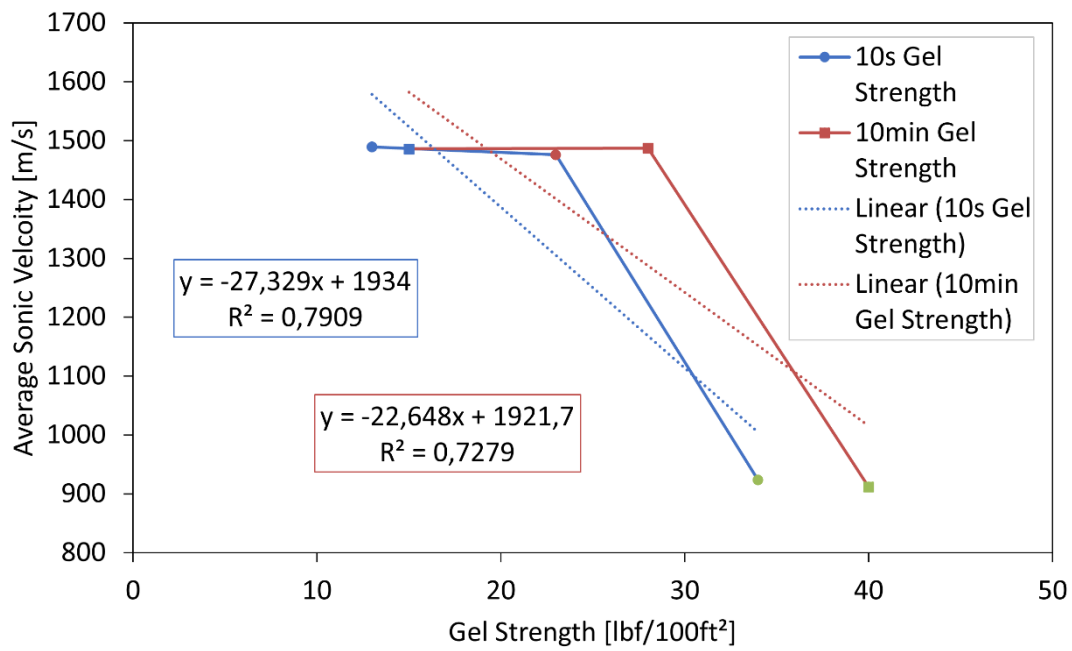


Figure 44: Gel strength [lbf/100ft²] vs. average sonic velocity [m/s]: xanthan gum - comparison of initial gel strength and 10-minute gel strength

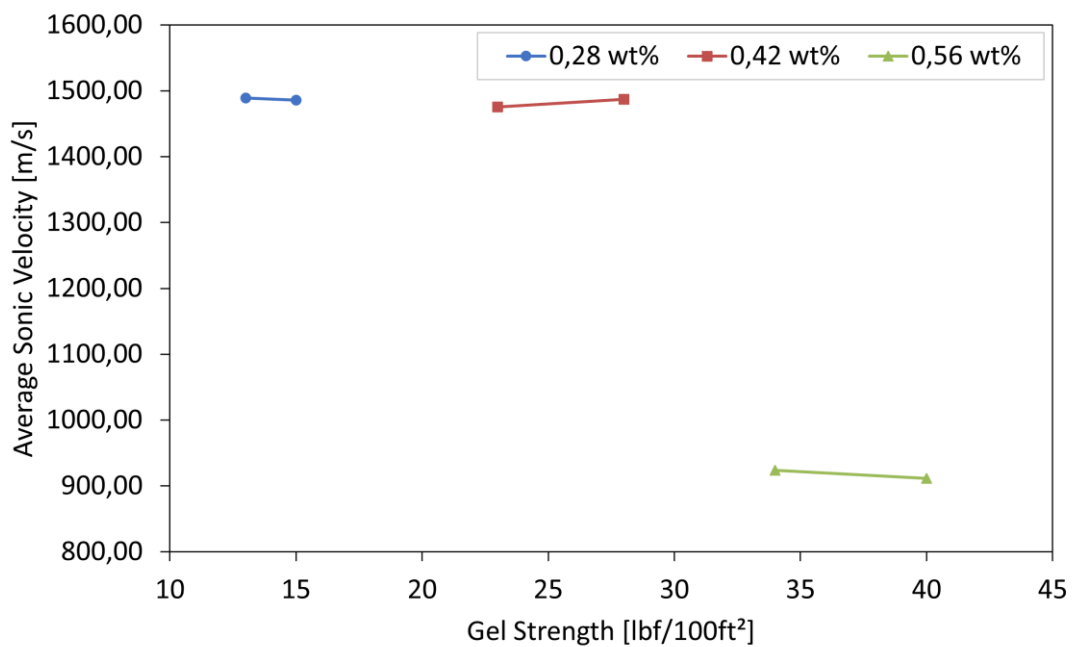


Figure 45: Gel strength [lbf/100ft²] vs. average sonic velocity[m/s]: xanthan gum - development of gel strength

Concentration Impact on Average Sonic Velocity:

Figure 46 shows how the concentration of xanthan gum changes the sonic velocity. The 10-second and 10-minute reading are very close to each other. Therefore, it can be assumed that the concentration has a bigger impact than the gel strength development.

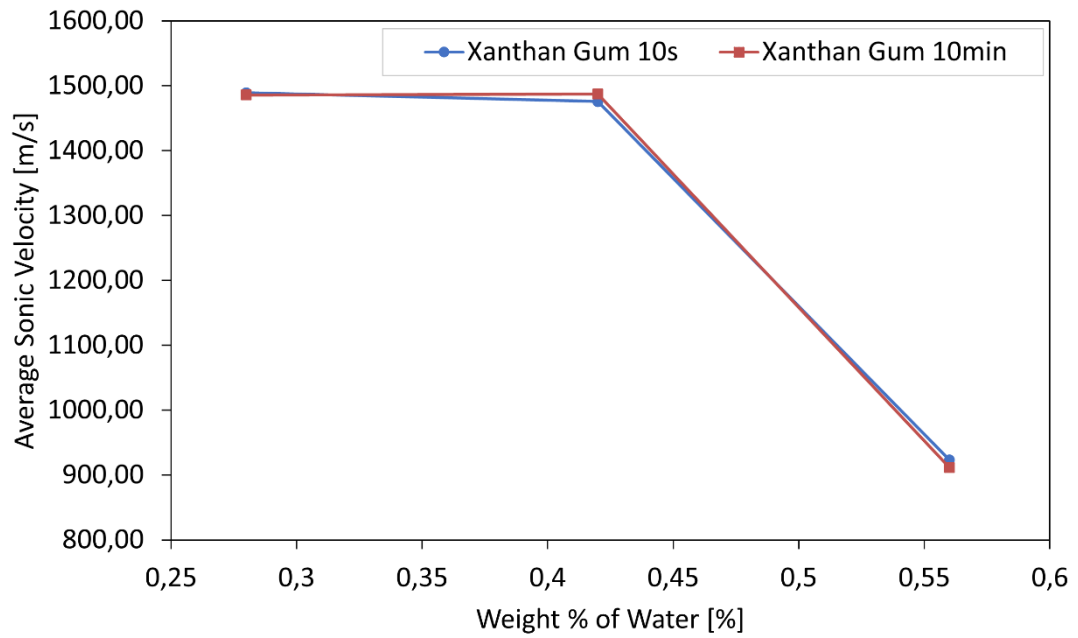


Figure 46: Weight % of water vs. average sonic velocity[m/s]: xanthan gum

5.1.1.3 Bentonite

Viscosity Data:

According to the RAS Software the 2 wt % and 3 wt % bentonite is best described with the Power Law fluid model and the 4 wt % bentonite with the GHB fluid model.

Table 17: Plastic viscosity and yield point bentonite

	Bentonite 2%	Bentonite 3%	Bentonite 4%
Plastic Viscosity [cp]	1,59	2,7	2,78
Yield point [lbf /100ft ²]	0	0	0,326

Plastic Viscosity – Average Sonic Velocity Comparison:

The colors in Table 18 represent the corresponding data points in the figures below. The focus of the study of bentonite is for the concentrations ranging from 2 wt % to 4 wt %. During the initial fluid preparation 0,5 wt % was also tested but no sufficient viscosity readings were taken from the viscometer, thus the data it has been decided to increase the concentration and keep the data points limited to three (2 wt %, 3wt % and 4 wt %). Still some data was gathered and is still displayed in some figures below. Figure 50 shows the comparison between the average ultrasonic velocity and the plastic viscosity of bentonite. A downward linear trend can be observed that with an increase in plastic viscosity the sonic velocity decreases. The highest sonic velocity can be observed at the lowest concentration of bentonite at 2 wt %.

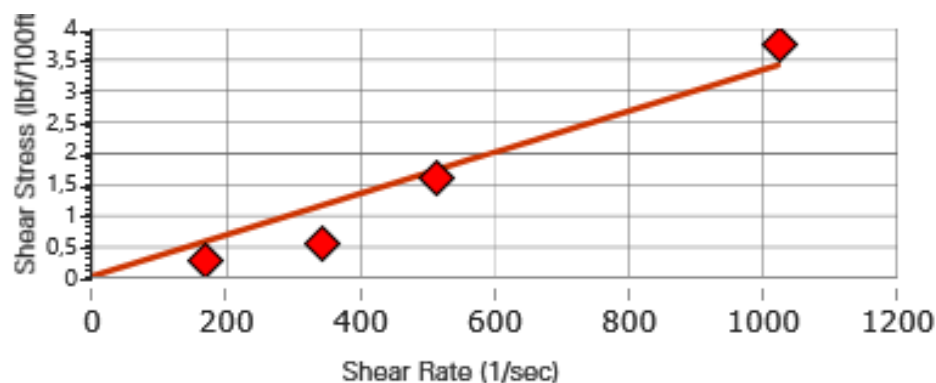


Figure 47: Bentonite 2% RAS analysis

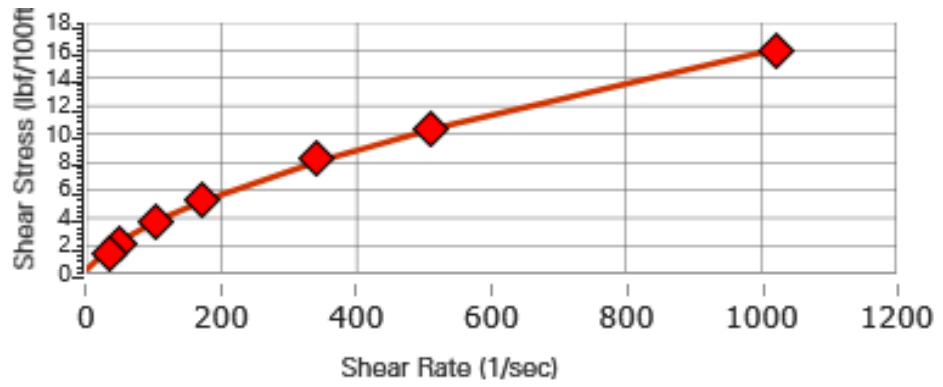


Figure 49: Bentonite 3% RAS analysis

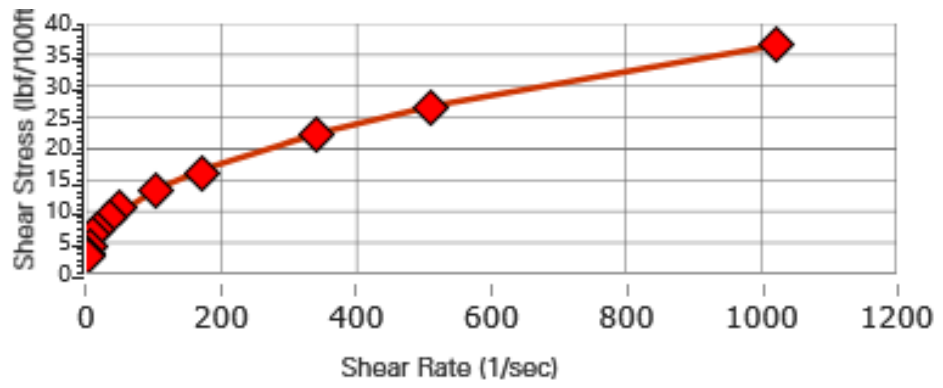


Figure 48: Bentonite 4% RAS analysis

Table 18: Plastic viscosity - average sonic velocity bentonite

Concentration [wt %]	Plastic Viscosity [cp]	Average Sonic Velocity [m/s]
0,5	-	1536,34
2	1,59	1518,51
3	2,7	1491,97
4	2,78	1480,29

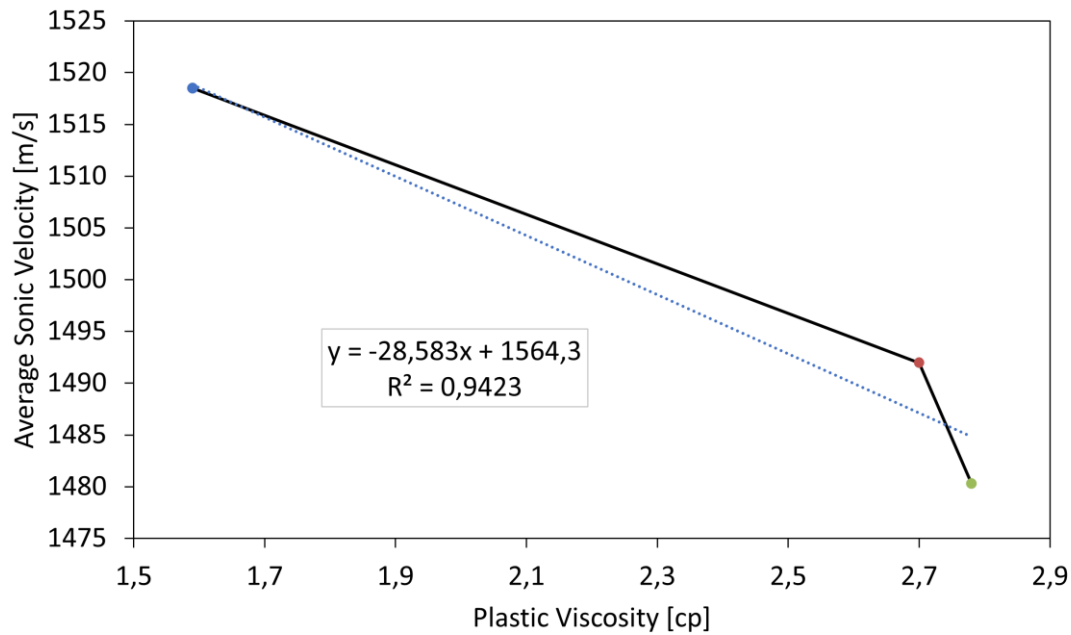


Figure 50: Plastic viscosity [cp] vs. average sonic velocity[m/s]: bentonite

Gel Strength Data:

The gel strength development of bentonite can be observed in Figure 51. The 0,5 wt % line and the 2 wt % line are overlapping. At low concentrations bentonite does not have a gel strength which can be measured by an analog viscometer. A gel strength reading can first be taken at 3 wt % and the shear stress increases over time. At 4 wt % it can be observed that the initial gel strength and the 10-minute gel strength are the same and don't change over time. In Figure 52 a trend can be observed that an increase in concentration of bentonite results in a decrease in ultrasonic velocity. Even though the gel strength does not change over time the sonic velocity does as can be seen in Figure 53. The observed change is very small around 1,43 m/s (decrease), 8,31 m/s (increase), 1,26 m/s (decrease) and 3,95 m/s (increase) from lowest to highest concentration respectively. No apparent trend can be observed, and it is unclear why the sonic velocity sometimes increases or decreases. The error of the system is on average is 0,22 %. At 1500 m/s this would result in $\pm 3,3$ m/s. Some of the anomalies probably owing to the system error.

Table 19: Gel strength - average sonic velocity bentonite

Concentration [wt %]	Time [hh:mm:ss]	Shear Stress [lbf/100ft ²]	Average Sonic Velocity [m/s]
0,5	00:00:10	0	1536,34
	00:10:00	0	1534,91
2	00:00:10	0	1518,51
	00:10:00	0	1526,82
3	00:00:10	1	1491,97
	00:10:00	1,5	1490,71
4	00:00:10	3	1480,29
	00:10:00	3	1484,24

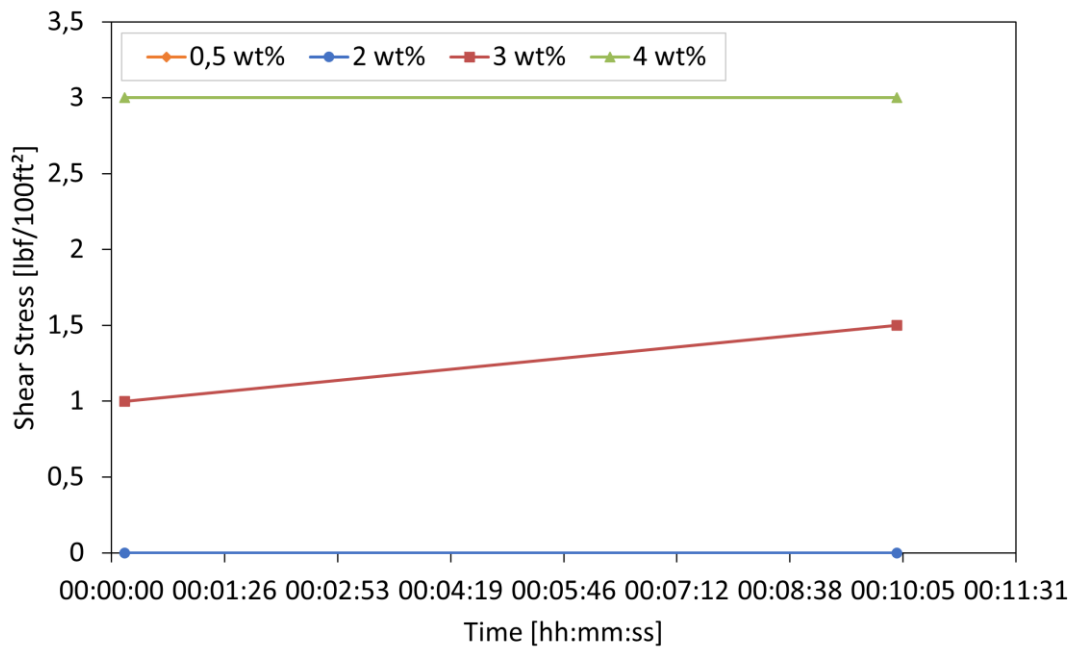


Figure 51: Gel strength [lbf/100ft²] bentonite

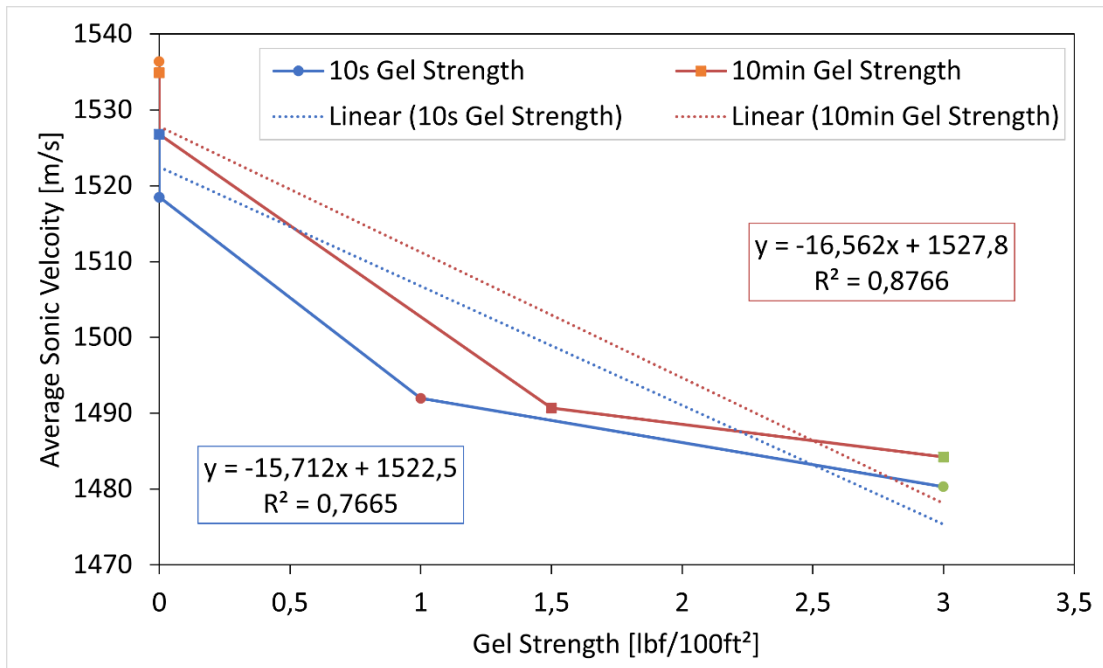


Figure 52: Gel strength [lbf/100ft²] vs. average sonic velocity [m/s]: bentonite- comparison of initial gel strength and 10min gel strength

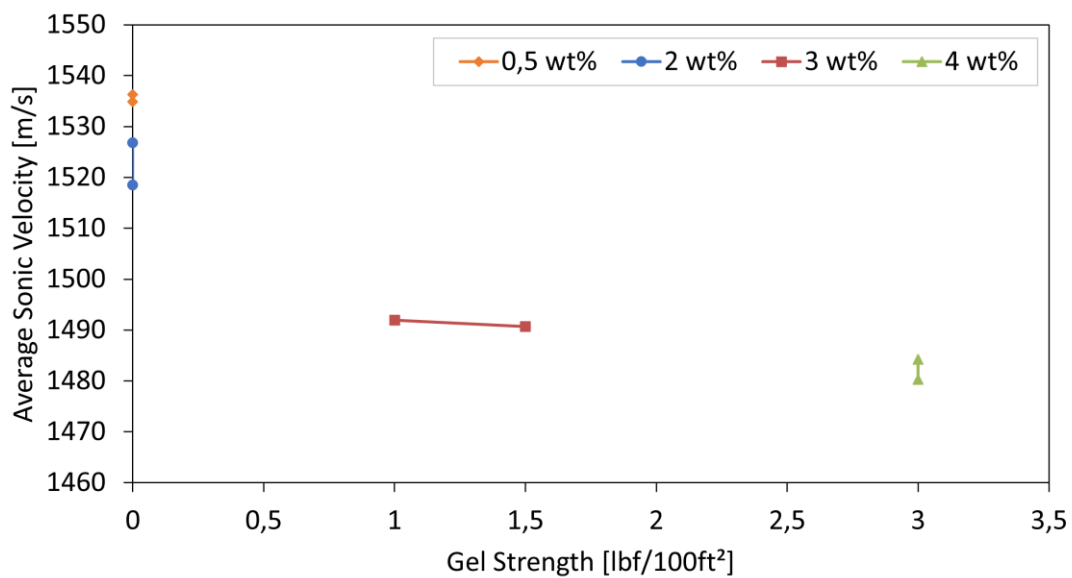


Figure 53: Gel strength [lbf/100ft²] vs. average sonic velocity [m/s]: bentonite - development of gel strength

Concentration Impact on Average Sonic Velocity:

Figure 54 shows that the concentration of bentonite has slight influence on the sonic velocity. A downward trend can be observed. Only a small difference between the 10-seconds and 10-minute gel-strength can be observed. Thus, it can be concluded that the concentration has little to no impact on the average sonic velocity when using bentonite as a viscosifier.

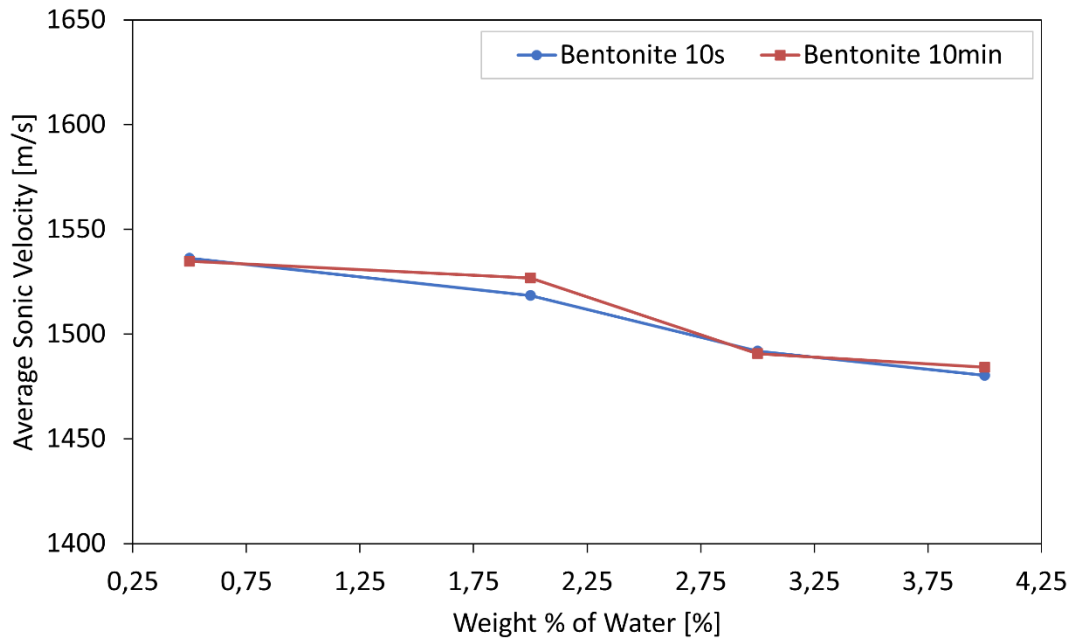


Figure 54: Weight % of water vs. average sonic velocity [m/s]: bentonite

5.1.1.4 Laponite

When using Laponite it is important to give the viscosifier some time to saturate (same as bentonite) with water after mixing. No significant change was observed after ~10 minutes of adding the laponite powder to the water or previous lower concentration mixture.

Viscosity Data:

According to the RAS software the 1 wt % laponite is best represented by the Power Law fluid model, the 1,5 wt % and 2 wt % laponite are best represented using GHB fluid model. The color scheme used in Table 20 represents the corresponding data in the figures below.

Table 20: Plastic viscosity and yield point laponite

	Laponite 1%	Laponite 1,5%	Laponite 2%
Plastic Viscosity [cp]	3,51	1,09	1,09
Yield point [lbf /100ft ²]	0	0,218	2,193

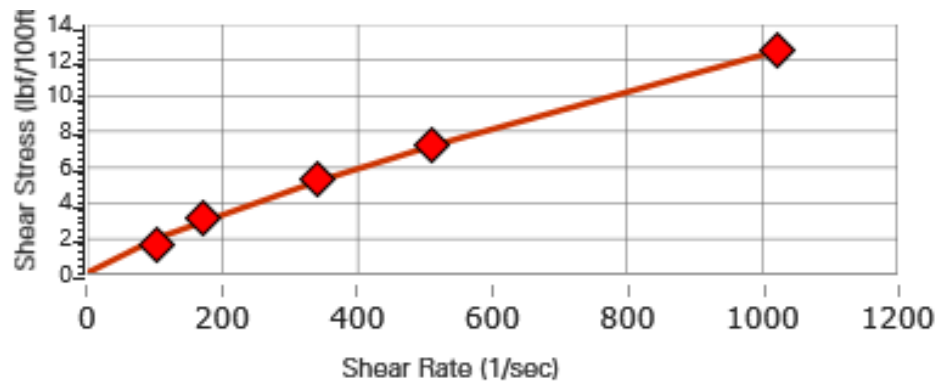


Figure 56: Laponite 1% RAS analysis

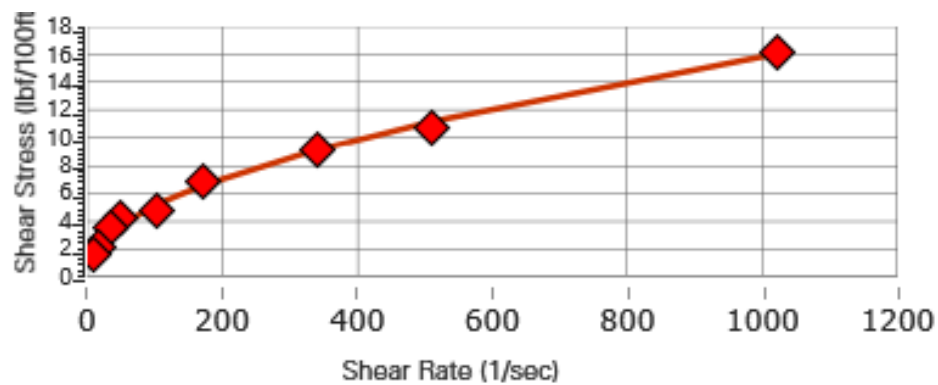


Figure 55: Laponite 1,5% RAS analysis

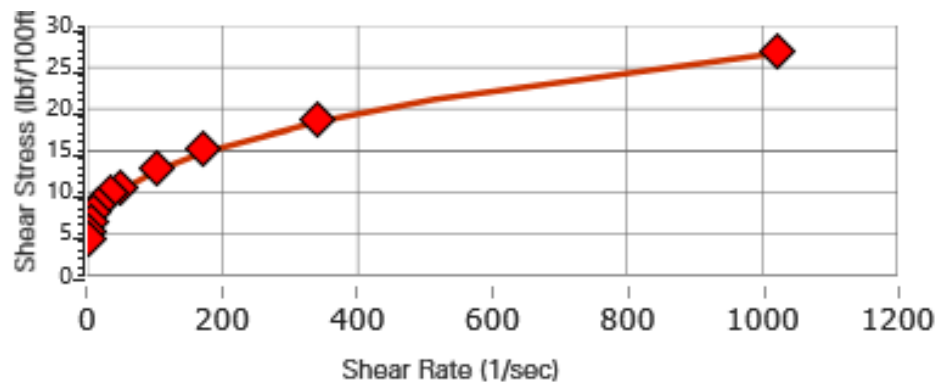


Figure 57: Laponite 2% RAS analysis

Plastic Viscosity – Average Sonic Velocity Comparison:

When using laponite the plastic viscosity reduces from 3,51 cp to 1,09 cp. This could be due to the change in fluid model calculation since with rise in laponite concentration increases yield point hence, different fluid model has been deemed best for calculating the plastic viscosity. No correlation between the plastic viscosity and the sonic velocity can be made as seen in Figure 58.

Table 21: Plastic viscosity - average sonic velocity laponite

Concentration [wt %]	Plastic Viscosity [cp]	Average Sonic Velocity [m/s]
1	3,51	1497,03
1,5	1,09	1502,45
2	1,09	1491,97

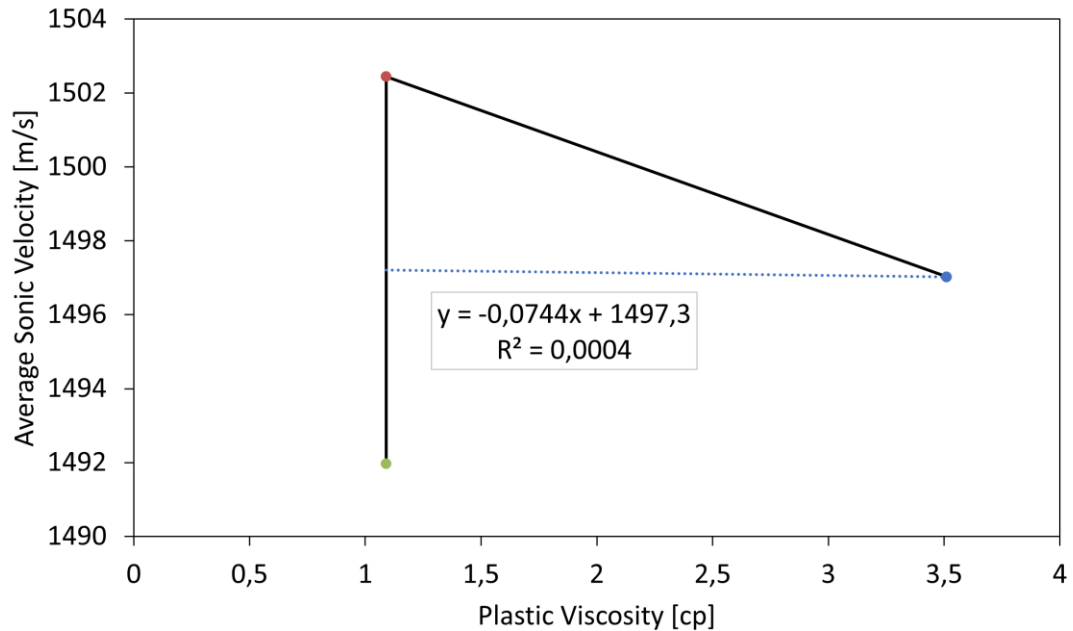


Figure 58: Plastic viscosity [cp] vs. average sonic velocity [m/s]: laponite

Gel Strength Data:

Figure 59 shows that laponite develops a gel strength over time. With increased concentration the difference between the 10-second and 10-minute gel strength becomes more prominent. Laponite 1,5 % shows satisfactory values for plastic viscosity, gel strength and yield point and is therefore selected to be used as the viscosifiers for the weighting material ultrasonic study (next sub-section). Some fluctuations can be observed for the 10-second gel strength in Figure 62. This can be a combination of human error (increased concentration results in more complicated measurement) and the system error. In comparison the 10-minute gel strength is more consistent. It was observed during the experiment that after 10minutes the amplitude increases, and responses of the ultrasonic signal becomes more prominent. This could be due to alignment of claylike particles to form the gel strength. This results in better transmission of the ultrasonic wave through the medium, because the particles are in contact with each other and can transfer the wave more efficiently. Figure 61 shows how the sonic velocity changes with time for each concentration. For 1 wt % the sonic velocity stays constant, for 1,5 wt % and 2 wt % the sonic velocity decreases from the 10-second gel strength to the 10-minute gel strength.

Table 22: Gel strength - average sonic velocity laponite

Concentration [wt %]	Time [hh:mm:ss]	Shear Stress [lbf/100ft ²]	Average Sonic Velocity [m/s]
1	00:00:10	0,5	1497,03
	00:10:00	15	1497,14
1,5	00:00:10	4	1502,45
	00:10:00	32	1498,41
2	00:00:10	9	1491,97
	00:10:00	95	1488,11

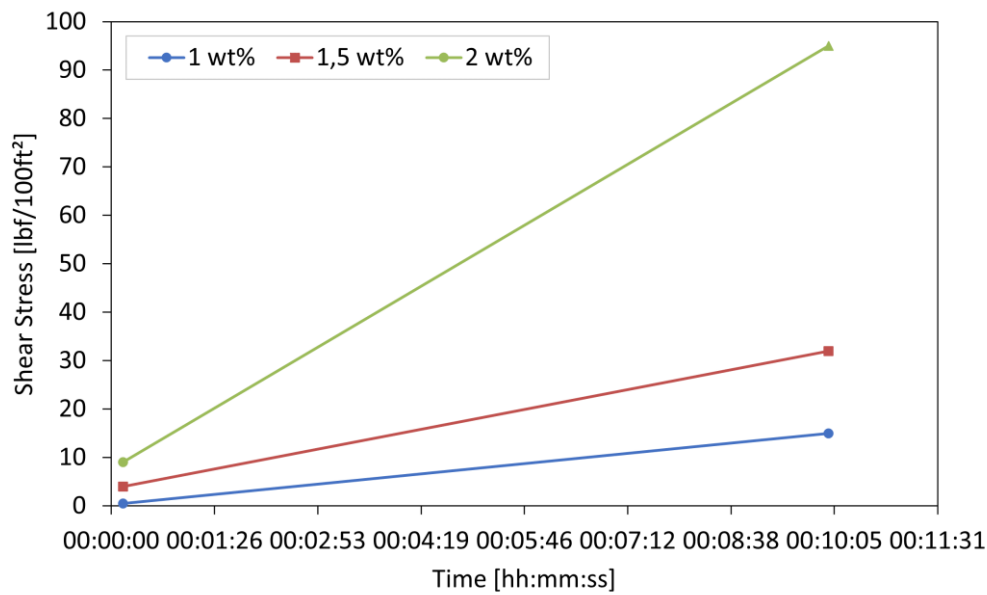


Figure 59: Gel strength [lbf/100ft²]: laponite

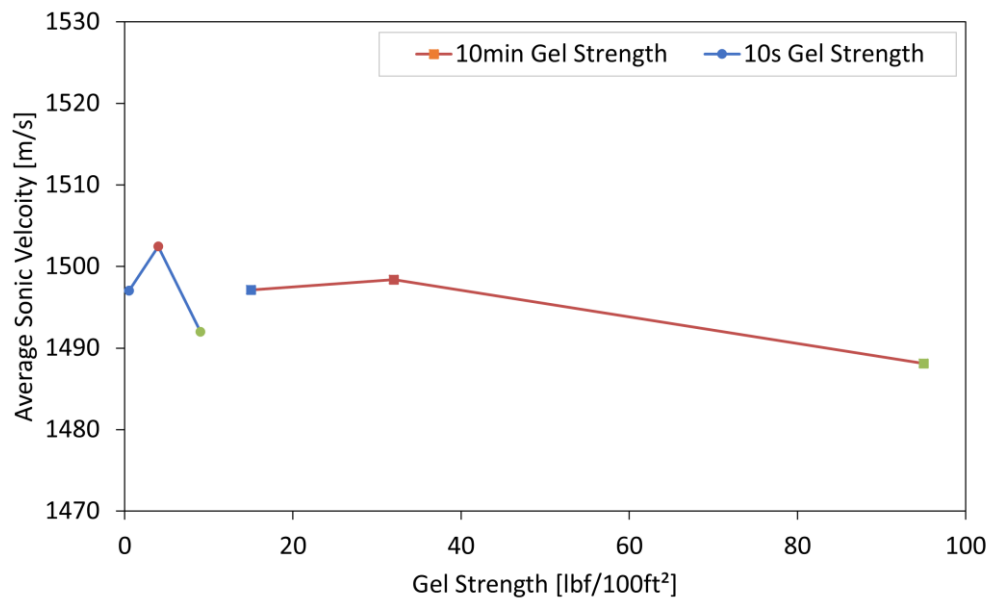


Figure 60: Gel strength [lbf/100ft²] vs. average sonic velocity [m/s]: laponite-comparison of initial gel strength and 10min gel strength

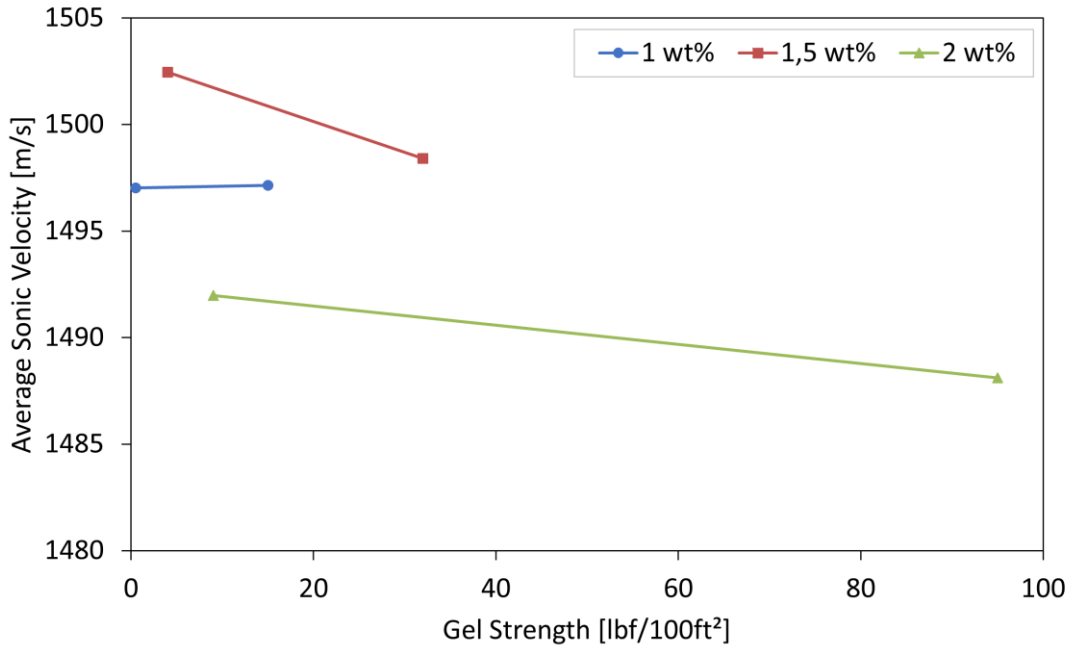


Figure 61: Gel strength [lbf/100ft²] vs. average sonic velocity[m/s]: laponite - development of gel strength

Concentration Impact on Average Sonic Velocity:

The concentration of laponite has only a small to no impact on the sonic velocity as can be seen in Figure 62.

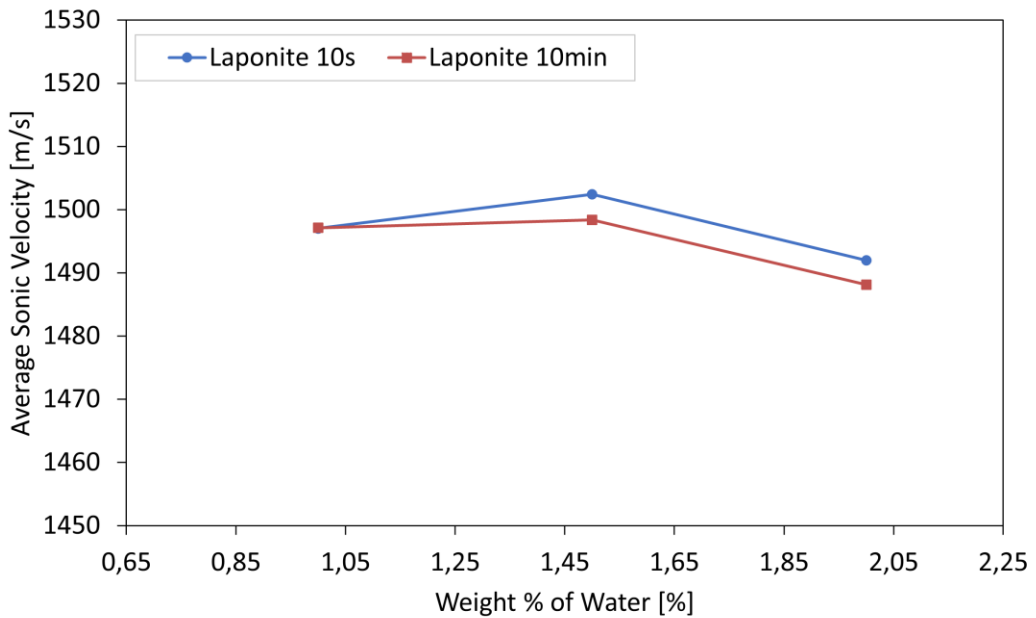


Figure 62: Weight % of water vs. average sonic velocity[m/s]: laponite

5.1.1.5 Carboxymethyl-cellulose (CMC)

Viscosity Data:

The RAS software suggested that the fluid model best fit for all concentrations of CMC is Power Law.

Table 23: Plastic viscosity and yield point CMC

	CMC 1%	CMC 1,5%	CMC 2%
Plastic Viscosity [cp]	4,76	9,08	15,09
Yield point [lbf/100ft ²]	0	0	0

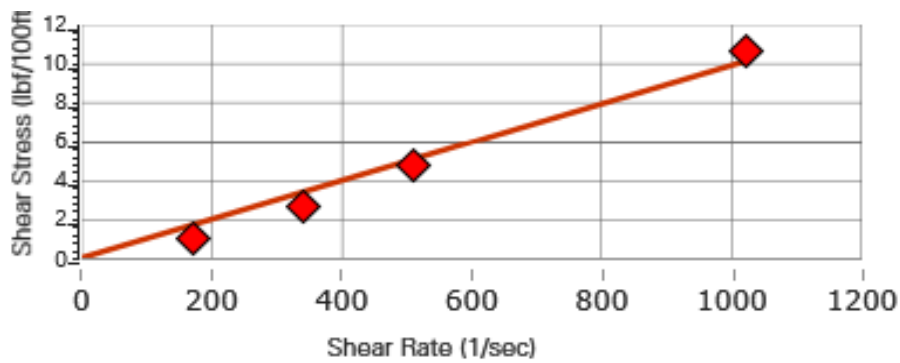


Figure 64: CMC 1% RAS analysis

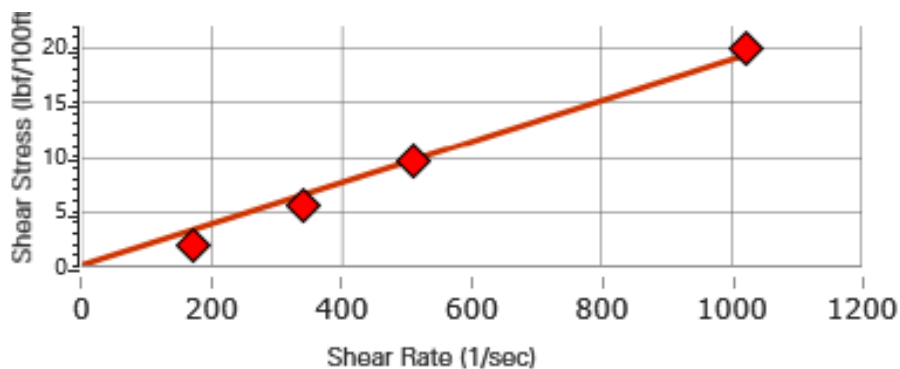


Figure 63: CMC 1,5% RAS analysis

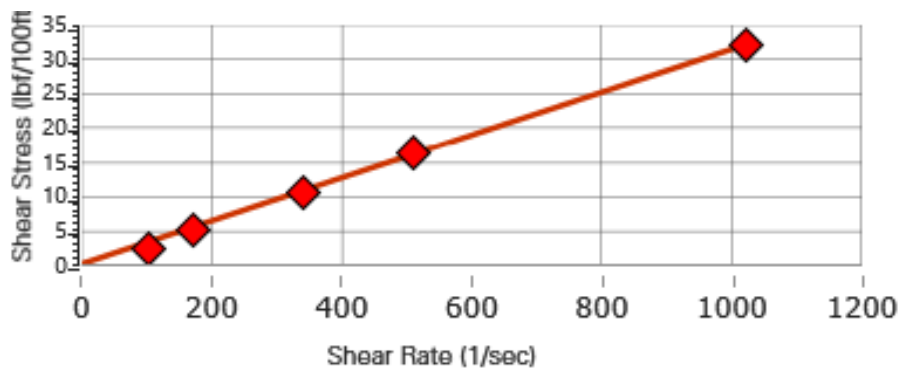


Figure 65: CMC 2% RAS analysis

Plastic Viscosity – Average Sonic Velocity Comparison:

The color scheme presented in Table 24 represents the data in all the figures below. A reduction in sonic velocity with an increase in plastic viscosity can be observed in Figure 66. The trend can be described with a linear trendline. The average sonic velocity difference between the lowest and highest concentration is 32 m/s.

Table 24: Plastic viscosity - average sonic velocity CMC

Concentration [wt %]	Plastic Viscosity [cp]	Sonic Velocity [m/s]
1	4,76	1523,97
1,5	9,08	1502,45
2	15,09	1491,97

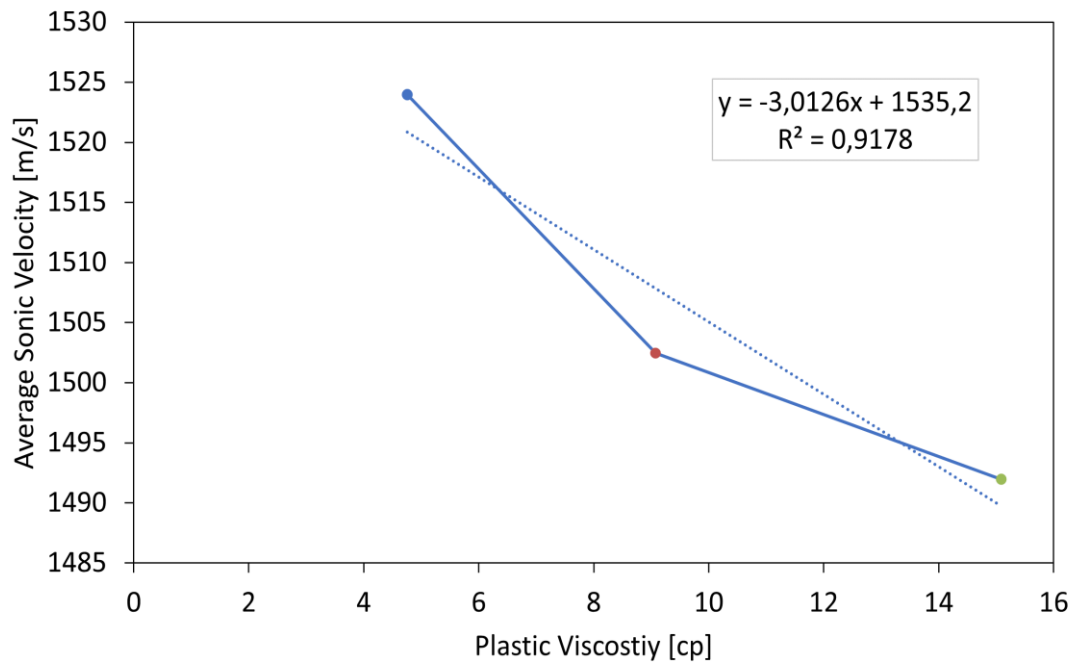


Figure 66: Plastic viscosity [cp] vs. average sonic velocity[m/s]: CMC

Gel Strength Data:

CMC does not develop a gel strength as seen in Figure 67. Therefore, the other analysis focusing on gel strength was not conducted.

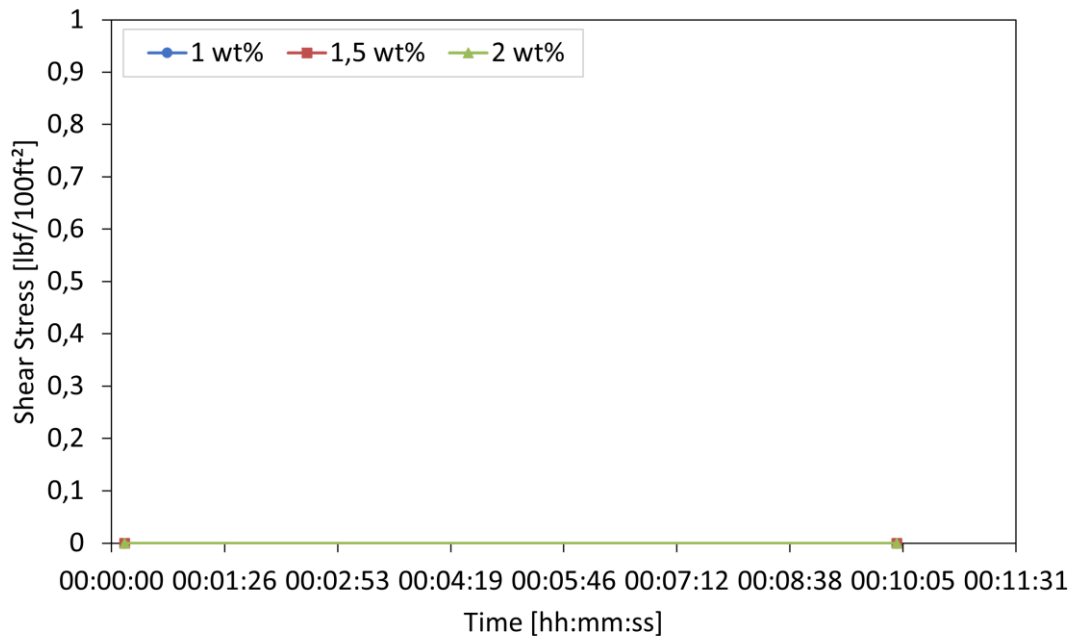


Figure 67: Gel strength [lbf/100ft²] CMC

Concentration Impact on Average Sonic Velocity:

An increase in wt % of water does not result in a change of average sonic velocity. Furthermore, since no gel strength is observed the 10 min reading is almost the same with only tiny variations. This effect can be seen in Figure 68. In conclusion the average sonic velocity of CMC is affected by the plastic viscosity or the concentration of the mixture. The presented data is not correlating with the data presented by (Abdul Kareem J- Al-Bermay and Nadia Hussein Sahib 2013). In their study the sonic velocity increases with an increase in concentration up to a sonic velocity of around 2000 m/s. This is even higher than any other additive tested during this study. Therefore, the results presented in that article can be assumed to have an error in measurement. A paper by (Guru et al. 2008) presents the study of compatibility of Pullulan (natural polymer used in the food industry) and CMC blends. The presented results in this study are in a comparable velocity range as the presented data in Figure 68. The measurements presented in the paper present a trend of increased sonic velocity with increased concentration. This is not corresponding to the presented data in this thesis. A theory why there is a discrepancy is that a blend of Pullulan and CMC was used which in turn has a different effect on the sonic velocity. Hence, more tests need to be conducted to be able to be certain that the presented measurement is valid.

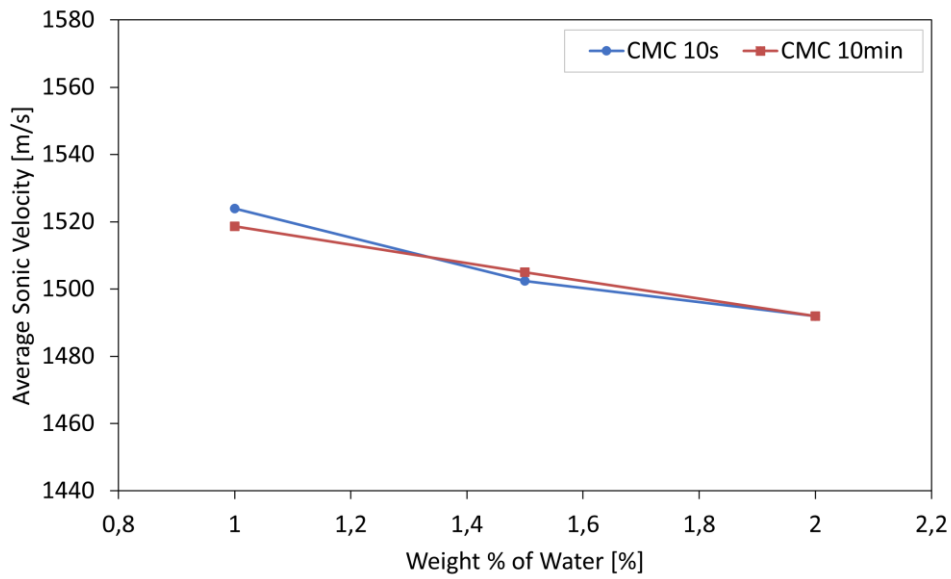


Figure 68: Weight % of water vs. average sonic velocity [m/s]: CMC

5.1.1.6 Flowzan

Viscosity Data:

The data presented in Table 25 has been calculated using the RAS software. The best fluid model for 0,25 wt % and 0,5 wt % is GHB and for 0,75wt % HB. The line displayed in Figure 71 is representing a GHB model instead of a HB model. This cannot be changed in the RAS software but the given values for yield point and plastic viscosity are accurate.

Table 25: Plastic viscosity and yield point flowzan

	Flowzan 0,25%	Flowzan 0,5%	Flowzan 0,75%
Plastic Viscosity [cp]	1,09	1,25	2
Yield point [lbf /100ft ²]	0,273	2,578	13,458

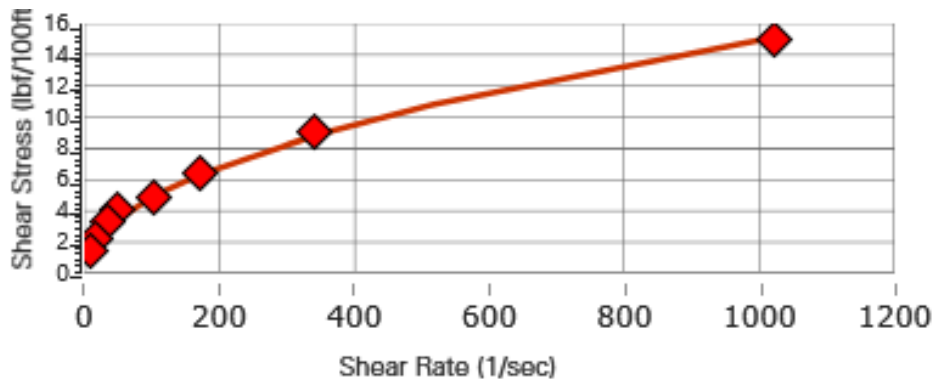


Figure 69: Flowzan 0,25% RAS analysis

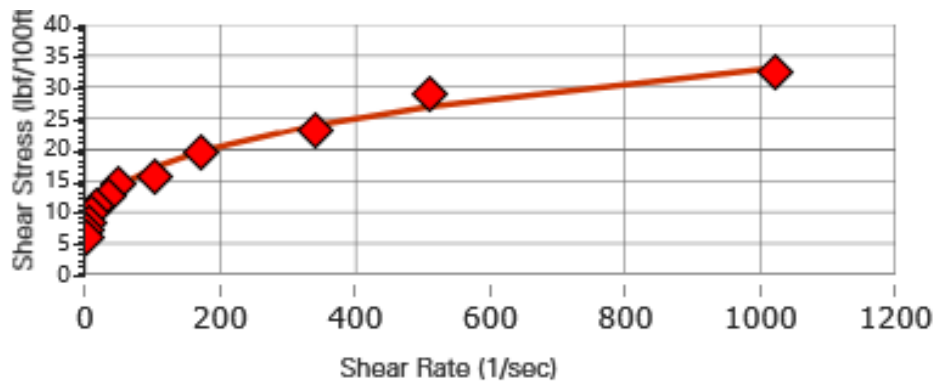


Figure 71: Flowzan 0,5% RAS analysis

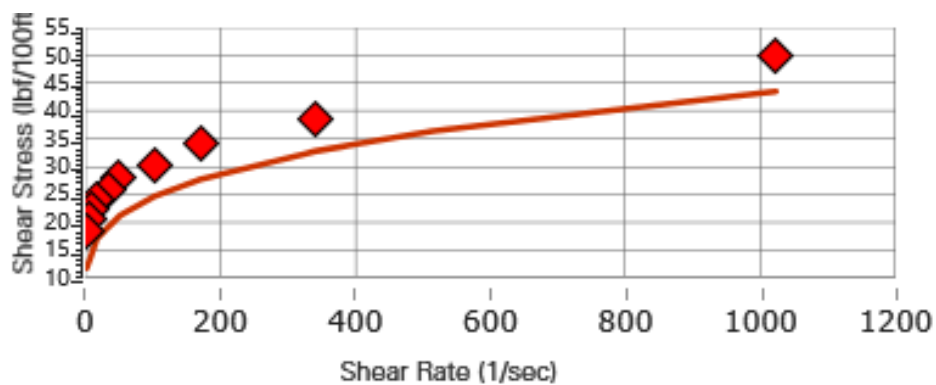


Figure 70: Flowzan 0,75% RAS analysis

Plastic Viscosity – Average Sonic Velocity Comparison:

In Table 26 presented color scheme is also used in the figures below to represent each data set. Figure 72 shows that with flowzan the sonic velocity decreases and then stays constant. The reasoning behind this is the same as stated in xanthan gum (discussed in section 4.5.1.2). With an increase in concentration of flowzan more bubbles are trapped in the fluid as seen in Figure 73. To mitigate this problem in the future it is suggested to use a vacuum chamber to remove all bubbles. Unfortunately for this study no vacuum chamber was available.

Table 26: Plastic viscosity - average sonic velocity flowzan

Concentration [wt %]	Plastic Viscosity [cp]	Average Sonic Velocity [m/s]
0,25	1,09	1452,48
0,5	1,25	1036,73
0,75	2	1033,33

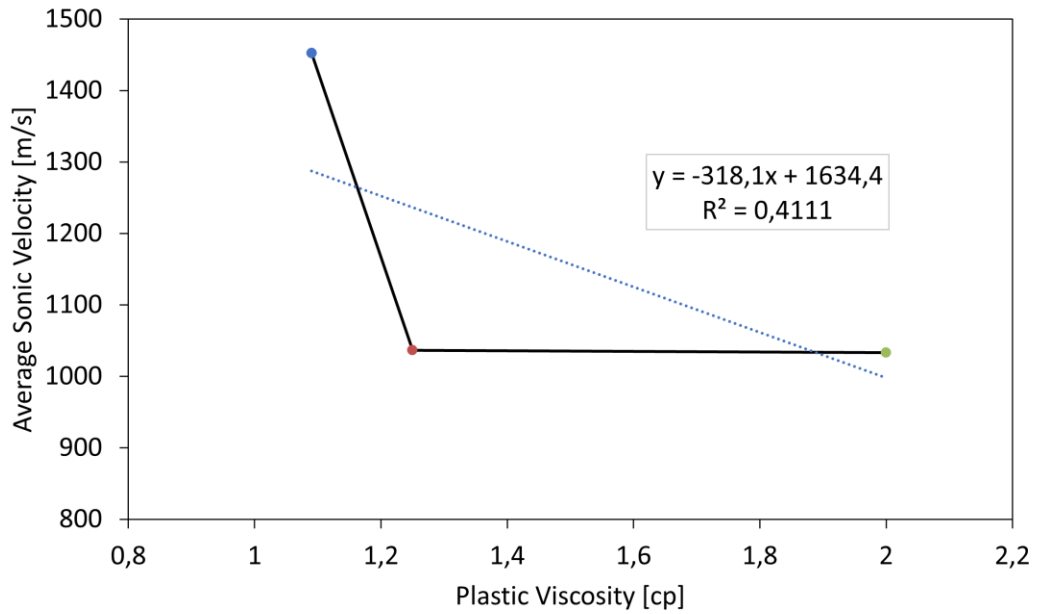


Figure 72: Plastic viscosity [cp] vs. average sonic velocity[m/s]: flowzan

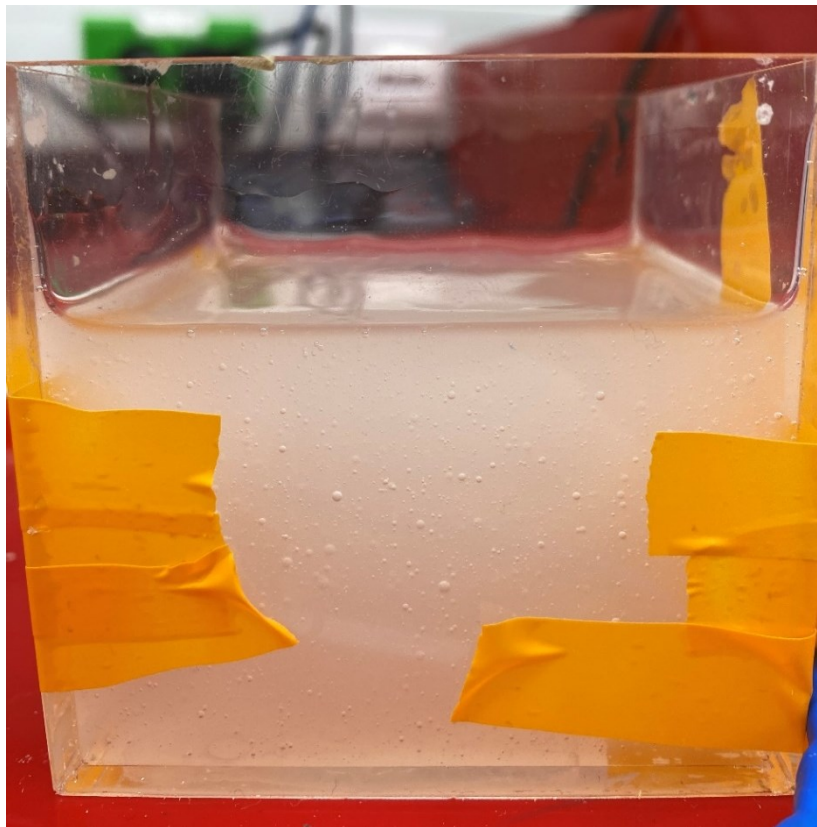


Figure 73: Flowzan 0,5% bubbles in suspension

Gel Strength Data:

Figure 74 shows how the gel strength develops from the 10-second reading to the 10-minute reading. With increased concentration both gel strength readings increase. The difference

between the 10-second and 10-minute gel strength is 1,5 lbf/100ft², 4,5 lbf/100ft² and 6,5 lbf/100ft² from lowest to highest concentration. Therefore, in this experiment the gel strength increases by 3 lbf/100ft² per 0,25 wt % when using flowzan. In Figure 75 the effect of the bubbles suspended in the fluid is observed again. Once sufficient bubbles are suspended only small changes in sonic velocity are observed. Figure 76 shows how the sonic velocity readings change for each concentration. For every concentration a small increase in average sonic velocity was measured.

Table 27: Gel strength - average sonic velocity flowzan

Concentration [wt %]	Time [hh:mm:ss]	Shear Stress [lbf/100ft ²]	Average Sonic Velocity [m/s]
0,25	00:00:10	1,5	1452,48
	00:10:00	3	1456,27
0,5	00:00:10	9,5	1036,73
	00:10:00	14	1039,3
0,75	00:00:10	18,5	1033,33
	00:10:00	25	1045,94

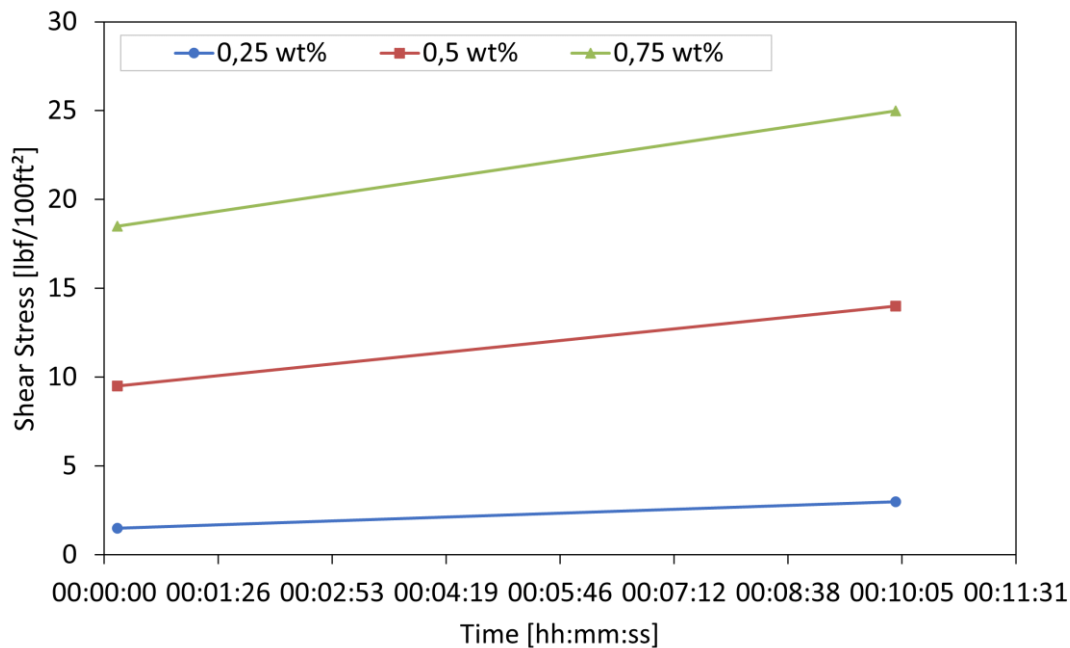


Figure 74: Gel strength [lbf/100ft²] flowzan

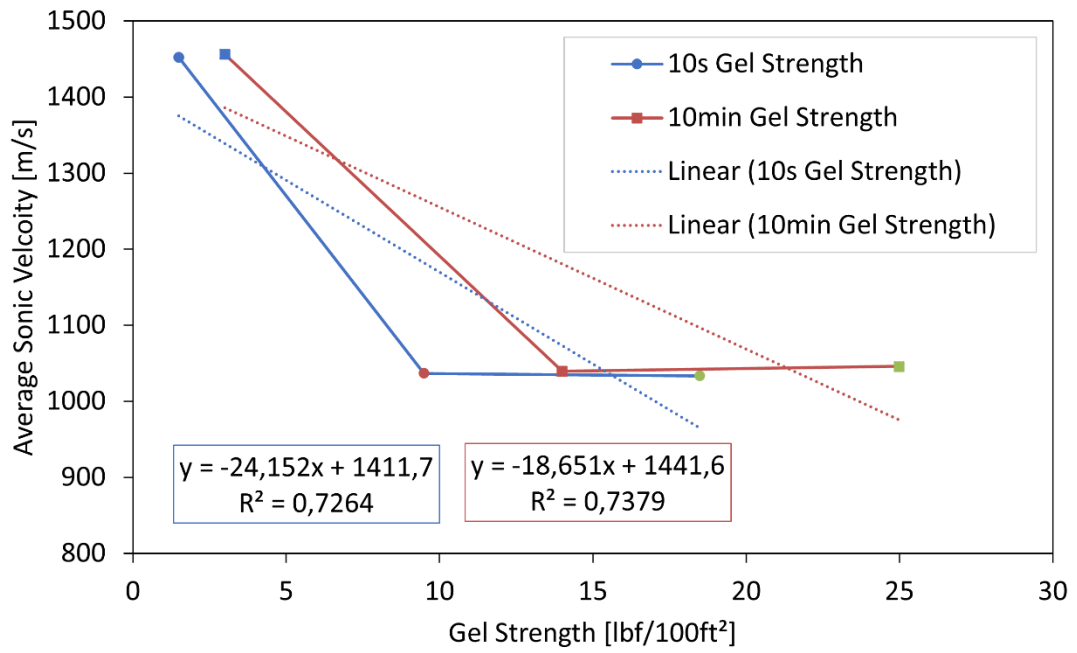


Figure 75: Gel strength [lbf/100ft²] vs. average sonic velocity [m/s]: flowzan - comparison of initial gel strength and 10min gel strength

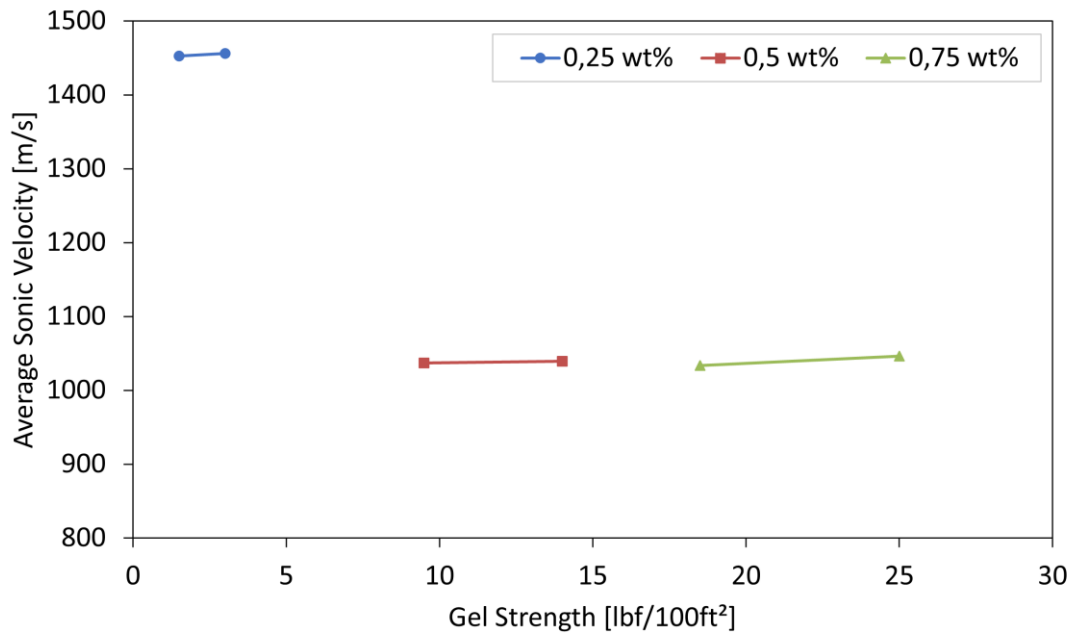


Figure 76: Gel strength [lbf/100ft²] vs. average sonic velocity [m/s]: flowzan - development of gel strength

Concentration Impact on Average Sonic Velocity:

The wt % of water concentration of flowzan has an impact on the sonic velocity only because of the bubbles that start to be suspended in the fluid, thus reducing the average sonic velocity drastically (drop of 420 m/s). In conclusion for flowzan the gel strength has an impact on the sonic velocity. Based on these results the concentration of flowzan has an impact on sonic velocity, since more air bubbles will be suspended in the fluid thus reducing the average sonic velocity drastically.

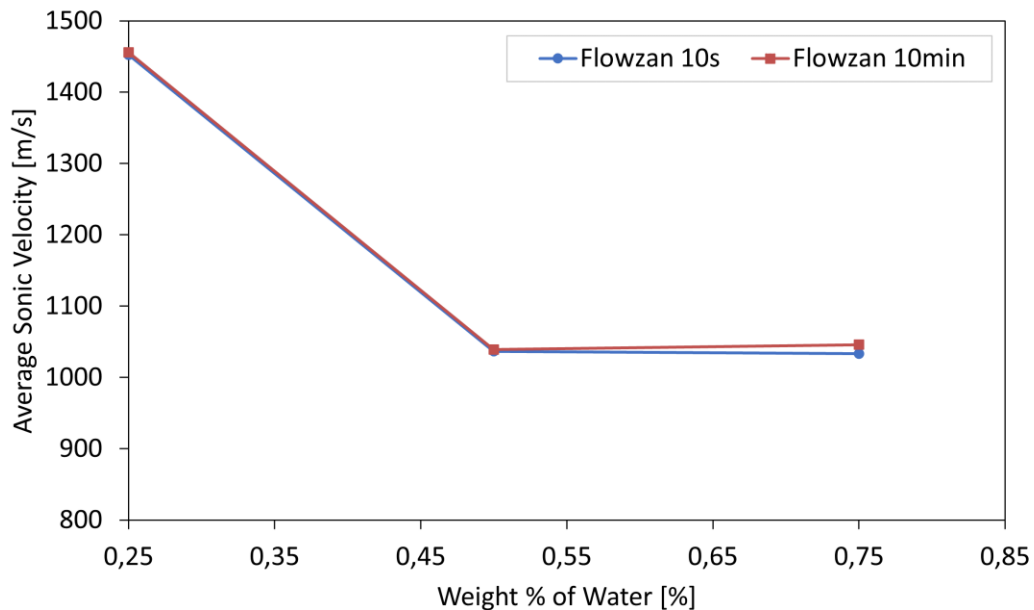


Figure 77: Weight % of water vs. average sonic velocity [m/s]: flowzan

5.1.2 Weighting Material

The density of all weighting materials is captured by a mud balance. The mass and volume of the soluble weighting materials dissolved in water is also measured to determine their density. This additional step has been taken because the pressurized mud balance had a systematic error thus not giving the correct density reading. Therefore, a graduated cylinder with an accuracy of ± 1 ml and a scale with $\pm 0,01$ g are used. The measurement is taken in SI-units and must then be converted to field units. To determine the average ultrasonic velocity of weighting materials in suspension (barite and CaCO_3) a viscosifier needs to be used. The selected viscosifier is laponite. Its low impact on ultrasonic velocity and lack of bubbles makes it a suitable viscosifier to analyze the data. The captured average ultrasonic velocity is then corrected for laponite. Therefore, the difference between the ultrasonic velocity of laponite and water is deducted from the average ultrasonic velocity of the weighting material.

Example:

For CaCO_3 2 wt % Laponite is used. During the test of laponite it was discovered that the average sonic velocity at this concentration is 1492 m/s. The difference between the measured average sonic velocity of water (1468,7 m/s) and 2 wt % laponite is 23,28 m/s. Every average sonic velocity value of the weighting material is then corrected by this value (23,28 m/s). This results in a shift in average sonic velocity as can be seen in Figure 78. After the correction the comparison between density and average ultrasonic velocity can be done.

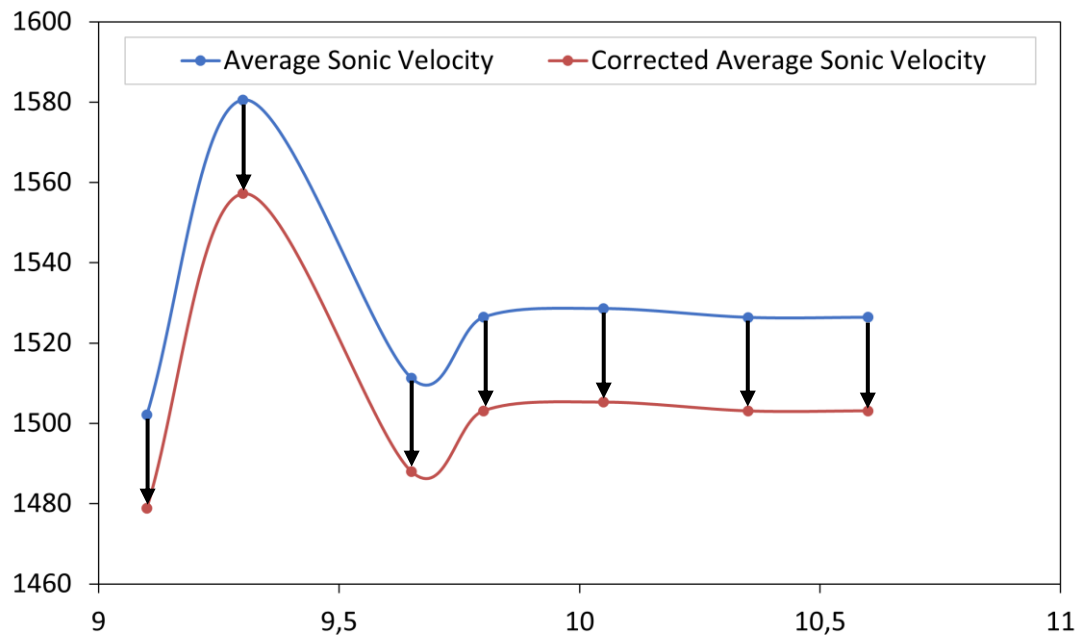


Figure 78: Viscosifier correction of CaCO_3

5.1.2.1 Barite

The result of the experiment can be observed in Figure 79. The value used to correct the data is 33,76 m/s. The data does not follow the linear trend properly, because due to the attenuation effect of the suspended barite it is really difficult to determine the average sonic velocity. The two apparent outliers are similar to the ones presented in (Motz et al. 1998). In the study by Motz, a mud was mixed using barite and bentonite. He also discovered that some densities have an increase in sonic velocity as can be seen in Figure 79 and Figure 80. He theorized that this is a mud specific property, but since in this study laponite was used as a viscosifier (instead of bentonite) and the same trend is observable it is more likely that the effect is due to the barite. Nevertheless, a downward trend is observable as previously seen during the feasibility study (Figure 10). This confirms that the trend observed is in fact due to the solids in suspension.

Table 28: Measured density and corrected average sonic velocity of barite.

Mud Balance Density [ppg]	Corrected Average Sonic Velocity [m/s]
9	1453,16
9,9	1463,82
10,85	1449,28
11,85	1449,28
12,95	1455,11
14	1449,32
15	1440,49

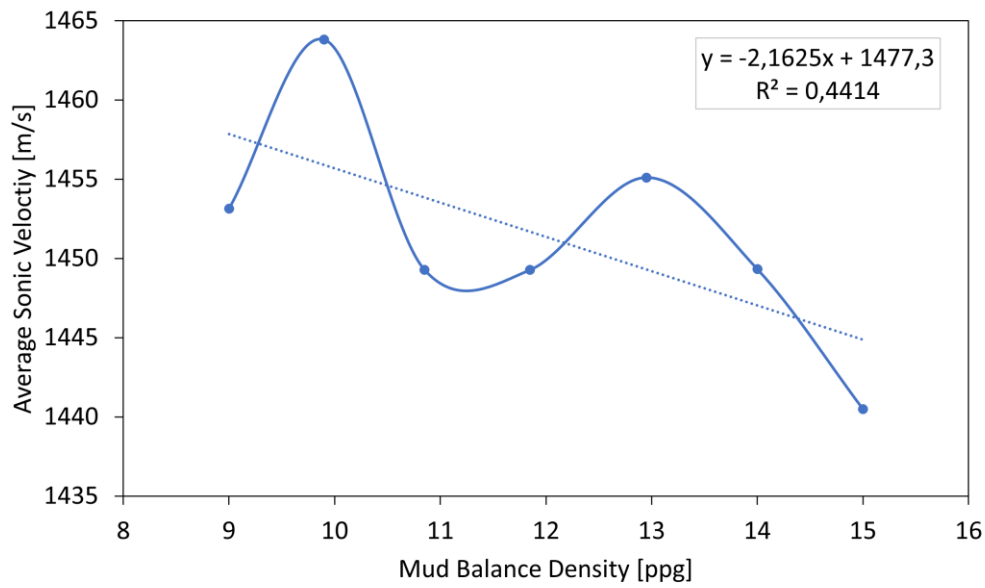


Figure 79: Comparison of average ultrasonic velocity [m/s] and mud balance density [ppg] of barite

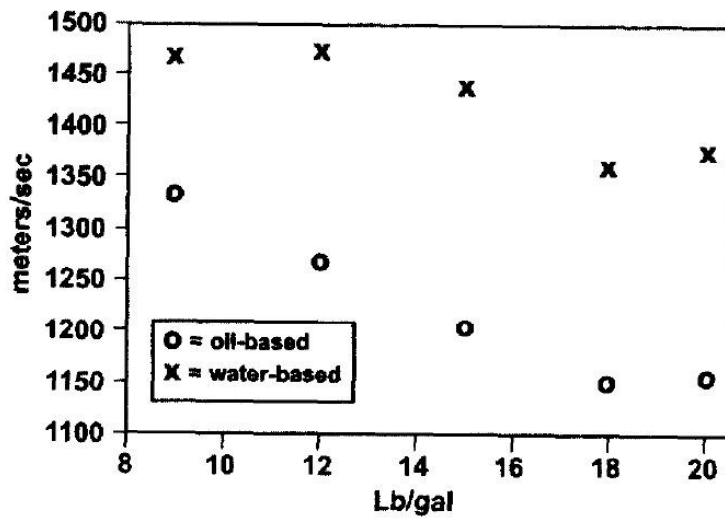


Figure 80: 180 kHz velocity versus mud weight (Motz et al. 1998)

5.1.2.2 Calcium Carbonate (CaCO₃)

The result of the experiment can be observed in Figure 81. The value used to correct the data is 23,28 m/s. It is very difficult to determine the average sonic velocity with confidence due to the attenuating effect of the suspended particles. Therefore, the average sonic velocity of 9,3 ppg might be a combination of human and system error. Another fascinating discovery is that starting at 9,8 ppg the change in average sonic velocity with increased density is very small. Further investigation into the ultrasonic behavior of different solid materials in suspension needs to be conducted to properly describe this phenomenon.

Table 29: Measured density and corrected average sonic velocity of CaCO₃.

Mud Balance Density [ppg]	Corrected Average Sonic Velocity [m/s]
9,1	1478,85
9,3	1557,27
9,65	1488,03
9,8	1503,14
10,05	1505,31
10,35	1503,12
10,6	1503,14

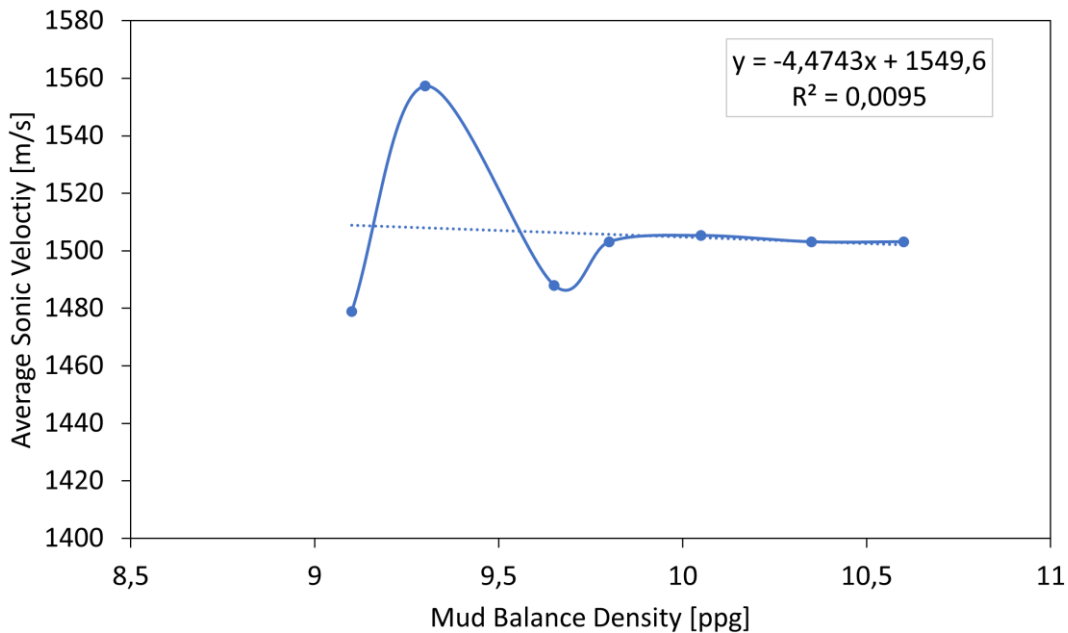


Figure 81: Comparison of average ultrasonic velocity [m/s] and mud balance density [ppg] of CaCO₃

5.1.2.3 Potassium Carbonate

K₂CO₃ is well described by a linear trend as can be seen in Figure 82. An increase in density results in an increase in average sonic velocity. Therefore, the increased amount of dissolved K₂CO₃ improves the capability of ultrasonic wave to propagate through the brine. The increased number of molecules allows for a better transmission of the wave since they are closely packed

together. This result is comparable to the water/brine mixture of the feasibility study (Figure 9). Both share the same behavior (increases average sonic velocity with an increase in density), and it can now be confirmed that the main contributor to this trend is the dissolved weighting material.

Table 30: Converted density and average sonic velocity of K_2CO_3 .

Converted Density [ppg]	Average Sonic Velocity [m/s]
9	1629,11
9,25	1654,18
9,48	1695,37
9,85	1752,88
9,93	1801,19
10,17	1854,17
10,48	1901,99

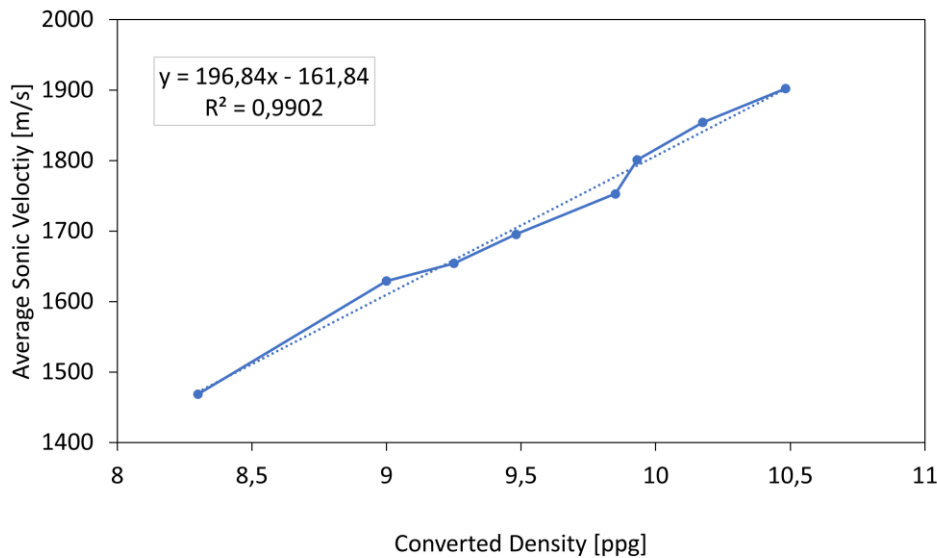


Figure 82: Comparison of average ultrasonic velocity [m/s] and converted density [ppg] of K_2CO_3

5.1.2.4 Sodium Carbonate (Na_2CO_3)

Na_2CO_3 is well described by a linear trend as can be seen in Figure 83. An increase in density results in an increase in average sonic velocity. Since Na_2CO_3 only substitutes the potassium of K_2CO_3 both share similar behavior. Comparing the 9 ppg average sonic velocity of K_2CO_3 (1629,11 m/s) and Na_2CO_3 (1679,63 m/s) shows that the ultrasonic wave propagates faster through the sodium carbonate brine. According to (O'Leary et al. 2015) this phenomenon is attributed to the effect of the adiabatic compressibility on sodium carbonate and potassium carbonate. In other words, if adiabatic compressibility decreases, it tends to increase the sonic velocity.

Table 31: Converted density and average sonic velocity of Na₂CO₃.

Converted Density [ppg]	Average Sonic Velocity [m/s]
8,50	1561,03
8,65	1596,20
8,75	1628,98
8,80	1655,08
9,00	1679,63
9,13	1718,60
9,28	1741,49

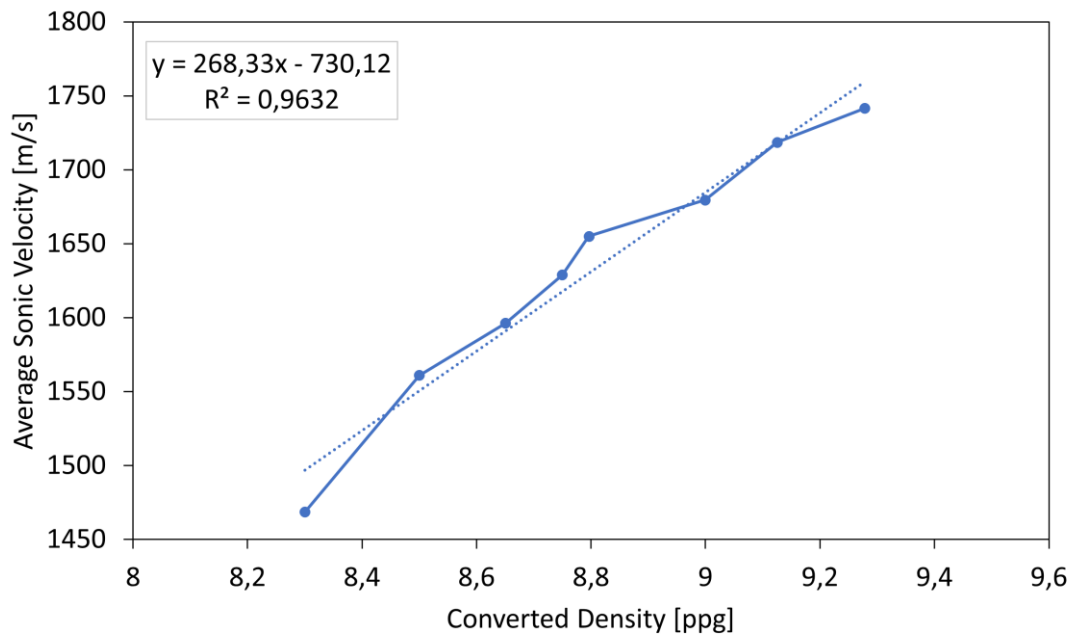


Figure 83: Comparison of average ultrasonic velocity [m/s] and mud balance density [ppg] of Na₂CO₃.

5.1.3 Other Additives

5.1.3.1 Citric Acid

Table 32 shows the experimental results of citric acid at varying concentrations. Water has also been included into the table to show how the pH changes with increased citric acid concentration. Citric acid is used in the oil and gas industry to adjust the pH of fluids and its effect can clearly be seen in the captured pH data. Figure 84 shows the effect of citric acid concentration on the sonic velocity. Between 0,5 wt % and 1,5 wt % only a difference of 3,39 m/s was recorded. Compared to water this is an increase of 13,43 m/s to 16,82 m/s at 0,5 wt % and 1,5wt % respectively. For this measurement the big testing chamber was used which has an average error of 0,22 % which equates to an error of $\pm 3,35$ m/s at highest concentration. Since this value is close to the 3,39 m/s it can be assumed that the sonic velocity is practically constant at these low concentrations. Still the concentration effect of citric acid on the sonic velocity is measurable and the results are comparable to those presented by (Jathi Ishwara Bhat et al. 2010) and can be used to correct future sonic velocities when citric acid needs to be added for pH control in baseline studies.

Table 32: Experimental data citric acid

Additive	Weight % of water	pH	Average Sonic Velocity [m/s]
Water	-	7,93	1507,80
Citric Acid	0,5	3,05	1521,23
	1	2,43	1521,88
	1,5	2,2	1524,62

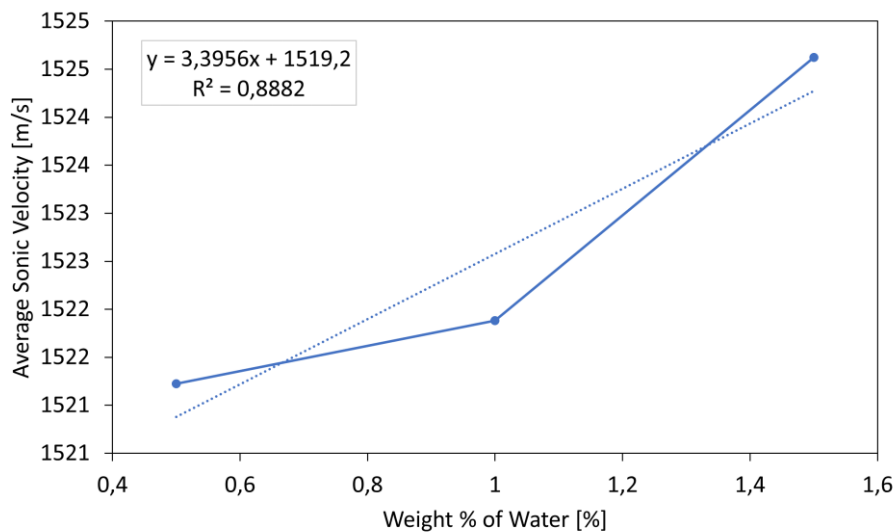


Figure 84: Weight % of water vs. average sonic velocity; citric acid

5.1.3.2 Caustic Soda

Table 33 shows the experimental results of caustic soda at varying concentrations. Water has also been included into the table to show how the pH changes with increased caustic soda concentration. Caustic soda is used in the oil and gas industry to adjust the pH of fluids and its effect can clearly be seen in the captured pH data. Figure 85 shows how the sonic velocity changes with increase in concentration of caustic soda. Between 0,5 wt % and 1,5 wt % a difference of 13,79 m/s was recorded. Compared to water this is an increase of 51,04 m/s to 64,83 m/s at 0,5 wt % and 1,5 wt % respectively. For this measurement, the big testing chamber was used which has an average error of 0,22 % which equates to an error of $\pm 3,46$ m/s at highest concentration. Since this value is not close to the 13,79 m/s it can be assumed that the sonic velocity is increasing with concentration. The concentration effect of caustic soda on the sonic velocity is obtainable and can be used to correct future sonic velocities when caustic soda needs to be added for pH control in baseline studies.

Even though the same amount of citric acid and caustic soda had been added to the testing fluid, caustic soda shows a stronger increase in sonic velocity. According to (Bitok J.K. 2013) the stronger increase in ultrasonic velocity is a consequence of the higher adiabatic coefficient of NaOH. During his research, it was also observed that even at low concentrations a big change in ultrasonic velocity is present. This result is comparable to the presented data in Table 33 and Figure 85.

Table 33: Experimental results for caustic soda

Additive	Weight % of water	pH	Average Sonic Velocity [m/s]
Water	-	7,93	1507,80
Caustic Soda (NaOH)	0,5	12,21	1558,84
	1	12,52	1566,80
	1,5	12,75	1572,63

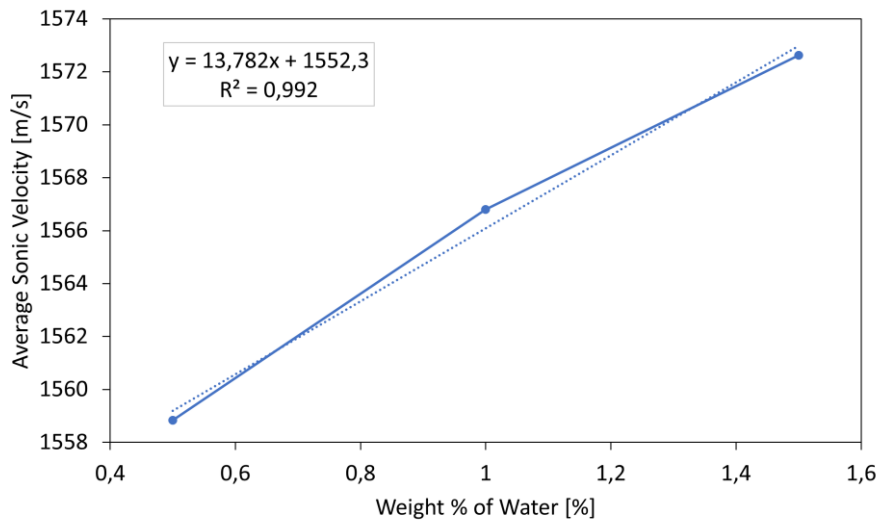


Figure 85: Weight % of water vs. average sonic velocity: caustic soda

5.1.3.3 Gypsum

The gathered average sonic velocity for gypsum can be observed in Figure 86. The increase in wt % results in a decrease in sonic velocity. The main difference between gypsum, caustic soda and citric acid is that gypsum is the only additive that is not dissolved in water. This again proves that suspended particles reduce the average sonic velocity with increasing concentrations. During the test it was observed that even at the lowest concentration (0,5 wt %) some gypsum is settling down at the bottom of the test chamber. When using a viscosifier to suspend these settled down particles, an even stronger reduction in average ultrasonic velocity is expected.

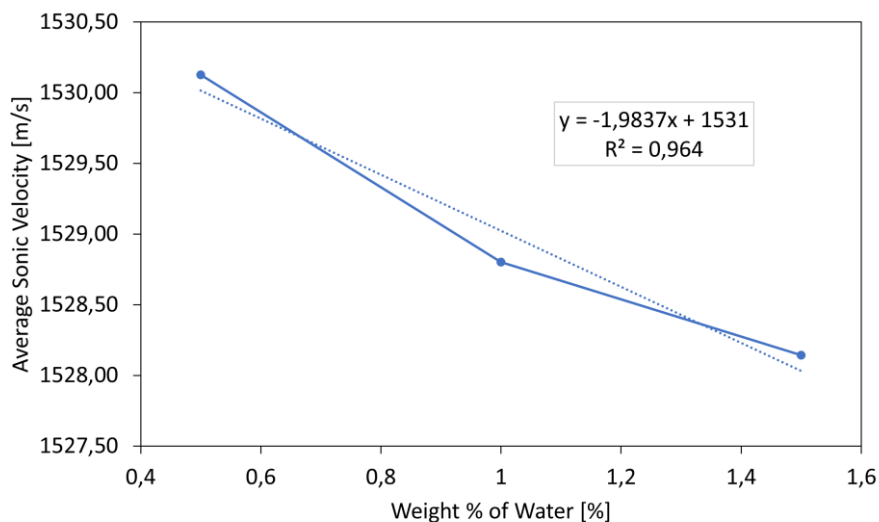


Figure 86: Weight % of water vs. average sonic velocity: gypsum

5.1.4 Proof of Concept Experiment

Three experiments are conducted, and the results are presented in the subsections below. These tests give an insight on how the presented master thesis can be used in the field or for future research.

5.1.4.1 Preliminary Fluid Study

The preliminary study is required to determine the coefficients presented in Table 35 required for Equation 1. The same measurement approach as for the weighting materials is used to determine the density and the average sonic velocity (Table 34). The captured data with the trendline equations can be seen in Figure 87 and Figure 88.

Table 34: Measured density, degree of intermixing and measured average sonic velocity of the preliminary fluid study.

Ratio	Degree of Intermixing	Density [ppg]	Average Sonic Velocity [m/s]
1:0	0,00%	9,15	1696,44
3:1	25,00%	9,5	1744,07
2:1	33,33%	9,55	1752,3
1:1	50,00%	9,7	1784,33
1:2	66,67%	9,85	1819,59
1:3	75,00%	9,9	1835,2
0:1	100,00%	10,1	1873,86

Table 35: Determined coefficients for density and intermixing calculations.

Coefficients for Density Calculation	
k	0,0051
d	0,5942
Coefficients for Intermixing Calculation	
k	0,0055
d	-9,3821

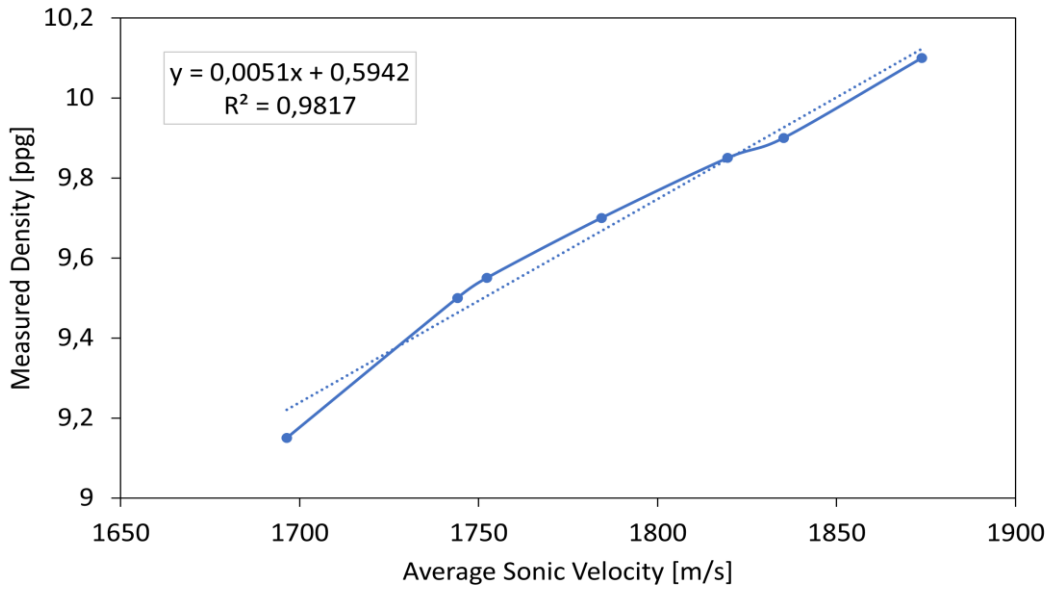


Figure 87: Measured density [ppg] compared to average sonic velocity [m/s] for the preliminary study.

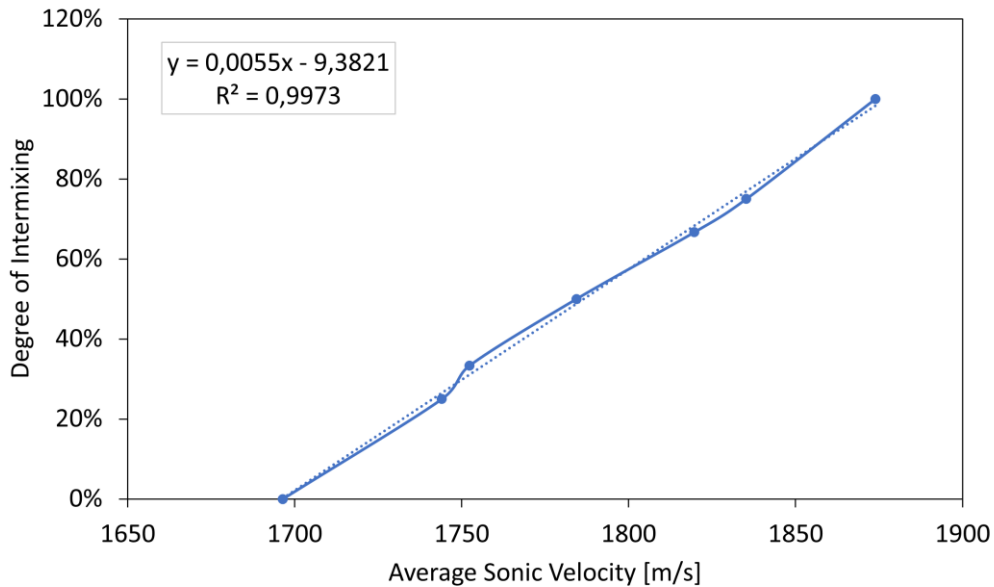


Figure 88: Degree of intermixing [%] compared to average sonic velocity [m/s] for the preliminary study.

5.1.4.2 Experiment 1

During this experiment, the first two samples are from the same batch of captured fluid. The experiment is still presented because Experiment 2 and 3 show that the first 200 ml of captured fluid share the same properties. Figure 89 shows the comparison between the density (calculated from the weight and volume measurement) and the calculated density using the

coefficients, generated during the initial study, and the measured average sonic velocity. To compare those two values a density error was determined as seen in Table 36. The resulting average error is 1,58 %. This value is acceptable, thus this technique to measure the density via the captured average sonic velocity can be applied in the presented manner. The effect of degree of intermixing on the average sonic velocity can be observed in Figure 90. The initial 25% of intermixing is caused by the presence of residual water in the disposal line. As the water is displaced, the degree of intermixing reduces until Fluid 1 is present. As the displacement continues the degree of intermixing continues to rise as a mixture of Fluid 1 and Fluid 2 is captured. A linear prediction is applied in Figure 91 to show how much additional volume is required to achieve full displacement. Approximately an additional 100ml are required as can be seen in Table 37. This means at 0,07 m/s flow velocity a total of 1,22 test section volumes needs to be displaced to achieve full displacement.

Table 36: Experimental data of Experiment 1

Sample	Density [kg/m ³]	Density [ppg]	Average Sonic Velocity [m/s]	Calculated Density [ppg]	Density Error	Calculated Degree of Intermixing
1	1061,19	8,86	1650,31	8,99	1,47%	25%
2	1070,93	8,94	1650,31	8,99	0,55%	25%
3	1069,40	8,92	1656,76	9,02	1,06%	22%
4	1086,58	9,07	1699,03	9,23	1,83%	2%
5	1136,47	9,48	1772,24	9,61	1,28%	42%
6	1142,39	9,53	1810,88	9,80	2,82%	63%
7	1162,43	9,70	1830,44	9,90	2,07%	74%

Table 37: Degree of intermixing and total volume prediction for Experiment 1

Sample	Volume [ml]	Summed Up Volumes [ml]	Degree of Intermixing
1	118	118	25%
2	118	236	25%
3	117	353	22%
4	114	467	2%
5	116	583	42%
6	92	675	63%
7	148	823	74%
Predicted Value		923,67	100%
Multiples of Test Section Volume		1,22	

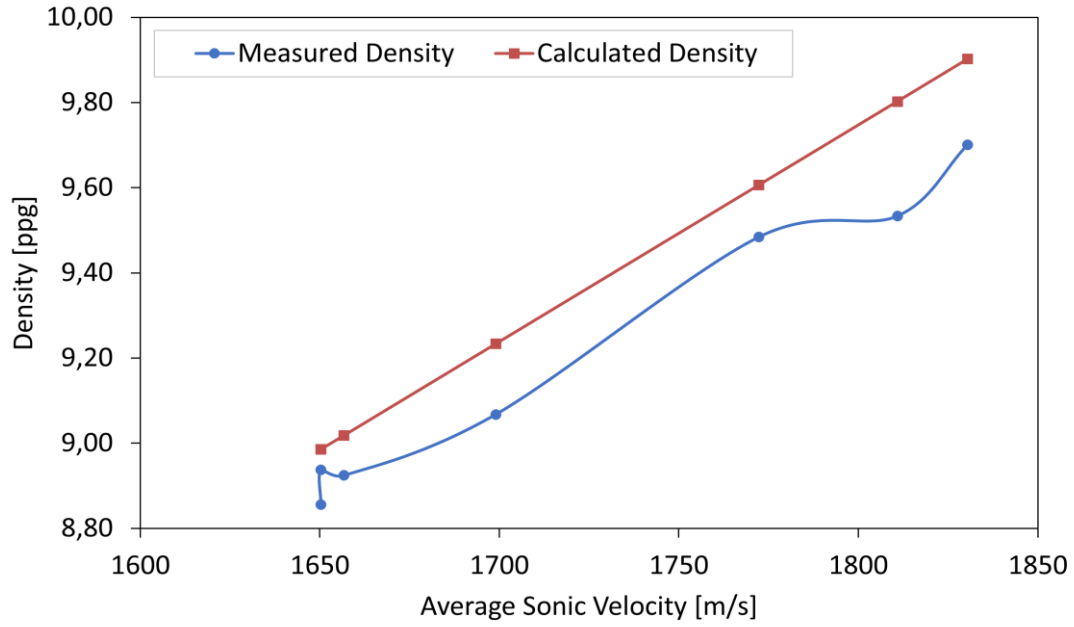


Figure 89: Comparison measured and calculated density [ppg] with average ultrasonic velocity [m/s] of Experiment 1

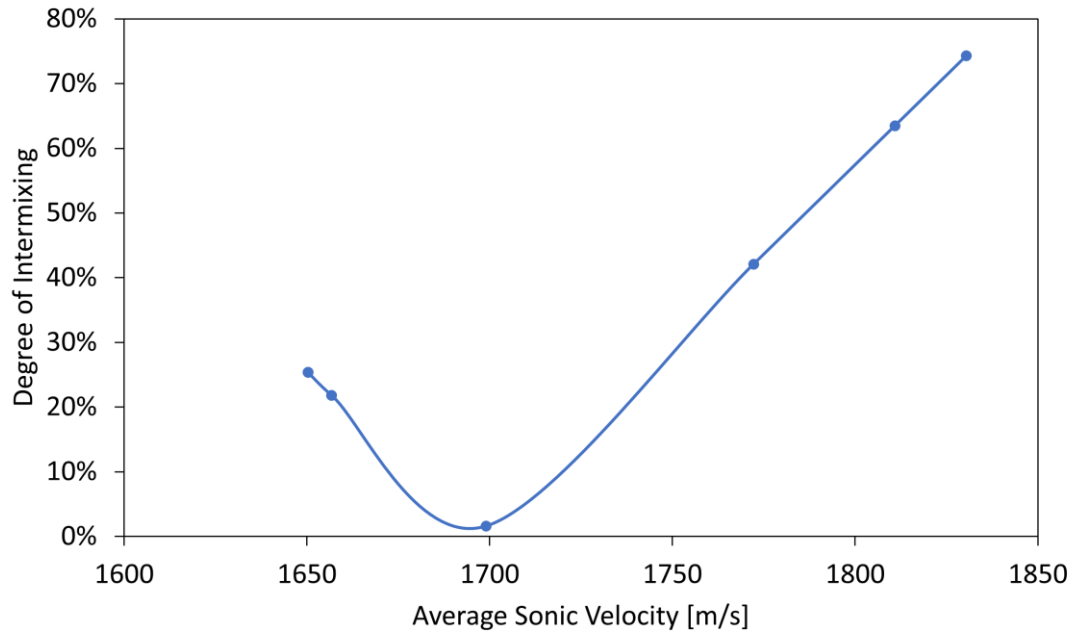


Figure 90: Comparison of degree of intermixing [%] and average sonic velocity [m/s] of Experiment 1

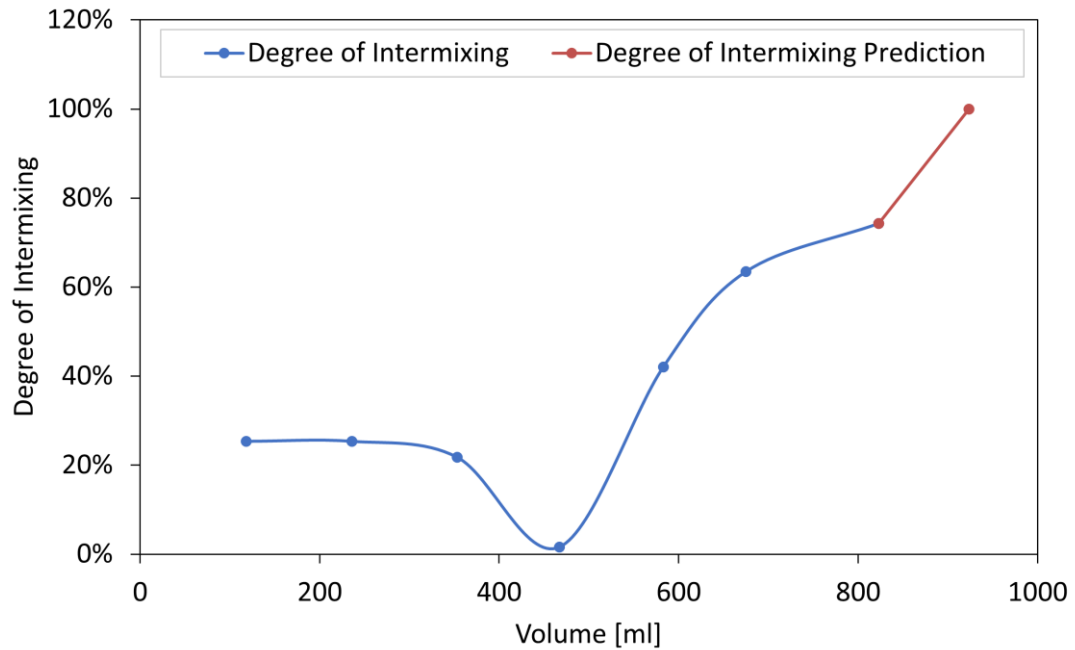


Figure 91: Comparison of degree of intermixing [%] with pumped volume [ml] and total volume prediction of Experiment 1

5.1.4.3 Experiment 2

Figure 92 shows the comparison between the density (calculated from the weight and volume measurement) and the calculated density using the coefficients, generated during the initial study, and the measured average sonic velocity. To compare those two values a density error was determined as seen in Table 38. The resulting average error is -0,92 %. This value is acceptable, thus this technique to measure the density via the captured average sonic velocity can be applied in the presented manner. The effect of degree of intermixing on the average sonic velocity can be observed in Figure 93. The datapoints for the first two (2) samples are very close together. Almost no change in average sonic velocity is recorded for the two fluid samples. A linear prediction is applied in Figure 94 to show how much additional volume is required to achieve full displacement. Approximately an additional 100 ml are required as can be seen in Table 37. This means at 0,16 m/s flow velocity a total of 1,21 test section volumes needs to be displaced to achieve full displacement. This prediction does not fit the degree of intermixing curve. The curve has the shape of a polynomial function; hence a linear prediction is not as accurate. Still, when a polynomial function is applied the resulting volume does not show a realistic value. To better predict the additional required volume to achieve full displacement more collection of samples with smaller volumes are required.

Table 38: Experimental data of Experiment 2

Sample	Density [kg/m ³]	Density [ppg]	Average Sonic Velocity [m/s]	Calculated Density [ppg]	Density Error	Calculated Degree of Intermixing
1	1118,43	9,33	1709,03	9,28	-0,53%	7%
2	1127,18	9,41	1706,55	9,27	-1,43%	6%
3	1149,66	9,59	1739,77	9,44	-1,60%	24%
4	1176,32	9,82	1788,25	9,69	-1,32%	51%
5	1181,95	9,86	1815,85	9,83	-0,36%	66%
6	1188,24	9,92	1826,5	9,88	-0,35%	72%
7	1196,64	9,99	1830,44	9,90	-0,84%	74%

Table 39: Degree of intermixing and total volume prediction for Experiment 2

Sample	Volume [ml]	Summed Up Volumes [ml]	Degree of Intermixing
1	115	115	7%
2	117	232	6%
3	116	348	24%
4	117	465	51%
5	118	583	66%
6	102	685	72%
7	140	825	74%
Predicted Value		923,14	100%
Multiples of Test Section Volume		1,21	

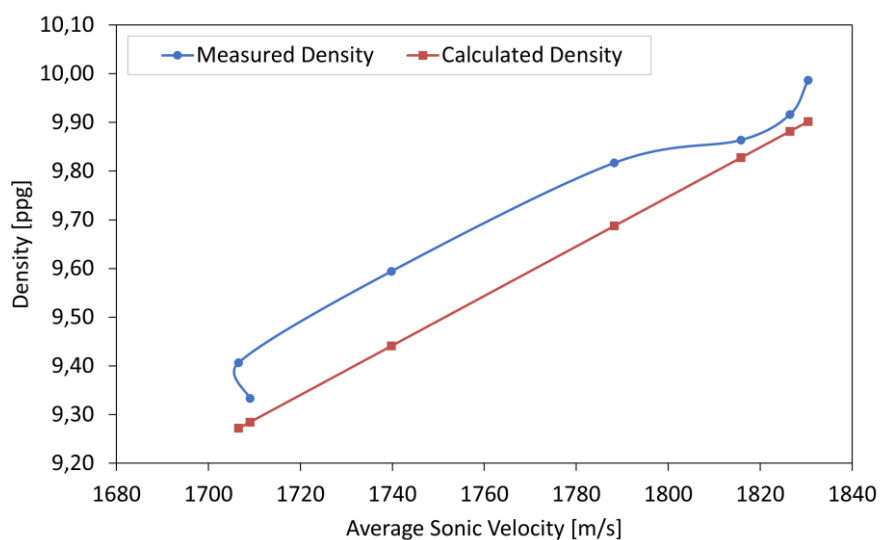


Figure 92: Comparison measured and calculated density [ppg] with average ultrasonic velocity [m/s] of Experiment 2

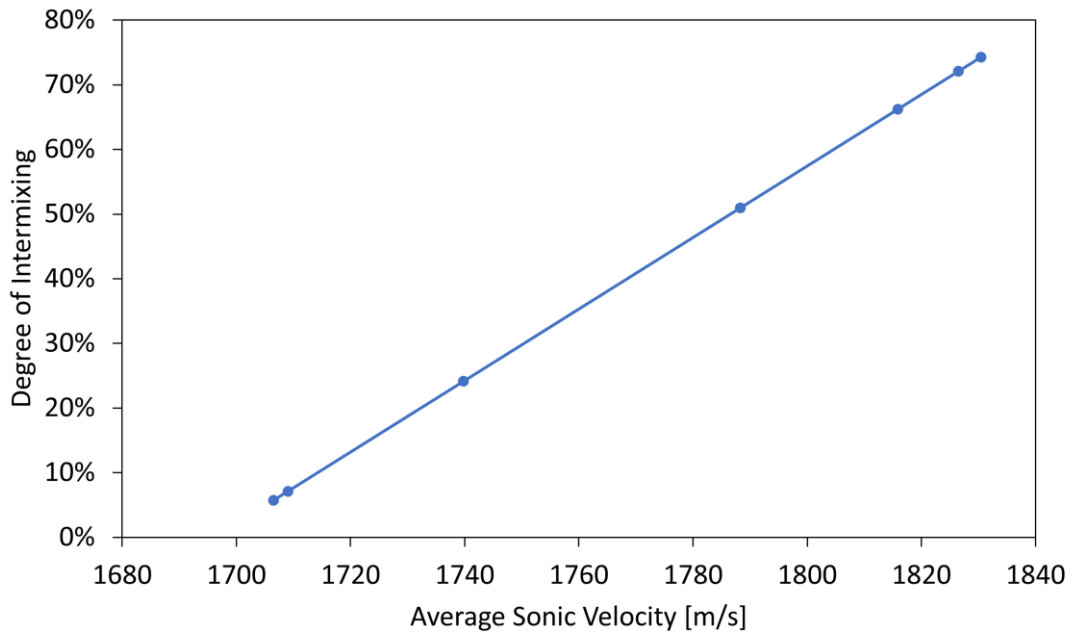


Figure 93: Comparison of degree of intermixing [%] and average sonic velocity [m/s] of Experiment 2

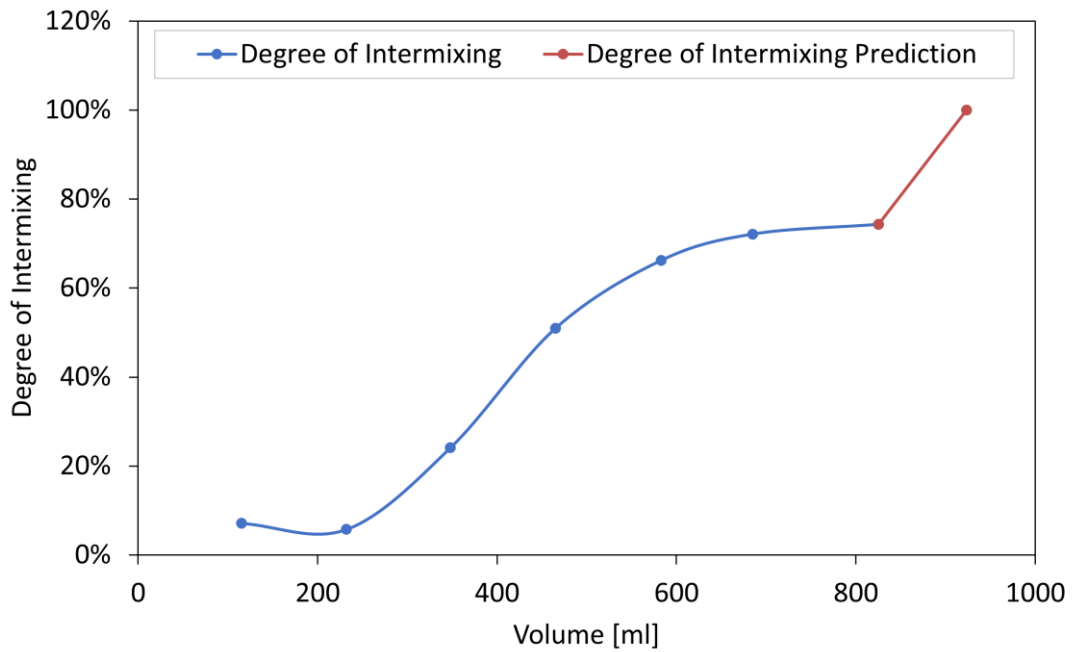


Figure 94: Comparison of degree of intermixing [%] with pumped volume [ml] and total volume prediction of Experiment 2

5.1.4.4 Experiment 3

Figure 95 shows the comparison between the density (calculated from the weight and volume measurement) and the calculated density using the coefficients, generated during the initial study, and the measured average sonic velocity. To compare those two values a density error

was determined as seen in Table 38. The resulting average error is -1,37 %. This value is acceptable, thus this technique to measure the density via the captured average sonic velocity can be applied in the presented manner. The effect of degree of intermixing on the average sonic velocity can be observed in Figure 96. The datapoints for the first two (2) samples are very close together. Almost no change in average sonic velocity is recorded for the two fluid samples. A linear prediction is applied in Figure 97 to show how much additional volume is required to achieve full displacement. Approximately an additional 90 ml are required as can be seen in Table 37. This means at 0,16 m/s flow velocity a total of 1,17 test section volumes needs to be displaced to achieve full displacement. This prediction does not fit the degree of intermixing curve. The curve has the shape of a polynomial function; hence a linear prediction is not as accurate. Still, when a polynomial function is applied the resulting volume does not show a realistic value. To better predict the additional required volume to achieve full displacement more collection of samples with smaller volumes are required.

Table 40: Experimental results Experiment 3.

Sample	Density [kg/m ³]	Density [ppg]	Average Sonic Velocity [m/s]	Calculated Density [ppg]	Density Error	Calculated Degree of Intermixing
1	1200,43	10,02	1832,34	9,91	-1,06%	75%
2	1212,50	10,12	1831,39	9,91	-2,09%	75%
3	1193,53	9,96	1814,91	9,82	-1,38%	66%
4	1163,73	9,71	1763,24	9,56	-1,56%	37%
5	1142,76	9,54	1742,35	9,45	-0,87%	26%
6	1140,42	9,52	1727,31	9,38	-1,47%	17%
7	1130,22	9,43	1715,96	9,32	-1,19%	11%

Table 41: Degree of intermixing and total volume prediction for Experiment 3

Sample	Volume [ml]	Summed Up Volumes [ml]	Degree of Intermixing
1	117	117	75%
2	120	237	75%
3	119	356	66%
4	118	474	37%
5	116	590	26%
6	118	708	17%
7	179	887	11%
Predicted Value		891,95	0%
Multiples of Test Section Volume		1,17	

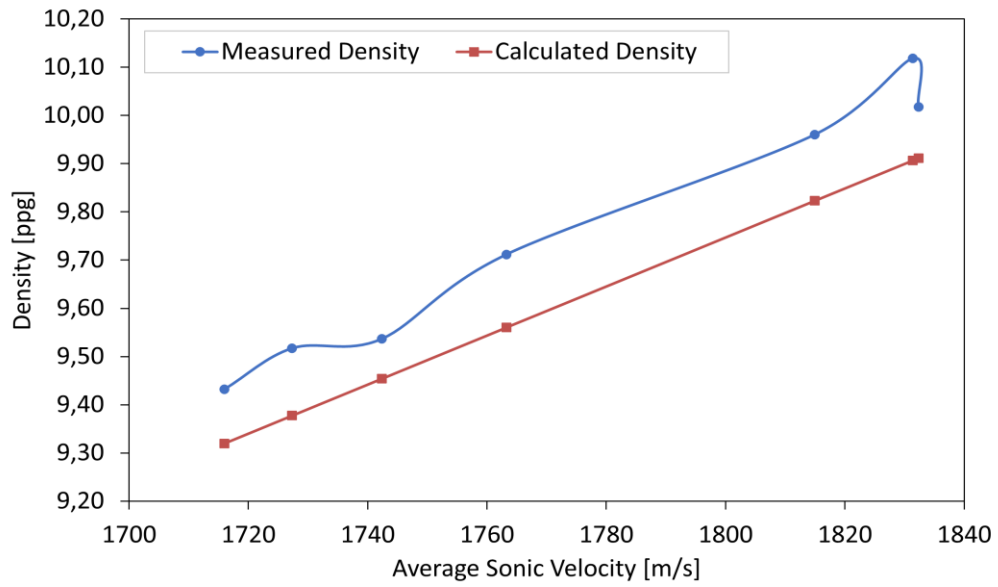


Figure 95: Comparison measured and calculated density [ppg] with average ultrasonic velocity [m/s] of Experiment 3

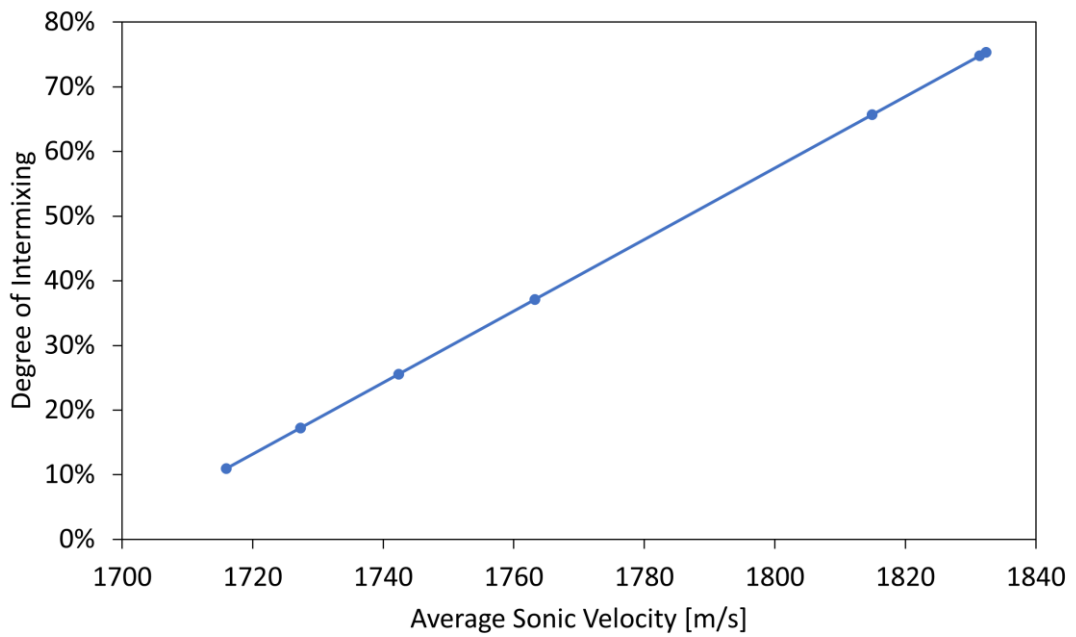


Figure 96: Comparison of degree of intermixing [%] and average sonic velocity [m/s] of Experiment 3

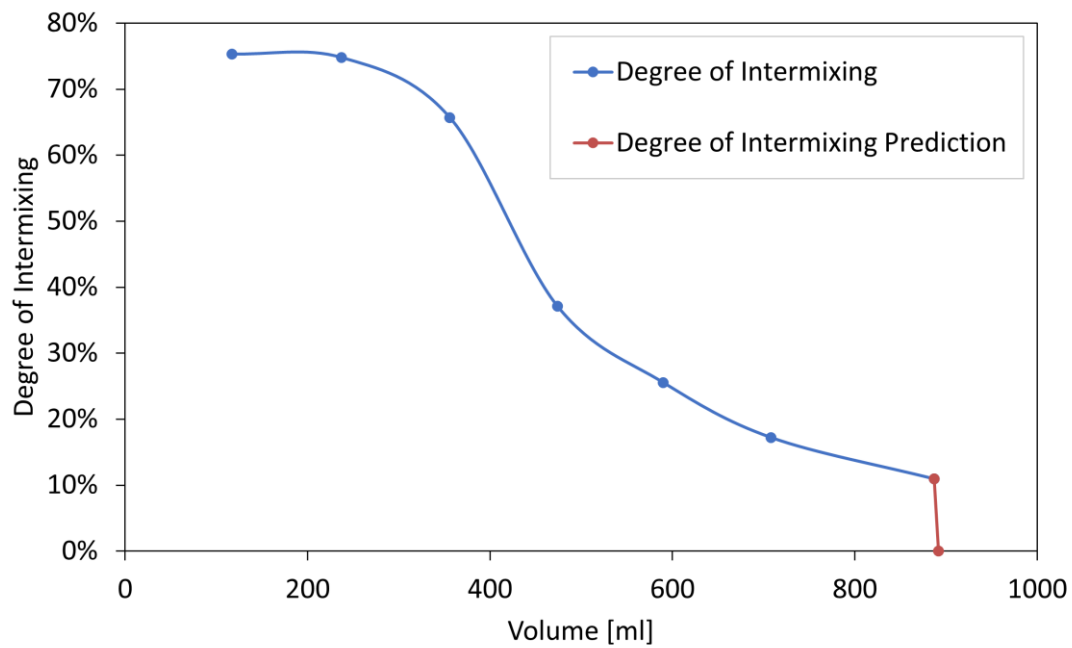


Figure 97: Comparison of degree of intermixing [%] with pumped volume [ml] and total volume prediction of Experiment 3

5.1.4.5 Triangulation Approach

The presented proof of concept experiment is a new approach to measure the degree of intermixing of a fluid. To validate this approach, it must be matched to a comparable data set. To do so the team at Montanuniversität Leoben conducted similar displacement tests and captured data using a highspeed camera and a spectrometer. The tests are conducted by displacing one fluid with a different weighted fluid. One of the fluids in this study is always water and the second fluid is a slightly weighted mud with viscosity (using PAC and 100 g of barite per 7l of water to have a contrast between the two fluids). The presented data below will only include two displacement experiments one at low flowrate and one at the medium setting of the pump. It needs to be noted that the fluids used during the highspeed, and spectrometer study are different from the ones presented in the experiments above. Unfortunately, it was not possible to rerun the experiment because the used spectrometer was lent to the team by a company. Nevertheless, the presented data is comparable to the degree of intermixing (Figure 91, Figure 94 and Figure 97). The darker fluid as seen in Figure 98 and Figure 99 is the test fluid and the white fluid is pure water. Furthermore, the presented data only shows the counts at a specific wavelength (365nm) which is the same as the emitted UV light. Before the test only water is in the test section and the UV-light can pass through the test section; hence giving high counts. Once displacement starts the light is increasingly obscured by the test fluid, thus reducing the counts until fully displaced. The average of the high values can be assumed as 0% displacement and the average of the low reading as 100% displacement. The shape of the presented data is comparable to the data captured in Experiment 1, 2 and 3. In future studies the data of the spectrometer, the highspeed camera and the ultrasonic sensors can be triangulated to confirm the validity of each measurement. The displacing fluid has a parabolic fluid front which is a trademark property of power law fluids as seen in Figure 98 and Figure 99. The fluctuation in the presented data is due to the UV-light source. A UV-bulb is used which is powered by the 50 Hz 230 V Austrian power grids. Here the frequency of the light is captured by the spectrometer because of its high capture frequency. In future experiments it is planned to use UV-LED lights to mitigate this problem. Additionally, the highspeed camera images have been correlated to the spectrometer data to represent what the captured data looks like in the test section. This whole experiment is presented in more detail in the master thesis of (Nico Masching 2023).

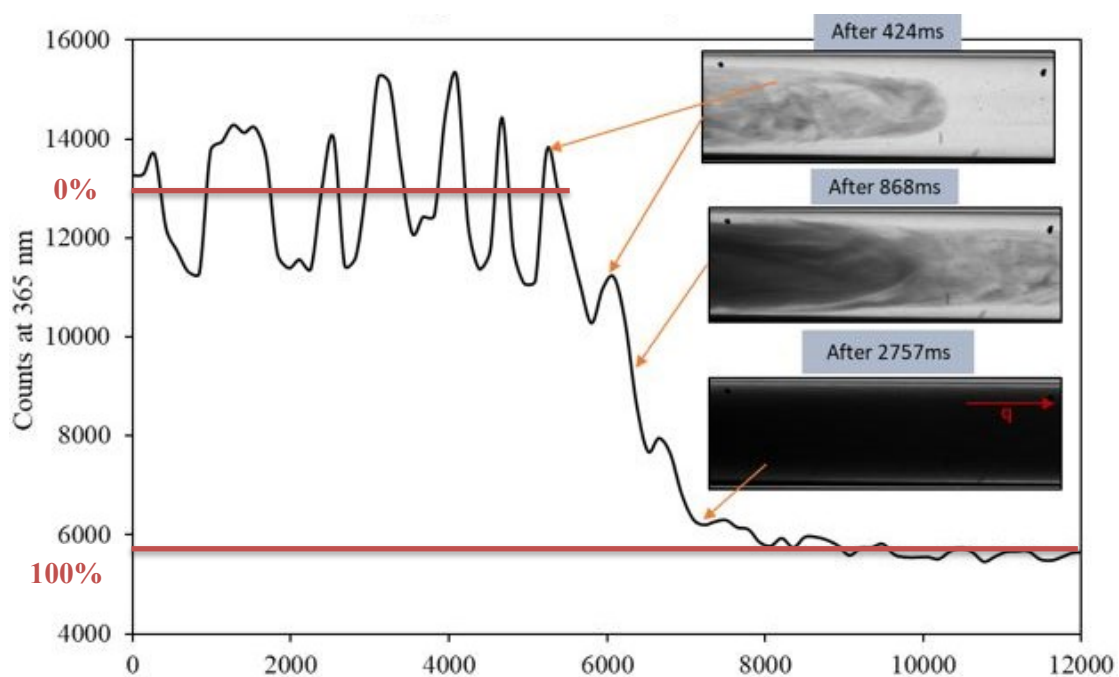


Figure 98: Spectrometer data of displacement experiment at 0,07m/s and 1,5 wt% PAC

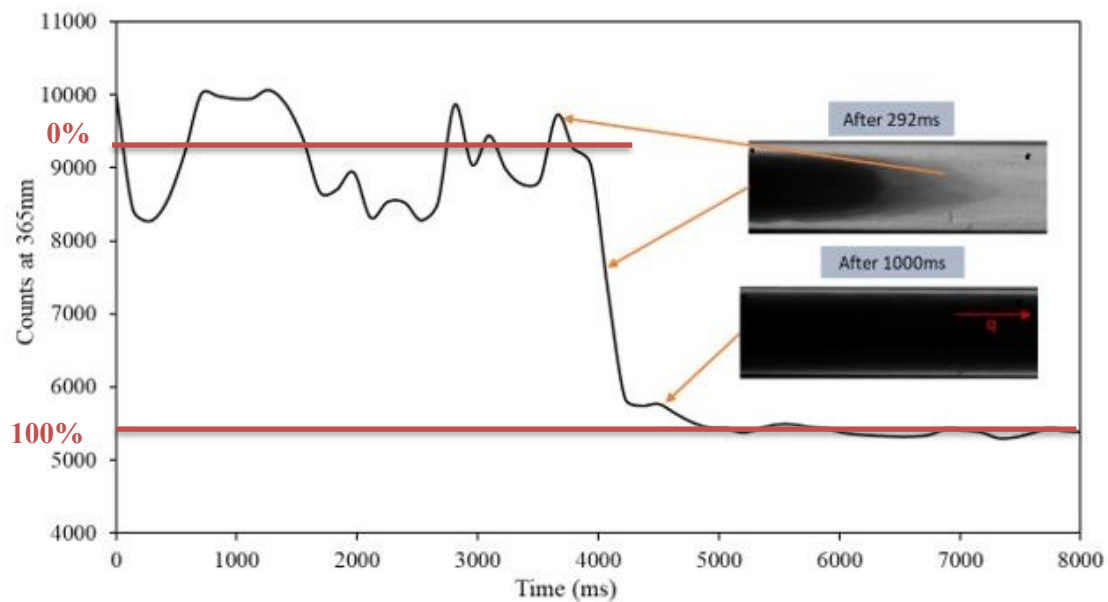


Figure 99: Spectrometer data of displacement experiment at 0,16m/s and 1,5 wt% PAC

Chapter 6

Conclusion

6.1 Summary

A feasibility study was conducted to see if it is possible to determine a density/average sonic velocity relationship. The feasibility study showed that the ultrasonic measurement approach is possible. During this study additional questions were developed which had been answered during the static single additive experiments.

In total 13 different additives had been analyzed using the custom-made ultrasonic setup. Therefore, fluids of different concentration of each additive were created and the average sonic velocity determined. Good results were achieved for viscosifiers which do not trap bubbles while being mixed. Especially xanthan gum and flowzan posed to be challenging fluids to determine their average sonic velocity due to the high number of bubbles. Good results were achieved using soluble weighting agents because their addition to the fluid makes it easier to measure the average sonic velocity. For insoluble weighting agents some challenges were faced due to their dampening effect on the ultrasonic wave. Good results have been achieved using other additives like citric acid and caustic soda. The results were comparable to the ones presented in soluble weighting agents. Gypsum posed some challenge due to its tendency to settle down. Based on this study an intrinsic understanding of the ultrasonic interaction with different commonly used additives were achieved.

Finally, a semi-dynamic proof of concept test was conducted to show how the acquired knowledge can be applied in the field. Two (2) muds of different density were mixed and displaced at different flowrates. Fluid discrimination, density evaluation, degree of intermixing calculation and required volume for full displacement prediction was successfully conducted and presented.

In conclusion fluid discrimination is possible, but a good understanding for each additive needs to be achieved. Only a fraction of used additives has been tested during this study and it is recommended to further develop the newly created data set. This approach has a future in the oil and gas industry to achieve a better understanding of the fluids in the borehole. The capability to determine the degree of intermixing can give a good insight if additional fluid volumes are required to have a full displacement.

6.2 Evaluation

The project objective was achieved during this work. The thesis has also identified directions and some questions for future work. The sonic velocity of single materials at different concentrations in water were captured and evaluated. A systematic approach to the measurement was presented and all challenges, achievements and results reported. The presented data is cross referenced with findings of other researchers and proposed theories were presented. Furthermore, the questions stated in the feasibility study were all successfully answered in the results and discussion section of this master thesis. A static density measurement for a mud/spacer was conducted during the feasibility study and the proof-of-concept experiment. No cement has been evaluated during this study because a lot of research has already been focused on this topic. A fully dynamic test on the benchtop could not be achieved due to setup restraints. The sensors could not be mounted onto the test section directly. As a compromise the fluid was captured in a semi-dynamic way (through the disposal line by opening and closing a valve).. A thorough compilation and analysis of the obtained data and an easy to implement approach for tests in the field was presented in this master thesis.

6.3 Future Work

During the tests of the viscosifiers, as expected they trap bubbles. It is possible to remove big bubbles by transferring the fluid from one container to another multiple times, but small bubbles remain. Another option is the application of a dispersant, but this could falsify the sonic velocity reading. Therefore, it is recommended to repeat the study and removing the bubbles in the fluid using a vacuum pump. This will result in an improved result.

While setting up the system, it was discovered that the oscilloscope is capturing noise created by electric devices in the room. Therefore, for future work it is recommended to use an electromagnetically sealed test setup.

Future setups can also be adjusted to be able to use sensors that can create stronger ultrasonic waves. This will allow for better penetration of fluids that are using insoluble weighting agents or viscosifiers that are suspending bubbles.

An interesting discovery was made while testing insoluble weighting agents and clay like viscosifiers. The sonic velocity did not change much during the test but the intensity of the signal changes significantly. During the gel strength test of laponite and bentonite it was discovered after 10 minutes that the intensity of the signal slightly increased. By comparing the area underneath the signal envelop it might be possible to determine the gel strength of a fluid. When using barite and calcium carbonate it was discovered that the intensity is reducing drastically with increased particle concentration. It is theorized that when comparing again the area underneath the signal envelope it is possible to determine the solids content in a fluid.

The overall experiment and gained knowledge are satisfactory, but more studies need to be employed to have a full understanding of drilling fluids. This is just the beginning of a database to capture all additives in the oil and gas industry. Therefore, more tests can be conducted in the future. Furthermore, only a semi-dynamic test has been conducted. Future setups can also be adjusted to be able to measure the average sonic velocity through a pipe setup. The setup can also be adjusted to again use a one sensor setup (sender and receiver in one sensor) to be able to measure an annular space.

References

- Abdul Kareem J- Al-Bermamy; Nadia Hussein Sahib (2013): Study Of Some Mechanical Properties Of High Viscosity Carboxy Methyl Cellulose Using Ultrasonic Wave System. In *Journal of University of Babylon* □□□□ □□□□□ □□□□ 21 (4), pp. 1439–1446.
- Adamowski, Julio; Buiocchi, Flávio; Simon, Claudio; Silva, Emílio; Sigelmann, Rubens (1995): Ultrasonic measurement of density of liquids. In *Acoustical Society of America Journal* 97, pp. 354–361. DOI: 10.1121/1.412320.
- Alkhaldi, M. H.; Nasr-El-Din, H. A.; Sarma, H. K. (2009): Application of Citric Acid in Acid Stimulation Treatments. In. Canadian International Petroleum Conference, PETSOC-2009-015, checked on 2/2/2023.
- APG Netzfrequenz (2023):
<https://markttransparenz.apg.at/markt/Markttransparenz/Netzregelung/Netzfrequenz>.
Available online at
<https://markttransparenz.apg.at/markt/Markttransparenz/Netzregelung/Netzfrequenz>, updated on 1/3/2023, checked on 1/3/2023.
- Barnard, A. J., JR. (1960): Organic Sequestering Agents (Chaberek, Stanley; Martell, Arthur E.). In *Journal of Chemical Education* 37 (4), p. 216. DOI: 10.1021/ed037p216.1.
- Bisley International (2022): What is CMC in Drilling Mud | Bisley International LLC.
Available online at <https://bisleyinternational.com/what-is-cmc-in-drilling-mud/>, updated on 7/18/2022, checked on 12/28/2022.
- Bitok J.K. (2013): Ultrasonic Studies in Aqueous Solutions, pp. 113–119. DOI: 10.5194/gi-2016-11-RC2.
- Bleiwas, Donald I.; Miller, M. Michael (2015): Barite: a case study of import reliance on an essential material for oil and gas exploration and development drilling. With assistance of

U.S. Geological Survey. Reston, VA (Scientific Investigations Report, 2014-5230). Available online at <http://pubs.er.usgs.gov/publication/sir20145230>.

Chen, Zhongming; Chaudhary, Saleem; Shine, Joe (2014): Intermixing of Cementing Fluids: Understanding Mud Displacement and Cement Placement. In *SPE/IADC Drilling Conference, Proceedings 1*. DOI: 10.2118/167922-MS.

Chevron Phillips Chemical (2023): FLOWZAN® Biopolymer. Available online at <https://www.cpchem.com/what-we-do/solutions/drilling-specialties/products/flowzanr-biopolymer>, updated on 2/8/2023, checked on 2/8/2023.

de Acj Arie Korte; H. J. H. Brouwers (2010): Ultrasonic sound speed measurement as method for the determining the hydration degree of gypsum. In.

eritia (2018): Gypsum (Gyp) Muds. In *AiPu Solids Control*, 4/19/2018. Available online at <https://drillingfluid.org/drilling-fluids-handbook/gypsum-gyp-muds.html>, checked on 12/28/2022.

foaming_agent (2022). Available online at https://glossary.slb.com/en/terms/f/foaming_agent, updated on 11/8/2022, checked on 11/8/2022.

Gogoi, Subrata; Talukdar, Prasenjit (2015): Use of Calcium Carbonate as bridging and weighting agent in the Non Damaging Drilling Fluid for some oilfields of Upper Assam Basin. In *International J. of Current Science 7*, pp. 18964–18981.

Guru, G.; Prasad, Pranish; Hosalike, Shivakumar; Rai, Sheshappa (2008): Studies on the Compatibility of Pullulan - Carboxymethyl Cellulose Blend Using Simple Techniques.

Hall, B. E.; Dill, W. R. (1988): Iron Control Additives for Limestone and Sandstone Acidizing of Sweet and Sour Wells. In. SPE Formation Damage Control Symposium, SPE-17157-MS, checked on 2/2/2023.

Halmshaw, R. (Ed.) (1996): Introduction to the Non-Destructive Testing of Welded Joints (Second Edition) : Woodhead Publishing Series in Welding and Other Joining Technologies: Woodhead Publishing.

Hemmati-Sarapardeh, Abdolhossein; Schaffie, Mahin; Ranjbar, Mohammad; Dong, Mingzhe; Li, Zhaomin (Eds.) (2022): Chemical Methods : Enhanced Oil Recovery Series: Gulf Professional Publishing.

Huang, Xian-Bin; Sun, Jin-Sheng; Huang, Yi; Yan, Bang-Chuan; Dong, Xiao-Dong; Liu, Fan; Wang, Ren (2021): Laponite: a promising nanomaterial to formulate high-performance water-based drilling fluids. In *Petroleum Science 18 (2)*, pp. 579–590. DOI: 10.1007/s12182-020-00516-z.

- Jandhyala, Siva Rama; Pangu, Ganesh; Deshpande, Abhimanyu; Wolterbeek, Tim; Cornelissen, Erik; van Eijden, Jip (2018): Volume Change of Cement Plugs: Spotlight on the Role of Boundary Conditions Using an Improved Testing Method. In. SPE Asia Pacific Oil and Gas Conference and Exhibition, D012S032R001, checked on 10/24/2022.
- Jathi Ishwara Bhat; M. N. Manjunatha; N. S. Shree Varaprasad (2010): Acoustic behaviour of citric acid in aqueous and partial aqueous media. In *Indian Journal of Pure & Applied Physics* 48, pp. 875–880.
- Khalifeh, Mahmoud; Saasen, Arild (2020): General Principles of Well Barriers. In Mahmoud Khalifeh, Arild Saasen (Eds.): *Introduction to Permanent Plug and Abandonment of Wells*. Cham: Springer International Publishing, pp. 11–69.
- Kimura, Shun; Kitayama, Kazumi; Takahashi, Hideharu; Kimoto, Kazushi; Kawamura, Katsuyuki; Kikura, Hiroshige (2018): Longitudinal and Shear Wave Velocities Measurement in Compacted Bentonite for Water Content. In *E3S Web of Conferences* 43, p. 1016. DOI: 10.1051/e3sconf/20184301016.
- Korte, A. C. J. de; Brouwers, H. J. H. (2011): Ultrasonic sound speed analysis of hydrating calcium sulphate hemihydrate. In *Journal of Materials Science* 46 (22), pp. 7228–7239. DOI: 10.1007/s10853-011-5682-6.
- Krautkrämer, Josef; Krautkrämer, Herbert (1990): *Ultrasonic testing of materials*. With assistance of W. Grabendörfer. 4th Fully revised edition. Berlin, Heidelberg: Springer Berlin Heidelberg. Available online at <https://ebookcentral.proquest.com/lib/kxp/detail.action?docID=3099756>.
- Krishna, Shwetank; Thonhauser, Gerhard; Kumar, Sunil; Elmgerbi, Asad; Ravi, Krishna (2022): Ultrasound velocity profiling technique for in-line rheological measurements: A prospective review. In *Measurement* 205, p. 112152. DOI: 10.1016/j.measurement.2022.112152.
- Lee, L., Rogers, P., Oakley, V. L., & Navarro, J. (1997): Investigations into the use of Laponite as a poulticing material in ceramics conservation (22). Available online at <http://www.vam.ac.uk/content/journals/conservation-journal/issue-22/investigations-into-the-use-of-laponite-as-a-poulticing-material-in-ceramics-conservation/>, checked on 2/8/2023.
- Mahmood, Ahmad Abdullah; Rasheed, Hassaan; Jan, Usman Ahmed; Khan, Anum Yousuf; Salazar, Jose (2022): Well Integrity Under Dynamic Stresses Using Flexible Cement Systems. In. IADC/SPE Asia Pacific Drilling Technology Conference and Exhibition, D022S004R003, checked on 10/24/2022.

- Manager, Aong (2017): how Drilling Fluid Additives are classified. In *AONG*, 8/1/2017. Available online at <https://www.arab-oil-naturalgas.com/how-drilling-fluid-additives-are-classified/>, checked on 11/8/2022.
- Manual, Drilling (2020): Rheometer Test Method | Drilling Fluid Viscometer. In *Drilling Manual*, 9/22/2020. Available online at <https://www.drillingmanual.com/drilling-fluid-vescometer-testing-rheometer-method/>, checked on 12/28/2022.
- Manual, Drilling (2021): Lost Circulation Material In Drilling. In *Drilling Manual*, 1/17/2021. Available online at <https://www.drillingmanual.com/lost-circulation-lcm-materials-drilling-oil-gas/#h-main-types-of-lost-circulation-material>, checked on 11/8/2022.
- Manual, Drilling (2022): Drilling Mud Properties Guide In Oil & Gas Wells. In *Drilling Manual*, 3/2/2022. Available online at <https://www.drillingmanual.com/drilling-mud-fluid-properties/#h-viscosity-properties-of-drilling-mud>, checked on 12/28/2022.
- Menezes, R. R.; Marques, L. N.; Campos, L. A.; Ferreira, H. S.; Santana, L.N.L.; Neves, G. A. (2010): Use of statistical design to study the influence of CMC on the rheological properties of bentonite dispersions for water-based drilling fluids. In *Applied Clay Science* 49 (1), pp. 13–20. DOI: 10.1016/j.clay.2010.03.013.
- Motz, Eric; Canny, Duane; Evans, Eddie (1998): Ultrasonic Velocity And Attenuation Measurements In High Density Drilling Muds. In. SPWLA 39th Annual Logging Symposium, SPWLA-1998-F, checked on 2/1/2023.
- Nabiyev, Kamran: The impact of different concentrations of viscosifiers on rheological properties of invert emulsion mud.
- Navarrete, R. C.; Himes, R. E.; Scheult, J. M. (2000): Applications of Xanthan Gum in Fluid-Loss Control and Related Formation Damage. In. SPE Permian Basin Oil and Gas Recovery Conference, SPE-59535-MS, checked on 12/28/2022.
- NEA Group (2023): Bentonite in Drilling Mud. Available online at <https://www.neuman-esser.de/en/company/media/bentonite-in-drilling-mud/>, updated on 2/8/2023, checked on 2/8/2023.
- Nico Masching (2023): Fluid Displacement Study of Various Non-Newtonian Fluids in a Digitalized Flow Setup. Master Thesis. Montanuniversität Leoben, Leoben, Austria. Drilling and Production Engineering.
- O’Leary, Mary; Lange, Rebecca; ai, Yixin (2015): The compressibility of CaCO₃-Li₂CO₃-Na₂CO₃-K₂CO₃ liquids: Application to natrocarbonatite and CO₂-bearing nephelinite

liquids from Oldoinyo Lengai. In *Contributions to Mineralogy and Petrology* 170. DOI: 10.1007/s00410-015-1157-0.

Oxy (2013): Product Stewardship Summary Potassium Carbonate. Available online at https://www.oxy.com/globalassets/documents/chemicals/stewardship/potassium-carbonate.pdf?_t_id=KVxbZhWrOcH593n81F1wjQ%3d%3d&_t_uuid=10_rPU7Tna6IHnScx21PA&_t_q=potassium+carbonate&_t_tags=language%3aen%2csiteid%3a7f9734a7-a207-4e8e-b441-c6286e2844cb%2candquerymatch&_t_hit.id=Oxy_Com_Logic_Models_Media_GenericFile_953ab5aa-8f56-499b-98db-a5db723e5b38&_t_hit.pos=1, checked on 1/2/2023.

Paul Wagner (2020a): Real-Time Monitoring of the Effect of Carbon Dioxide on the Cement Sheath. University of Leoben. Available online at [https://pure.unileoben.ac.at/portal/en/publications/realtime-monitoring-of-the-effect-of-carbon-dioxide-on-the-cement-sheath\(55dd59e9-d598-4e20-a9a4-63aceb3beada\).html?customType=theses](https://pure.unileoben.ac.at/portal/en/publications/realtime-monitoring-of-the-effect-of-carbon-dioxide-on-the-cement-sheath(55dd59e9-d598-4e20-a9a4-63aceb3beada).html?customType=theses).

Paul Wagner (2020b): Real-Time Monitoring of the Effect of Carbon Dioxide on the Cement Sheath. University of Leoben. Available online at [https://pure.unileoben.ac.at/portal/en/publications/realtime-monitoring-of-the-effect-of-carbon-dioxide-on-the-cement-sheath\(55dd59e9-d598-4e20-a9a4-63aceb3beada\).html?customType=theses](https://pure.unileoben.ac.at/portal/en/publications/realtime-monitoring-of-the-effect-of-carbon-dioxide-on-the-cement-sheath(55dd59e9-d598-4e20-a9a4-63aceb3beada).html?customType=theses).

Persianutab (2021): Citric acid in drilling fluids. Available online at <https://persianutab.com/citric-acid-in-drilling-fluids/?lang=en>, updated on 3/6/2021, checked on 2/2/2023.

Pico (2020): PicoScope 6 User's Guide. Available online at <https://www.picotech.com/download/manuals/picoscope-6-users-guide.pdf>, checked on 3/1/2023.

Poletto, Flavio; Carcione, José; Lovo, Massimo; Miranda, F. (2002): Acoustic velocity of seismic-while-drilling (SWD) borehole guided waves. In *Geophysics* 67. DOI: 10.1190/1.1484534.

POVEY, MALCOLM J.W. (Ed.) (1997): *Ultrasonic Techniques for Fluids Characterization*. San Diego: Academic Press.

Rig Worker (2022): Gel Strength Measurement Procedures - Drilling Engineering. Available online at <https://www.rigworker.com/engineering-3/gel-strength-measurement-procedures.html>, updated on 10/10/2022, checked on 11/8/2022.

Shadravan, Arash; Narvaez, Guido; Alegria, Adriana; Carman, Paul; Perez, Cresencio; Erger, Robert (2015): Engineering the Mud-Spacer-Cement Rheological Hierarchy Improves Wellbore Integrity. In. SPE E&P Health, Safety, Security and Environmental Conference-Americas, SPE-173534-MS, checked on 10/23/2022.

SLB Energy Glossary - Bentonite (2023). Available online at <https://glossary.slb.com/en/terms/b/bentonite>, updated on 2/8/2023, checked on 2/8/2023.

SLB Energy Glossary - calcium carbonate (2023). Available online at https://glossary.slb.com/en/terms/c/calcium_carbonate, updated on 2/1/2023, checked on 2/1/2023.

SLB Energy Glossary - Caustic soda (2023). Available online at https://glossary.slb.com/en/terms/c/caustic_soda, updated on 2/2/2023, checked on 2/2/2023.

SLB Energy Glossary - Citric acid (2023). Available online at https://glossary.slb.com/en/terms/c/citric_acid, updated on 2/2/2023, checked on 2/2/2023.

SLB Energy Glossary - CMC (2023). Available online at <https://glossary.slb.com/en/terms/c/cmc>, updated on 2/8/2023, checked on 2/8/2023.

SLB Energy Glossary - Gyp mud (2023). Available online at https://glossary.slb.com/en/terms/g/gyp_mud, updated on 2/8/2023, checked on 2/8/2023.

SLB Energy Glossary - potassium mud (2023). Available online at https://glossary.slb.com/en/terms/p/potassium_mud, updated on 2/1/2023, checked on 2/1/2023.

SLB Energy Glossary - Sodium carbonate (2023). Available online at https://glossary.slb.com/en/terms/s/sodium_carbonate, updated on 2/2/2023, checked on 2/2/2023.

SLB Energy Glossary - Xanthan Gum (2023). Available online at https://glossary.slb.com/en/terms/x/xanthan_gum, updated on 2/8/2023, checked on 2/8/2023.

Solubility Table of Compounds in Water at Temperature (2022). Available online at <https://www.sigmaaldrich.com/AT/de/support/calculators-and-apps/solubility-table-compounds-water-temperature>, updated on 12/28/2022, checked on 12/28/2022.

Sven Curis (2022a): Real Time In-Situ Monitoring of Cement Carbonation with Acoustic System. University of Leoben. Available online at [https://pure.unileoben.ac.at/portal/en/publications/real-time-insitu-monitoring-of-cement-carbonation-with-acoustic-system\(300d9977-3b7f-43a4-8662-7ba97139c6bd\).html?customType=theses](https://pure.unileoben.ac.at/portal/en/publications/real-time-insitu-monitoring-of-cement-carbonation-with-acoustic-system(300d9977-3b7f-43a4-8662-7ba97139c6bd).html?customType=theses).

- Sven Curis (2022b): Real Time In-Situ Monitoring of Cement Carbonation with Acoustic System. University of Leoben. Available online at [https://pure.unileoben.ac.at/portal/en/publications/real-time-insitu-monitoring-of-cement-carbonation-with-acoustic-system\(300d9977-3b7f-43a4-8662-7ba97139c6bd\).html?customType=theses](https://pure.unileoben.ac.at/portal/en/publications/real-time-insitu-monitoring-of-cement-carbonation-with-acoustic-system(300d9977-3b7f-43a4-8662-7ba97139c6bd).html?customType=theses).
- Tay, Chuang Hwee; Salazar, Jose; Main, Darren; Plack, Heiko; Rublevskiy, Anton; Reid, James (2020): Conductor Batch Drilling Rig Time Optimization by Cementing with Low-Density Low-Temperature Fast Setting Cement. In. SPE Latin American and Caribbean Petroleum Engineering Conference, D021S011R002, checked on 10/24/2022.
- Taylor, K. C.; Nasr-El-Din, H. A.; Al-Alawi, M. J. (1999): Systematic Study of Iron Control Chemicals Used During Well Stimulation. In *SPE J.* 4 (01), pp. 19–24. DOI: 10.2118/54602-PA.
- TCI China (2021): PAC Polyanionic Cellulose | Oilfield Drilling Fluids Chemicals Experts. Available online at <https://www.tcichina.co.uk/pac/>, updated on 1/15/2021, checked on 2/8/2023.
- Westlake Chemical (2018): Product Stewardship Summary - Liquid Caustic Soda. Available online at https://www.westlake.com/sites/default/files/Liquid%20Caustic%20Soda-DiaphragmMembrane-PS%20Summary%20-%20Ed1%20-%20Final_July2018_0.pdf, checked on 2/2/2023.
- Wiklund, Johan; Stading, Mats; Trägårdh, Christian (2010): Monitoring liquid displacement of model and industrial fluids in pipes by in-line ultrasonic rheometry. In *Journal of Food Engineering* 99 (3), pp. 330–337. DOI: 10.1016/j.jfoodeng.2010.03.011.
- Xanthan Suspensions | Resolute Oil (2023). Available online at <https://resoluteoil.com/applications/oil-and-gas/xanthan-suspensions/>, updated on 2/8/2023, checked on 2/8/2023.
- Xiong, Zheng-Qiang; Li, Xiao-Dong; Fu, Fan; Li, Yan-Ning (2019): Performance evaluation of laponite as a mud-making material for drilling fluids. In *Petroleum Science* 16 (4), pp. 890–900. DOI: 10.1007/s12182-018-0298-y.

List of Figures

Figure 1: Depiction of refraction from medium 1 into medium 2 (Burrascano et al. 2015)....	19
Figure 2: 9ppg barite ultrasonic measurement	21
Figure 3: 10ppg barite ultrasonic measurement	21
Figure 4: All mixed fluids for the feasibility study.....	33
Figure 5: Schematic for feasibility study	33
Figure 6: Octogon inhouse software	34
Figure 7: Flowchart for the feasibility study.....	35
Figure 8: All feasibility data represented in one graph.....	37
Figure 9: Average sonic velocity [m/s] with reference to measured density [ppg] of fluid 1 & 2	37
Figure 10: Average sonic velocity [m/s] with reference to measured density [ppg] of fluid 2 & 4	38
Figure 11: Average sonic velocity [m/s] with reference to measured density [ppg] of fluid 3 & 4	38
Figure 12: Testing methodology	42
Figure 13: Measurement for each surface of the acrylic cube (in mm)	44
Figure 14: All pieces of the acrylic cube before assembling	44
Figure 15: Finished acrylic cube.....	44
Figure 16: Schematic of the experimental setup	46
Figure 17: Custom-made ultrasonic test setup with big testing chamber	46
Figure 18: Types of gel strength in muds Source: (SLB Glossary 2022)	49
Figure 19: Waterproof pH-meter	51
Figure 20: pH-strip quick test of fluid 1 at 0,5wt %	51
Figure 21: Testing procedure for main experiment.....	53
Figure 22: Schematic design of the benchtop experimental setup.....	54
Figure 23: Capture setup toolbar.....	59
Figure 24: channel controls.....	60
Figure 25: Signal generator settings.....	61
Figure 26: Trigger control settings.....	61
Figure 27: 10ppg K ₂ CO ₃ mud viscous separation with bubbles captured in it.	64
Figure 28: Fluid 1 displaced by Fluid 2 at medium flowrate.	64
Figure 29: Fluid 2 displaced by Fluid 1 at medium flowrate.	64
Figure 30: Ultrasonic signal - water 2nd measurement	65
Figure 31: PAC 1% RAS analysis	67
Figure 33: PAC 2% RAS analysis	67
Figure 32: PAC 1,5% RAS analysis	67
Figure 34: Plastic viscosity [cp] vs. average sonic velocity [m/s]: PAC	68
Figure 35: Gel strength [lbf/100ft ²] PAC.....	69
Figure 36: Weight % of water vs. Average sonic velocity [m/s]: PAC	69
Figure 38: XGUM 0,42% RAS analysis.....	70
Figure 37: XGUM 0,28% RAS analysis.....	70
Figure 39: XGUM 0,56% RAS analysis.....	70
Figure 40: Plastic viscosity[cp] vs. average sonic velocity [m/s]: xanthan gum	71
Figure 42: Ultrasonic signal 0,56 wt % xanthan gum.....	72
Figure 41: Ultrasonic signal 0,28 wt % xanthan gum.....	72
Figure 43: Gel strength [lbf/100ft ²]: xanthan gum.....	73
Figure 44: Gel strength [lbf/100ft ²] vs. average sonic velocity [m/s]: xanthan gum - comparison of initial gel strength and 10-minute gel strength	74
Figure 45: Gel strength [lbf/100ft ²] vs. average sonic velocity[m/s]: xanthan gum - development of gel strength	74
Figure 46: Weight % of water vs. average sonic velocity[m/s]: xanthan gum	75

Figure 47: Bentonite 2% RAS analysis.....	76
Figure 49: Bentonite 4% RAS analysis.....	77
Figure 48: Bentonite 3% RAS analysis.....	77
Figure 50: Plastic viscosity [cp] vs. average sonic velocity[m/s]: bentonite	78
Figure 51: Gel strength [lbf/100ft ²] bentonite.....	79
Figure 52: Gel strength [lbf/100ft ²] vs. average sonic velocity [m/s]: bentonite- comparison of initial gel strength and 10min gel strength.....	80
Figure 53: Gel strength [lbf/100ft ²] vs. average sonic velocity [m/s]: bentonite - development of gel strength	80
Figure 54: Weight % of water vs. average sonic velocity [m/s]: bentonite	81
Figure 56: Laponite 1,5% RAS analysis.....	82
Figure 55: Laponite 1% RAS analysis.....	82
Figure 57: Laponite 2% RAS analysis.....	82
Figure 58: Plastic viscosity [cp] vs. average sonic velocity [m/s]: laponite	83
Figure 59: Gel strength [lbf/100ft ²]: laponite.....	84
Figure 60: Weight % of water vs. average sonic velocity[m/s]: laponite	85
Figure 61: Gel strength [lbf/100ft ²] vs. average sonic velocity[m/s]: laponite - development of gel strength.....	85
Figure 62: Gel strength [lbf/100ft ²] vs. average sonic velocity [m/s]: laponite-comparison of initial gel strength and 10min gel strength.....	84
Figure 64: CMC 1,5% RAS analysis	86
Figure 63: CMC 1% RAS analysis	86
Figure 65: CMC 2% RAS analysis	86
Figure 66: Plastic viscosity [cp} vs. average sonic velocity[m/s]: CMC.....	87
Figure 67: Gel strength [lbf/100ft ²] CMC.....	88
Figure 68: Weight % of water vs. average sonic velocity [m/s]: CMC	89
Figure 69: Flowzan 0,25% RAS analysis	89
Figure 71: Flowzan 0,75% RAS analysis	90
Figure 70: Flowzan 0,5% RAS analysis	90
Figure 72: Plastic viscosity [cp] vs. average sonic velocity[m/s]: flowzan	91
Figure 73: Flowzan 0,5% bubbles in suspension.....	91
Figure 74: Gel strength [lbf/100ft ²] flowzan.....	92
Figure 75: Gel strength [lbf/100ft ²] vs. average sonic velocity [m/s]: flowzan - comparison of initial gel strength and 10min gel strength.....	93
Figure 76: Gel strength [lbf/100ft ²] vs. average sonic velocity [m/s]: flowzan - development of gel strength	93
Figure 77: Weight % of water vs. average sonic velocity [m/s]: flowzan	94
Figure 78: Viscosifier correction of CaCO ₃	95
Figure 79: Comparison of average ultrasonic velocity [m/s] and mud balance density [ppg] of barite	96
Figure 80: 180kHz velocity versus mud weight (Motz et al. 1998).....	96
Figure 81: Comparison of average ultrasonic velocity [m/s] and mud balance density [ppg] of CaCO ₃	97
Figure 82: Comparison of average ultrasonic velocity [m/s] and converted density [ppg] of K ₂ CO ₃	98
Figure 83: Comparison of average ultrasonic velocity [m/s] and mud balance density [ppg] of Na ₂ CO ₃	99
Figure 84: Weight % of water vs. average sonic velocity; citric acid.....	100
Figure 85: Weight % of water vs. average sonic velocity: caustic soda	102
Figure 86: Weight % of water vs. average sonic velocity: gypsum.....	102
Figure 87: Measured density [ppg] compared to average sonic velocity [m/s] for the preliminary study.....	104
Figure 88: Degree of intermixing [%] compared to average sonic velocity [m/s] for the preliminary study.	104

Figure 89: Comparison measured and calculated density [ppg] with average ultrasonic velocity [m/s] of Experiment 1	106
Figure 90: Comparison of degree of intermixing [%] and average sonic velocity [m/s] of Experiment 1	106
Figure 91: Comparison of degree of intermixing [%] with pumped volume [ml] and total volume prediction of Experiment 1	107
Figure 92: Comparison measured and calculated density [ppg] with average ultrasonic velocity [m/s] of Experiment 2	108
Figure 93: Comparison of degree of intermixing [%] and average sonic velocity [m/s] of Experiment 2	109
Figure 94: Comparison of degree of intermixing [%] with pumped volume [ml] and total volume prediction of Experiment 2	109
Figure 95: Comparison measured and calculated density [ppg] with average ultrasonic velocity [m/s] of Experiment 3	111
Figure 96: Comparison of degree of intermixing [%] and average sonic velocity [m/s] of Experiment 3	111
Figure 97: Comparison of degree of intermixing [%] with pumped volume [ml] and total volume prediction of Experiment 3	112
Figure 98: Spectrometer data of displacement experiment at 0,07m/s and 1,5 wt% PAC	114
Figure 240: Spectrometer data of displacement experiment at 0,16m/s and 1,5 wt% PAC 100%	114
Figure 99: Spectrometer data of displacement experiment at 0,16m/s and 1,5 wt% PAC	114

List of Tables

Table 1: Fluid description feasibility study.....	31
Table 2: Feasibility study amount of additives	32
Table 3: Feasibility study-mixing ratios and measured densities	32
Table 4: Acquired data of the feasibility study	36
Table 5: Chosen materials and their categories	48
Table 6: Selected viscosifiers with respective wt %	49
Table 7: Selected weighting materials with target density.....	50
Table 8: Chosen other additives with target wt % (eritia 2018).	50
Table 9: Error determination - comparison external and local data.....	56
Table 10: Mixing Ratios and Corresponding Measured Density.....	63
Table 11: PAC - plastic viscosity and yield point.....	67
Table 12: Plastic viscosity - average sonic velocity PAC.....	68
Table 13: Gel strength - average sonic velocity PAC.....	69
Table 14: Plastic viscosity and yield point xanthan gum.....	70
Table 15: Plastic viscosity - average sonic velocity xanthan gum.....	71
Table 16: Gel strength - average sonic velocity xanthan gum.....	73
Table 17: Plastic viscosity and yield point bentonite.....	76
Table 18: Plastic viscosity - average sonic velocity bentonite.....	77
Table 19: Gel strength - average sonic velocity bentonite.....	79
Table 20: Plastic viscosity and yield point laponite.....	81
Table 21: Plastic viscosity - average sonic velocity laponite.....	83
Table 22: Gel strength - average sonic velocity laponite.....	84
Table 23: Plastic viscosity and yield point CMC.....	86
Table 24: Plastic viscosity - average sonic velocity CMC.....	87
Table 25: Plastic viscosity and yield point flowzan.....	89
Table 26: Plastic viscosity - average sonic velocity flowzan.....	90
Table 27: Gel strength - average sonic velocity flowzan.....	92
Table 28: Measured density and corrected average sonic velocity of barite.	96
Table 29: Measured density and corrected average sonic velocity of CaCO ₃	97
Table 30: Converted density and average sonic velocity of K ₂ CO ₃	98
Table 31: Converted density and average sonic velocity of Na ₂ CO ₃	99
Table 32: Experimental data citric acid	100
Table 33: Experimental results for caustic soda	101
Table 34: Measured density, degree of intermixing and measured average sonic velocity of the preliminary fluid study.....	103
Table 35: Determined coefficients for density and intermixing calculations.	103
Table 36: Experimental data of Experiment 1	105
Table 37: Degree of intermixing and total volume prediction for Experiment 1.....	105
Table 38: Experimental data of Experiment 2	108
Table 39: Degree of intermixing and total volume prediction for Experiment 2.....	108
Table 40: Experimental results Experiment 3.....	110
Table 41: Degree of intermixing and total volume prediction for Experiment 3.....	110

Nomenclature

k	slope	[]
d	Intersection on the y-axis	[]
v	Ultrasonic/average velocity	[m/s]
s	Distance	[m]
t	Time	[s]
$v_{internal}$	Velocity captured with ultrasonic setup of Montanuniversity Leoben	[m/s]
$v_{external}$	Velocity captured with ultrasonic setup of Octogon	[m/s]
V_i	Volume of substance “i”	[m ³]
ρ_i	Density of substance “i”	[kg/m ³]
τ	Shear stress	[lbf/100ft ²]
γ	Shear rate	[RPM]
τ_0	Fluid stress at near-zero shear rate	[lbf/100ft ²]
γ_∞	Finite high shear limiting viscosity	[RPM]
m	Variable shear stress exponent	[]
n	Variable shear rate exponent	[]
τ_{ref}	Reference that equals 47,88Pa=1 lb/ft ²	[]

Abbreviations

PAC	Polyanionic cellulose
CMC	Carboxymethyl cellulose
CaCO ₃	Calcium carbonate
K ₂ CO ₃	Potassium carbonate
Na ₂ CO ₃	Sodium carbonate
ppg	Pounds per gallon
PPE	Personal protective equipment
Wt %	Weight percent
R&D	Research and development
RPM	Rotation per minute
mm	Milli meter
IADC	International association of drilling contractors
LCM	Lost circulation material
RAS	Regression Analysis Software
GHB	General Herschel Bulkley
HB	Herschel Bulkley